State Atomic Energy Corporation "Rosatom"

FEDERAL STATE UNITARIAN ENTERPRISE
"SCIENTIFIC RESEARCH INSTITUTE
SCIENTIFIC INDASTRIAL ASSOCIATION "LUCH"
FSUE SRI SIA "LUCH"

APPROVED
General Director
Professor, PhD.

S.V. Alekseev

STUDY OF FUEL ASSEMBLIES UNDER SEVERE ACCIDENT TOP QUENCHING CONDITIONS IN THE PARAMETER TEST SERIES
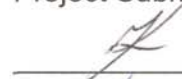
Scientific and Researrch Final Report
on the work of ISTC Project No. 3690

Project Manager

_____ V.I. Nalivaev

Project Submanagers:

_____ A.E. Kiselev

_____ V.P. Semishkin

Podolsk 2009

Authors

from FSUE SRI SIA "LUCH"

L.S. Degtyareva, V.P. Deniskin, D.N. Ignatiev, V.S. Konstantinov, V.I. Nalivaev, N.Ya. Parshin, E.B. Popov, D.M. Soldatkin, V.N. Turchin

from IBRAE RAS

A.D. Vasilev, A.E. Kiselev, D.Yu. Tomashchik, T.A. Yudina

from OKB "GIDROPRESS"

V.P. Semishkin, E.A. Frizen, V.V. Shchekoldin

Abstract

The Final Report deals with the results of the computational and experimental studies performed according to the Work Plan of ISTC Project No. 3690 "Studies of fuel assemblies under severe accident top quenching conditions in the PARAMETER-SF test series". The Project was executed jointly by three organizations: FSUE SRI SIA "LUCH", IBRAE RAS, OKB "GIDROPRESS" with participation of the leading specialists from JSC "VNIINM", RRC "Kurchatov Institute", A.I. Leipunsky SRC RF - IPPE and under methodical support of foreign collaborators (FZK, GRS, JRC-ITU, PSI, EdF, CEA, AEKI, INRNE).

Within the framework of the Project two experiments of PARAMETER-SF series (SF3 and SF4) were conducted as well as material studies of the model assembly tested in the SF2 experiment under the preceding ISTC Project No. 3194 were done. The tested bundles were made up of 19 fuel rod simulators. The bundles are identical to those used in VVER-1000 with respect to material and dimensions.

In PARAMETER-SF2 experiment, the initial stage of severe LB LOCA accident is studied when top and bottom flooding with water is initiated after core drying and its heating-up to ~ 1500°C.

In PARAMETER-SF3 experiment, the specific peculiarities of cooling and changes in structure of materials of VVER-1000 assembly under the conditions of severe accident with top flooding of the assembly heated to temperature of ~1600°C were investigated.

The possibility of assembly flooding intensively oxidized with steam-air mixture when unstable cladding temperature escalation occurs was in focus of the PARAMETER-SF4 experiment.

Results of the tests are intended for studying the processes occurring during water flooding of the overheated core in the course of severe LOCA accident at the NPP with VVER, and under similar situations in PWR, and could be used for verification of computer codes.

The report includes: 75 pages, 4 Tables, 81 Figures, 2 Annexes.

CONTENTS

Introduction

VVER design shall meet the safety criteria and principles established in NP-001-97 (PNAE G-01-011-97), NP-082-07 and in other regulatory documents of Russia. Safety guides and other recommendations issued by International Atomic Energy Agency (IAEA), and the requirements of European Utilities for NPP with PWR (EUR Safety requirements, Volume 2, Chapter 2.1) should be taken into account as well.

According to the regulatory documents the design shall take into account the additional conditions, for instance, beyond design basis accidents for implementation of measures or procedures on accident management. For NPP with VVER (PWR), the unfavourable consequences associated with the core melting are expected for beyond design basis accident of LB LOCA. LB LOCA in VVER-1000 can be caused by damage of the primary pipelines and, in the first turn, of the main coolant pipeline (MCP) Dnom850. Usually the initiating event is assumed to be a break of Dnom850 at the reactor inlet or outlet. Generally speaking, the fact of the coolant system (or of the reactor plant vessel at the latest stage of severe accident) depressurization creates conditions for air ingress from the containment into the reactor vessel and, consequently, into the core that would influence the heat transfer and the core flooding under severe accident.

Studying the phenomenology of oxidation processes of fuel rod claddings made of E110 alloy in steam-air environment is of interest both for development of the adequate numerical models for computer codes, on the one hand, and for verification of the implemented code models against the integral bench experiment data with considerable temperature inhomogeneity over the test assembly volume. The practical interest presents the study of a possibility of flooding the assembly intensively oxidized with steam-air mixture when fuel rod temperature escalation occurs. The outcomes should be used for elaboration of the severe accident management guides and for estimation of hydrogen generated during flooding.

In the SF4 experiment conducted under Project No. 3690, the experimental data on the temperature behaviour of overheated VVER bundle under air ingress conditions including flooding stage were obtained. The data will enable to extend the base of knowledge on mechanical and physical-chemical behaviour of claddings of the overheated fuel rods, including the parameters of interaction of zirconium melt with uranium dioxide fuel pellets.

The Project was executed jointly by three organizations:

-   FSUE SRI SIA "LUCH" – conducting the experiments, post-test calculations and material studies;

- IBRAE RAS – the experiment scenarios development, pre- and post-test numerical modelling;

- OKB "GIDROPRESS" – the experiment scenarios development, pre- and post-test modelling.

The leading specialists from JSC "VNIINM", RRC "Kurchatov Institute", A.I. Leipunsky SRC RF - IPPE took part in the work under the Project with the methodical support of foreign collaborators (FZK, GRS, JRC-ITU, PSI, EdF, CEA, AEKI, INRNE).

According to the Work Plan of ISTC Project No. 3690 the following tasks were fulfilled:

- *Task 1* – Post-test material investigations of VVER-1000 model assembly, tested in the PARAMETER-SF2 experiment under severe accident with top and bottom quenching;

- *Task 2* – Study of peculiarities of cooling and change in the structure of materials of VVER-1000 assembly under severe accident during top quenching of the assembly, overheated to temperature of ~ 1600°C (PARAMETER-SF3);

- *Task 3* – Study of behaviour of 19-rods model FA of VVER-1000 under severe accident with air ingress (PARAMETER-SF4).

The performed experiments enabled to:

- obtain the information on the behaviour of structural components of 19-rods model FA of VVER-1000 overheated to ~ 1600°C during top quenching;

- study the temperature behaviour of the model FA of VVER-1000 under the conditions of air oxidation and subsequent bottom quenching;

- obtain the information on the degree of oxidation of structural components of the model FA of VVER-1000 and structural-phase changes in claddings of the model FA of VVER-1000 by the results of post-test studies;

- study the time history of oxygen absorption and hydrogen release.

Results of tests are intended for better understanding of the phenomenology of the processes occurring during water flooding of the core overheated under severe LOCA at NPP with VVER and under similar situations at PWR, and can be used for verification of computer codes.

1. POST-TEST ANALYSIS OF SF2 ASSEMBLY

1.1. Methods of encapsulation and sectioning of the model FA

Experiment PARAMETER-SF2 was performed with the aim of studying the behaviour of a 19-rods model FA of VVER-1000 under simulated severe accident conditions. In the experiment the initial stage of severe accident with large coolant leak from the primary circuit of VVER-1000 RP was simulated when the core drying occurs, then its heating-up to ~ 1500°C and top and bottom water quenching.

After the experiment the test section was disassembled and the state of model FA inside the test section was fixated with a compound (epoxy resin ЭД-20) in vertical position.

After the compound hardened, the assembly was removed from the test section, photographed and cut over the length into fragments and slabs. Sectioning of the bundle was done with the use of cutting-off machine Delta-Abrasimet with diamond blade of thickness 1.7 mm. Thickness of cross section slabs was chosen to be 15…20 mm to be ensured in their integrity keeping during their cutting out.

To remove voids and cavities, remained after FA filling with the compound, the cross section slabs vacuum impregnation was made with epoxy resin EPO – THIN at the "Buehler" impregnator. Then the cross section slabs have been ground and polished.

The macro photos of the ground cross section slabs were taken by the digital camera SONY (8 mps). Further on, the available macrographs were used for comparative evaluation of the degree of the assembly damage at different elevations.

1.2. Methods of material studies of the model FA

Methods of material studies of the model FA are described in detail in [1]. Methodical approaches to material studies of the PARAMETER-SF2 assembly are developed on the basis of the analysis of the cladding thermocouples readings [2].

According to the thermocouples readings, the hottest zone was observed in the assembly upper part at the elevations of 900…1300 mm and, consequently, the highest degree of oxidation of the shroud and claddings corresponded to this zone. Therefore, the metallographic measurements of layer thickness in this area were done with more details (using slabs from the elevations of 902, 951, 1033, 1103 1203, 1246 and 1296 mm, Figures 1, 2).

For claddings at all cross section slabs, the thickness of metal layers and compact oxides were measured. Measurements were carried out on each cladding in four directions and averaged. By the results of measurements, curves of distribution of thickness of metal part of claddings and of compact oxide over the assembly length were

plotted. The data are also presented on thickness of oxide layers calculated as a difference between the original cladding thickness (690 μm) and the thickness of metal remaining part (considering Pilling-Bedworth factor).

Metallographic analysis of cross section slabs was performed with the optical microscope OLYMPUS using the computer code package OMNIMET. Electron microscope studies of cross-sections were performed with the scanning electron microscope JEOL JSM – 6460 LV.

X-ray analysis was applied to specimens cut out of the shroud (Z ~ 250, 500, 900 and 1200 mm, specimen size – 15x20 mm). We did not manage to prepare similar specimens of claddings because any attempt to withdraw claddings from cross section slabs filed with epoxy resin resulted in cladding damage.

X-ray phase analysis of specimens was performed on the outside surface (because the concavity of the inside surface does not allow analysis in the inside), as well as at the depth of 30 and 200 μm from the external surface and in the middle of the shroud tube (~1000 μm). At the elevation of 900 mm, where the maximum hydrogen content was revealed in the course of studies, the additional studies were performed at the depth of 1300, 1400, 1500 and 1600 μm. Material was removed by etching in the mixture of hydrogen peroxide, nitrogen and hydrofluoric acids. Thickness of the etched layers was measured with the help of micrometer.

X-ray of specimens was performed with the diffractometer DRON-6 with the use of CuKα – radiation, and the amount of ZrH$_2$ phase was measured by ratio of integral intensities of analytical lines. Line (111) – the most intensive in the diffraction spectrum of ZrH$_2$, was used as the analytical line. Measurements were performed in each studied section in layer-by-layer radiography phase analysis. The most suitable specimens for performing the quantitative X-ray phase analyses are powders. Owing to this, in sections (Z ~ 250, 500, 900 and 1200 mm), measurements of ZrH$_2$ phase content were performed also on powder samples. Lattice periods of β - and ω - phases were determined with an error of ±0.01 Å.

Accuracy of determination of *a* and *c* periods of α-solid solution depended on the width of diffraction lines, i.e. on the degree of the lattice distortion. In the most favourable cases an error in determination of *a* and *c* periods did not exceed ±0.001 Å.

1.3. Results of material studies

Results of material studies are given in more details in the R&D report of [1].

Analysis of the results of post-test material studies showed that temperature gradient over the bundle length caused different degree of its damages.

The state of the assembly lower part (Z = 0…400 mm) does not practically differ from the original state, and oxide thickness on the outer surface does not exceed 5…10 μm.

At 500…1300 mm elevations, a multilayered spalling off zirconium dioxide was found. Thickness of compact oxide and the remaining metal part of claddings was measured on each fuel rod. Results of these measurements are plotted in Figures 3 – 6. Comparison of the results of metallographic studies and thermocouples readings enabled to suppose that such extended zone with the pronounced "breakaway" effect was formed probably during the assembly pre-oxidizing.

In the middle part of the assembly (Z = 500…800 mm) the fuel rod simulators are displaced relative to the original arrangement in the assembly cross-section, the outer cladding surface is covered with multilayered zirconium dioxide, separating from metal substrate, but its thickness does not exceed ~ 100 μm.

In the upper part of the assembly (Z = 900…1300 mm) the original arrangement is greatly distorted (Figure 2). The claddings are oxidized both on the outer (to 650 μm), and on the inner (to 50 μm) surfaces. Zirconium dioxide has different morphology. The inner part of the oxide scale is a compact well connected with the metal layer zirconium dioxide that was grown evidently at the transient stage. In the hottest zone for the compact oxide the cracking in azimuth direction with trend to separation of the outer part is typical. One can suppose that this effect resulted from thermal shock during top flooding. Thickness of compact zirconium dioxide attached to metal layer increases with elevation increase and reaches the maximum value at the elevations of 1250-1300 mm, and distribution of its thickness through the assembly cross-section at the given elevations is significantly nonhomogeneous and varies within the range of 100…350 μm.

On the compact dioxide there is the zirconium dioxide of multilayered structure, separating from the cladding. The metal part of the claddings presents the oxygen-stabilized α phase (α - Zr (O)). The fuel rod claddings are embrittled, i.e. have through-wall cracks, however fragmentation of fuel rods is limited. No fuel relocation and fuel-clad interaction were revealed in the assembly.

Results of X-ray phase analysis of the shroud specimens are presented in Table 1.

Table 1

Results of phase analysis by X-ray

Assembly coordinate, mm	Thickness of etched layer, μm	Phase composition	Lattice periods, a Å		Results of layer-by-layer analysis Content of H, % at.	Results of analysis of powder samples * Content of H, % at.
Shroud original state	-	α - Zr + β - Nb	α - Zr	a = 3.229, c = 5.144	-	-
			β - Nb	3.548		
250 mm	0 (external surface)	α - Zr(O) + ZrO$_2$ monoclinic	α - Zr	a = 3.230, c = 5.149	-	-
	20	α - Zr + β - Nb	α - Zr	a = 3.231, c = 5.148	-	-
			β - Nb	3.34		
	300	α - Zr + β - Nb	α - Zr	a = 3.230, c = 5.148	-	-
			β - Nb	3.34		
	middle section	α - Zr + β - Nb	α - Zr	a = 3.230, c = 5.148	-	-
			β - Nb	3.34		
500	0 (external surface)	Zr(C$_x$O$_{1-x}$) + α - Zr	Zr(C$_x$O$_{1-x}$)	4.66	-	9
			α - Zr	a = 3.249, c = 5.178		
	20	α - Zr + β - Zr + ω - Zr + δ-ZrH$_2$	α - Zr	a = 3.239, c = 5.164	10	
			β - Zr	3.56		
			ω - Zr	a = 5.02, c = 3.10		
			δ-ZrH$_2$	4.75		
	300	α - Zr + β - Zr + δ-ZrH$_2$+ ω - Zr(traces)	α - Zr	a = 3.235, c = 5.152	8	
			β - Zr	3.56		
			δ-ZrH$_2$	4.75		
	middle section	α - Zr + δ-ZrH$_2$+ β - Zr	α - Zr	a = 3.235, c = 5.161	6	
			β - Zr	3.55		
			δ-ZrH$_2$	4.75		
900	0 (external surface)	Zr(CO) + α - Zr	Zr(CO)	4.67	-	23
			α - Zr	a = 3.227, c = 5.150		

	Depth, μm	Phase composition	Phase	Lattice parameter	ZrH₂ content*	
	20	α - Zr + δ-ZrH$_2$	α - Zr	a = 3.225, c = 5.147	24	
			δ-ZrH$_2$	4.77		
	300	α - Zr + δ-ZrH$_2$	α - Zr	a = 3.225, c = 5.145	21	
			δ-ZrH$_2$	4.77		
	1000	α - Zr + δ-ZrH$_2$	α - Zr	a = 3.224, c = 5.150	20	
			δ-ZrH$_2$	4.77		
	1300	α - Zr + δ-ZrH$_2$			17	
	1400	α - Zr + δ-ZrH$_2$			17	
	1500	α - Zr + δ-ZrH$_2$			17	
	1600	α - Zr + δ-ZrH$_2$			16	
1200	0 (external surface)	Zr(CO) + α - Zr	Zr(CO)	4.67	-	18
			α - Zr	a = 3.236, c = 5.178		
	20	α - Zr+ δ-ZrH$_2$ + β - Zr + β - Nb	α - Zr	a = 3.225, c = 5.150	21	
			δ-ZrH$_2$	4.76		
			β - Zr	3.56		
			β - Nb	3.33		
	300	α - Zr + δ-ZrH$_2$ + β - Zr + β - Nb	α - Zr	a = 3.229, c = 5.153	20	
			δ-ZrH$_2$	4.77		
			β - Zr	3.56		
			β - Nb	3.34		
	middle section	α - Zr + δ-ZrH$_2$ + β - Zr + β - Nb	α - Zr	a = 3.229, c = 5.178	18	
			δ-ZrH$_2$	4.77		
			β - Zr	3.57		
			β - Nb	3.34		

* - content of ZrH₂ phase was measured on powder samples got by filing the shroud fragments with diamond needle file from the external surface to the depth of not more than half of the shroud.

On the basis of the results of metallographic studies the evaluation was done for the maximum possible hydrogen mass that could release into steam-gas environment during the experiment. Taking into account the results of measurements of hydrogen content in the shroud the upper limit of released hydrogen mass is estimated to be 31 g. The obtained value is in a good agreement with the results of measurements (~ 28 g), [2].

2. PARAMETER-SF3 EXPERIMENT

2.1. Pre-test calculations of PARAMETER-SF3 experiment

The main purpose of the pre-test calculations was justification of the scenario of PARAMETER-SF3 experiment and elaboration of recommendations on its performance.

Pre-test scenario of the experiment is presented in Table 2.

Table 2

Pre-test scenario of PARAMETER-SF3 experiment

No.	Stage	Main Parameters			
		FA temperature, K	Medium	Heating rate, K/s	Time, s
1	Joule heating up of FA in argon flow	~300-670	Argon at temperature 720 K (argon flow rate - 2 g/s)	–	0-1500
2	Joule heating up of FA in the flow of steam-argon mixture	670→770	Steam-argon mixture (argon/ steam flow rate at inlet - 2/3.5 g/s at temperature 720/770 K)	–	1500-3500
3	FA heating up to 1470 K	770→1470	Steam-argon mixture (argon/ steam flow rate at inlet - 2/3.5 g/s at temperature 720/770 K)	0.25 (initial), 0.1 (final)	3500-7500
4	FA pre-oxidation	~1470	Steam-argon mixture (argon/ steam flow rate at inlet - 2/3.5 g/s at temperature 720/770 K)	–	7500-11500
5	Transient phase	1470→1870	Steam-argon mixture (argon/ steam flow at inlet - 2/3.5 g/s at temperature 720/770 K)	0.4 (initial)	11500-12400
6	Top flooding of the assembly (as soon as FA will reach Tmax=1870 K)	Up to saturation	Water (flow rate 40 g/s, water temperature ~300 K	–	As soon as saturation temperature will be reached

To fit the proposed scenario the mode of electric power supply was optimized.

Pre-test calculations were performed with the computer codes SOCRAT (IBRAE RAS), RELAP/SCDAPSIM MOD3.2 (OKB "GIDROPRESS"), ICARE/CATHARE (RRC "Kurchatov Institute"), PARAM-TG (FSUE SRI SIA "LUCH"), ATHLET-CD (GRS), SCDAP/ RELAP/ FZK-PSI (PSI).

13

Annex 1 presents the detailed description of the specific features of thermohydraulic simulation, nodalizations, initial and boundary conditions and the results of numerical calculations of the experiment

By the results of calculations the recommendations were given to experimenters on the test performing and correction of electrical power in the "on-line" mode if the measured parameters differ substantially from the predicted values.

In spite of some scattering in predicted temperature and hydrogen release, results of pre-test studies including the analytical work done on revealing the most important factors of uncertainties, allowed defining the initial and boundary conditions of the experiment.

2.2. Results of PARAMETER-SF3 experiment

PARAMETER-SF3 experiment was conducted on 31 October, 2008, and the full information on the experimental results are presented in [3].

In PARAMETER-SF3 experiment, the initial stage of severe accident with LB LOCA was simulated when the core drying occurs, then its heating-up to $\sim 1600°$C and top water flooding.

SF3 experiment was performed with the aim of studying the behaviour of a 19-rods model FA of VVER-1000 under simulated severe accident conditions including the stage of low rate top flooding, and namely:

- Study of behaviour of structural components of a 19-rods model FA of VVER-1000 (fuel pellets and claddings, shroud, spacing grids);
- Study of oxidation degree of structural components of a 19-rods model FA of VVER-1000;
- Study of interaction and structural-phase changes in the materials of a model FA of VVER-1000 (fuel pellets and claddings);
- Study of hydrogen release.

The process systems of PARAMETER test facility were prepared for the experiment according to the functional diagram (Figure 7).

The experiment consisted of five stages:

- *preparation stage* (0 – 4506 s) – stabilization of the assigned flow rates of argon ($G_{Ar\ in} \approx 2$ g/s) and steam ($G_{st\ in} \approx 3.5$ g/s) at FA temperature of $T_{FA} \approx 500°$C, check of state of the assembly and process systems;

- *assembly heating-up to temperature of $\approx 1200°C$* (4506 – 9760 s);

- *pre-oxidation* (9760 – 13725 s) – FA holdup at temperature $\approx 1200°C$ in the hottest zone during $\sim$ 3970 s. The maximum temperature deviations in the hottest cross-section (1250 mm) – $\sim \pm 50°C$;

- *assembly heating-up to maximum temperature* (13725 – 14481 s) – increase in FA temperature in the hottest section to $1600°C$;

- *flooding* (14486 – 14960 s) – top flooding of the assembly at the flow rate of Gtf $\approx$ 40 g/s.

In Figures 8 and 9 the results of measurement of the main experimental parameters are given: flow rate and temperature of argon (G_{argon}, $T_{Ar\,in}$) and steam (G_{steam}, $T_{st\,in}$) at the test section inlet; gas mixture flow rate R4 at the outlet to special ventilation (Figure 8); electric parameters (Figure 9): power (P), current (I), voltage (U).

Thermocouples readings arranged over the length of fuel rod claddings during the whole experiment are presented in Figure 10.

Figure 11 presents the results of measurement of volumetric hydrogen concentration by the continuous hydrogen measurement device SOV-3 and in ten sampling tanks (Vol.1,…,Vol.10). Curve of volumetric hydrogen concentration is plotted considering response time of SOV-3 system but the time delay in hydrogen measurements connected with the gas transport is not taken into account. One can see from the Figure that indications of SOV-3 and the results of gas sampling analysis are in a good agreement.

Analysis of the results of hydrogen measurement with SOV-3 system indicated that during the experiment $\sim$ 34 g of hydrogen was generated, and maximum rate of hydrogen generation was $\sim$ 0.02 g/s (Figure 12).

2.3. Results of material studies of the SF3 model assembly

After the PARAMETER-SF3 experiment, the model FA encapsulation, sectioning and material studies were performed and the results are presented in Annex 2.

In the course of dismounting of the test section and preparing the FA for encapsulation the assembly lower part (from 1300 mm and below) separated from the upper part and the personnel was forced to withdraw it out of the shroud.

After visual inspection and photo documentation of the assembly appearance it was placed into a plastic vessel and filled with a compound (epoxy resin ЭД-20) in horizontal position. For spacing the fuel rods of the third row of the assembly and the vessel walls the copper bands were used.

After solidifying the compound the assembly was withdrawn from the plastic vessel and cut into slabs.

Just during visual examination of the assembly it became clear that direct measurement of the zirconium dioxide layer thickness on cladding surfaces are not available along the whole assembly length (500-1500 mm) due to pronounced spalling of oxide scale (only at the elevation of 400 mm the direct measurements of oxide thickness were performed because of the claddings reveal no spallation). In this case the only method for assessment of oxidation degree of claddings is evaluation by thickness of the remaining metal layer. Difference between the initial cladding thickness and the measured thickness of the remaining metal part considering Pilling-Bedworth factor that reflects the change in volume during transformation of metal to oxide gives the oxide thickness. This procedure is widely used, for instance, in QUENCH-12, PARAMETER-SF2 tests, however for the assembly in PARAMETER-SF3 test its modification was required. The matter is that in the course of the experiment PARAMETER-SF3 within the time interval from ~5000 s to 14500 s the pressure was increasing inside fuel rods and so the pressure differential on claddings was 0.1…0.3 MPa. At the beginning of the experiment (when the claddings were not oxidized practically), this pressure differential led to their deformation in the form of ballooning, and consequently, to cladding thinning. As the cladding deformation is nonuniform over the length and azimuth of each fuel rod, the additional measurements of inner diameters were needed for each cladding at all selected cross-sections.

Alongside with measurements of thickness of metal layers and inner diameter of claddings the measurements were performed for thickness of compact oxide scales and sub-oxide layers on the outer and inner surfaces of fuel rod claddings.

Analysis of post-test material studies showed that:

- the state of the assembly lower part (Z = 0…400 mm) does not practically differ from the original state, and oxide thickness on the outer surface does not exceed 2-10 μm;

- within the range of 500…1300 mm elevations there is a multilayered zirconium dioxide spalling off on the fuel rod claddings;

- in the middle part of the assembly (Z = 500…800 mm) the fuel rod simulators are displaced in respect to the initial position in the assembly cross-section (Figure 13), the outer cladding surfaces are covered with multilayered zirconium dioxide, separating from metal surface, and its thickness on some fuel rods (at 800 mm elevation) reaches ~ 400 μm.

In the upper part (Z = 900…1300 mm) the assembly state is greatly distorted (Figure 14). The claddings are oxidized both on the outside (to 550 μm), and on the inside (to 50 μm) surfaces. Zirconium dioxide has different morphology. The inside part of the oxide scale is a compact, well-bound with the metal part, zirconium dioxide of columnar structure that was formed, evidently, at the transient stage. Its thickness increases at

higher elevations and reaches the maximum value at the elevations of 1250-1300 mm, and distribution of its thickness through the assembly section at the given elevation is greatly irregular and varies within the range of 100…350 μm. In the hottest zone in the compact oxide of three fuel rods the precipitations of the second phase α - Zr(O) are revealed that is evidently indicated their high-temperature (above ~1500 °C) oxidation and formation of ZrO_2 cubic modification. On the compact dioxide one can see the zirconium dioxide of multiplayer structure, separating from cladding. The metal part of claddings presents the oxygen-stabilized α phase (α - Zr (O)). The fuel rod claddings are embrittled, i.e. have the through cracks, and fragmented. No fuel-clad interaction is revealed in the assembly.

In the studied assembly cross-sections the considerable non-uniform oxidation of fuel rods is observed.

Thickness of zirconium dioxide on surfaces of fuel rods (Figure 15) and shroud (Figure 16), calculated on the basis of measurements of metal layer thickness, confirm thermocouples readings that indicates that location of the hottest zone at the elevation was at 1300 mm.

The mass of hydrogen generated due to oxidation and calculated "from above" corresponds to the value of ~42 g. To make a comparison with the measured mass it is necessary to consider additionally the mass of hydrogen absorbed by FA components, at least, due to the shroud hydrogenation.

2.4. Post-test calculations of PARAMETER-SF3 experiment

The main purpose of simulation in PARAMETER-SF3 experiment at PARAMETER facility was the most possible accurate solution of thermal problem. Calculated values of parameters of chemical interactions were of the secondary character and allowed evaluation the consistency of measurement of temperatures and hydrogen production.

Post-test calculations of the experiment were carried out with the use of computer codes SOCRAT, RELAP/SCDAPSIM MOD3.2, ICARE/CATHARE, PARAM-TG, ATHLET-CD.

Annex 1 gives a detailed description of nodalizations, initial and boundary conditions and the results of numerical calculation of SF3 experiment, the analytical support was made for a possibility of top flooding.

During top flooding the water penetration into the model assembly is hindered due to presence of steam streaming upwards the assembly. At reaching the definite mass steam flow rate, called the critical flow rate under counter-current flow limitation, the occurrence of the so-called counter-current flow limitation mode shall be observed when

the flows become unstable, the waves of large length are formed on the surface, the pressure differential increases and water starts to move upwards. Analysis of this process is described in detail in Annex 1. The obtained results showed that the top flooding will be successful at the maximum temperature of FA heating below ~1700°C, otherwise, the counter-current flow limitation mechanism could lead to overheating of fuel rods. In SF3 experiment the maximum temperature of ~1600°C were realized, and the flooding was successful that does not contradict the results of the analytical study performed.

Comparative analysis of the results of numerical simulation of PARAMETER-SF3 experiment, conducted with the use of various computer codes, enables to conclude that all of them give a satisfactory description of temperature behaviour and of the processes occurring in the FA (Figures 17 – 25).

3. PARAMETER-SF4 EXPERIMENT

3.1. Pre-test calculations of PARAMETER-SF4 experiment

The purpose of PARAMETER-SF4 experiment was studying the behaviour of the pre-oxidized assembly under the conditions of air ingress with a small flow rate and subsequent flooding.

The proposed temperature scenario corresponded, on the whole, to the scenario of QUENCH-10 experiment. Specific features of SF4 experiment were the following, [4]:

1.   Temperature of the assembly pre-oxidation in steam flow – 1200ºC;

2.   Oxidation degree of the assembly – to 300 (400) μm;

3.   Maximum temperature before flooding onset was 1750ºC to avoid temperature escalation and damage of the assembly.

For justification of the experiment scenario the pre-test numerical analysis was made by the calculation teams of participants and collaborators of the Project [5, 6, 7]. The parameters to be determined were electric power, air flow rate, flooding water flow rate.

The following computer codes were used for the pre-test calculations: SOCRAT, ICARE/CATHARE, ATHLET-CD, RELAP/SCDAPSIM MOD3.2, MAAP4 (EdF), SCDAP/RELAP/FZK-PSI, PARAM-TG.

In two codes – SOCRAT and RELAP/SCDAPSIM MOD3.2 - air oxidation model is not available. To treat air oxidation the available steam oxidation model was adapted in SOCRAT code. In other codes, the air oxidation models are available but their verification is needed.

Key conditions and parameters at the air ingress phase were:

- − long-term holding of the assembly under oxygen starvation conditions (for formation of zirconium nitrides);
- − assembly flooding at maximum temperature of 1750ºC.

To meet the temperature condition the criterion was developed that limits the assembly heat up rate at the hottest elevation. Due to the fact that the hottest elevation is shifted at the air ingress stage and its calculated position is evaluated with a high degree of uncertainty, the low heat up rate (below 1 K/s) was chosen as the acceptance criterion. If the oxygen starvation period in the experiment is rather long and the maximum temperatures are not reached, the experimentalists will be able to increase the heat up rate following the thermocouples readings.

Another criterion of acceptability became the oxygen starvation conditions duration. The codes give a prediction for the moment when oxygen starvation conditions come *in the assembly*, while in the course of the experiment these conditions are recorded by the OLCT20 device and the sampling system located in a bypass to the off-gas line

(Figure 26), i.e. recorded with a time delay. For the PARAMETER test facility the acceptable minimum calculated period of oxygen starvation was estimated to be 150-200 s. When oxygen starvation conditions is recorded by the device, for instance, for 200 s, then the minimum calculated oxygen starvation period should be increased to 350-400 s.

The third criterion of acceptability was keeping the assembly geometry.

As the first step, the calculations were performed with the air flow rate of 0.8 g/s. This value corresponds to the air flow rate in QUENCH-10 experiment considering the scale factor determined by the ratio of perimeters of elements Zry (or ZrNb1%).

For simulation of PARAMETER-SF4 experiment, the input deck were derived from the post-test calculations of PARAMETER-SF3 considering changes in the boundary conditions. The value of electric energy at the pre-oxidation stage and the duration of plateau were chosen to meet the assigned conditions (1200°C, 300 μm). At the cool down stage decrease of electric power to 5.5 kW was simulated, and this power value was kept at the air ingress stage (Figure 44).

At the pre-oxidation stage the hot spot was predicted at the elevations of 1200-1250 mm (calculations with codes ATHLET-CD and SOCRAT). In the calculations with SCDAP/RELAP/FZK-PSI code one can see some deviation from the temperature profile at the upper end of the heated zone (due to limitations in modeling upper part of bundle), but this does not influence the evaluation of the hottest zone location before flooding onset because it is predicted in the middle part of the assembly heated section. By the end of the air ingress stage the codes predict a hot spot shift downwards: ATHLET-CD – to the elevation of 700 mm, SOCRAT – to the elevation of 1000 mm, SCDAP/RELAP/FZK-PSI – to the elevation of 500 mm (Figures 46 – 49).

On the whole, the calculations indicated that at the air flow rate of 0.8 g/s the oxygen starvation conditions could be probably reached (Figure 46), but the starvation period might be too short (in the calculations with the code ATHLET-CD the starvation period was estimated to be 60 s). The predicted cladding heat up rates are rather high >5 K/s (Figure 45). For the shroud, at the end of air ingress stage the code ATHLET-CD showed the heat up rates of ~30 K/s that leads to its melting predicted before flooding (Figure 50). In calculations with the codes SOCRAT and SCDAP/RELAP/FZK-PSI the shroud heat up rates are less but still rather high (10 K/s).

The main factors, that could influence the heat up rate at the air ingress stage, are thickness of oxide layer on the surface of zirconium components, air flow rate, electrical power, coolant flow rate (at the air ingress stage it is a mixture of air and argon). For

optimization of the scenario a set of variant calculations was performed with different boundary conditions.

Change in the oxide scale thickness profile

At the pre-oxidation stage with the steam flow rate of 3.5 g/s the pronounced axial temperature gradient is observed in the test section of PARAMETER facility that, in its turn, governs a distribution of oxide scale thickness along the heated zone (Figure 51). As a result a thick layer of zirconium oxide is grown on the claddings surface at the elevation of 1250 mm (~300 μm) and a thin layer at the elevations of 500-800 mm (~50-100 μm). In other words, at the elevations where air oxidation is predicted to occur intensively the protective property of the oxide layer is rather poor. Therefore in the calculations the possibility of axial redistribution of the oxide scale thickness was evaluated that could be realized by decrease in the steam flow rate. The calculations were carried out with the steam flow rate of 1 g/s (this flow rate provides no oxygen starvation conditions in the bundle). However the results of calculations showed that with the flow rate of 1g/s the profiling of temperatures and thickness of oxide scales does not be changed substantially (Figure 51).

Variation of argon flow rate

Due to lack of knowledge on air oxidation kinetics, heat source due to air oxidation can be underestimated. In this case there is a high probability of the assembly melting, especially if high temperatures are reached at the elevations between thermocouples locations. The reliable method to avoid the local melting is provision of the conditions when all chemical heat is removed from the assembly. Then the assembly heating-up will be performed only by electric power, and Joule heat is uniformly distributed over the assembly length. Calculations with the air flow rate of 0.5 g/s and argon flow rate of 4 g/s indicate that the heat of oxidation reaction is comparable with convective and radial heat losses. With the air flow rate of 0.33 g/s the oxidation power is slightly less and therefore this case was considered to be more preferable. In the calculations with the air flow rate of 0.33 g/s the assembly heating up at the beginning of the air ingress stage calculates at the rate of 0.5 K/s (Figure 54). Decrease in the heat up rate to 0.2 K/s at temperature above 1800 K is achieved by switching off the electric power. The oxygen starvation conditions come at temperature of 1850 K and last for 1500 s. Sensitivity studies showed that the heat-up rate and duration of oxygen starvation conditions depend weakly on the oxide scale thickness (Figures 52 – 55). This scenario seemed to be acceptable but performed starting-up and adjustment with the argon flow rate of 4 g/s revealed that pressure in the assembly increases to ~0.7 MPa, and at the locations of the oxygen measurement

OLCT20 device and of the hydrogen measurement system SOV-3 (see Figure 26) the pressure is out of their operation range.

Variation of air flow rate

So, a single variable parameter that governs substantially the duration of starvation period is the air flow rate. At the air flow rate of 0.8 g/s oxygen starvation would probably be reached but the time period of starvation would probably be quite short to record by the oxygen measurement system in the on-line mode. The flow rate of 0.25 g/s results in starvation front propagation too far down (Figures 56 – 58). Therefore for final calculations for justification of the experiment scenario the air flow rate of 0.5 g/s was chosen. Table 3 presents the scenario for the final calculations proposed by Jon Birchley from PSI and supported by other participants of the pre-test calculations.

Table 3

Pre-test scenario of PARAMETER-SF4 experiment

No.	Stage	Main parameters			
		FA temperature, K	Medium	Heating rate, K/c	Time, s
1	Joule heating up of FA in argon flow	~300-670	Argon at temperature 720 K (argon flowrate - 2 g/s)		0-1500
2	Joule heating up of FA in the flow of steam-argon mixture	670→770	Steam-argon mixture (argon/steam flowrate at inlet - 2/3.5 g/s at temperature 720/770 K)		1500-3500
3	FA heating up to 1470 K (transient phase I)	770→1470	Steam-argon mixture (argon/steam flowrate at inlet - 2/3.5 g/s at temperature 720/770 K)	0.3 (beginning), 0.1 (end)	3500-8000
4	FA pre-oxidation	~1470	Steam-argon mixture (argon/steam flowrate at inlet - 2/3.5 g/s at temperature 720/770 K)		8000-14000
5	FA cool down to 1170 K (transient phase II)	1470→1170	Steam-argon mixture (argon/steam flowrate at inlet - 2/3.5 g/s at temperature 720/770 K)		14000-16000

6	Air ingress	1170→2020	Air-argon mixture (argon/air flowrate at inlet - 2/0.5 g/s at temperature 720/300 K)	~0.3	As soon as FA will reach temperature of 2020K
7	FA bottom flooding (as soon as FA will reach Tmax=2020 K)	Up to saturation	Water (flowrate of 80 g/s at temperature ~300 K)		As soon as saturation temperature will be reached

Final pre-test calculations of SF4 experiment

Boundary conditions for the pre-test calculations are presented in Figures 59 – 67. It should be noted that SF4 experiment was performed according to these conditions at least at the pre-heating, pre-oxidation, cooling down and air ingress stages. For comparison the experimental data are plotted as well.

Steam flow rate at the pre-heating, pre-oxidation, cooling down stages is 3.5 g/s, both in calculations and in the experiment. Beginning of steam injection and its switching off in the experiment are in good agreement with the boundary conditions for the pre-test calculations. Argon flow rate throughout the experiment is 2 g/s, both in calculations and in the experiment.

Electric power at the pre-heating and pre-oxidation stages was tuned by users themselves to oxidize the assembly at the hottest elevation at temperature of 1200ºC and to grow oxide scale with the thickness of 300 μm in calculations.

At the cool down stage the scenario provided the decrease of electric power to 5.5 kW; in calculations with the codes MAAP4, PARAM-TG the electric power was tuned to cool the bundle down to temperature of 900ºC exactly.

The codes predict the hottest zone at the elevation of 1250 mm, as in the experiment or somewhat lower (see Figure 28). At the pre-oxidation stage there are deviations from temperature 1200ºC in calculated temperatures, and this leads to differences in thickness of oxide scale (Figures 27, 28). Figure 29 gives a distribution of oxide scale thickness on fuel rod cladding surfaces by the end of pre-oxidation (t=13950 s). For the assembly upper part the differences are substantial, but for the lower elevations of 400-800 mm, where the hottest zone is predicted by the codes before flood onset, the calculated thicknesses are close, except for the data calculated with ICARE code. Therefore the effect of pre-oxidation degree on the hot spot shift during air oxidation could be recognized hardly by the given calculations.

By the end of pre-oxidation stage most of the codes predict similar hydrogen mass of 21 – 22.5 g (Figure 40), close to measured one in the experiment (21 g). Differences in

hydrogen masses, calculated with the codes ATHLET-CD and ICARE, are caused by the above-mentioned deviations of calculated temperatures from the assigned value (1200ºC).

Before the beginning of air injection the maximum calculated temperatures in the assembly are different (vary from 900ºC to ~1000ºC – Figure 30), because the scenario provided a definite value of electric power at this stage, but not its varying for reaching the required temperature of 900ºC. In the experiment, the temperature of 900ºC was reached exactly at the assigned time interval but with lower electric power – 4 kW (Figure 31).

At the air ingress stage the pronounced hot spot shift was observed. Figure 32 gives the temperature profile measured for various time moments. By the beginning of the stage (16000 s) the hottest zone was at the elevation of 1250 mm, in 700 s (16700 s) the hot spot shifted down to the elevation of 1100 mm, in 1200 s (17200 s) – to the elevation of 700 mm. Before the flooding onset, the hottest zone was at the elevation of 500 mm (Figure 33).

The code SOCRAT with the adapted steam oxidation model predicts a rather wide hot spot from 700 to 1200 mm, the code MAAP4 gives a location of the hot spot at the elevation of 800 mm. The predictions of the codes ICARE (550 mm), ATHLET-CD (500 mm) and RELAP/IRS (500 mm) turned out to be in good agreement with the measured data. It should be noted that temperatures before flooding onset, calculated with the code ATHLET-CD, are in good agreement with measured ones along the whole heated length (see Figure 33).

Due to differences in predictions of the hottest zone location, the data to be compared at air ingress phase are maximum temperature evolution (see Figure 35). Up to temperature of ~1200ºC most of the codes calculate close heat up of ~0.5 K/s. Above this temperature the codes SOCRAT, ATHLET-CD, MAAP4 and PARAM-TG predict quite slow temperature escalation.

Duration of oxygen starvation conditions are presented in Table 4. As seen from the Table, the codes ATHLET-CD, MAAP4 predict a short but acceptable duration, however this time can be insufficient to recognize these conditions in the on-line mode. Calculations with the code RELAP/IRS look more acceptable because they meet all the requirements: both quite low heat up rates and long-term starvation conditions (600 s).

In the experiment, up to 1200ºC the rate of maximum temperature rise was slightly lower than calculated one (about 0.4 K/s), probably due to some differences in electric power (see Figure 36). Above temperature of 1200ºC, the rate was within the calculated range (about 1.4 K/s).

Table 4

Calculated parameters of oxygen starvation conditions

Computer code	Time when starvation condition come, s / Temperature, °C	Duration of starvation period, s
ATHLET-CD	16640 / 1350	200
MAAP4	16721 / 1500	160
SCDAP/RELAP/FZK-PSI	16750 / 1550	600
SOCRAT	16560 / 1600	600
PARAM-TG	16560 / 1450	110

At the flooding stage one can see significant discrepancies between predicted and observed behaviours. In the experiment the electric power was switched off when thermocouples at the elevation of 500 mm read the temperature about 1750°C. In ~20 s the system of water injection into the assembly was switched on. The air injection was stopped in ~100 s. Between the water injection onset and the moment of switching off the air supply system the thermocouples read a slow cooling down of the elevations of 0-200 mm, temperature ran away at the elevation of 400 mm, delayed temperature escalation at the elevations of 500-700 mm, slow cooling down of the assembly upper part at the elevations of 900-1500 mm (Figures 37 – 39).

At the elevation of 400 mm the low-temperature thermocouples were used, therefore there is no possibility to observe the temperature evolution at this elevation above 1400ºC. At the elevations of 500-1500 mm the high-temperature thermocouples were used, however at the flooding stage most of them failed. Material study revealed extensive melting of the assembly over the heated part.

Some codes (ICARE, MAAP4) demonstrate a quick cooling down of the assembly without substantial temperature escalation at the flooding stage of (Figure 35). The code SOCRAT predicts dissolution of oxide scale on surface of the shroud and periphery rods under oxygen starvation conditions, strong oxidation of the uncovered metal with steam at the flooding stage, strong heat release due to oxidation reaction, heating up and melting. Nevertheless, the code predicts that in ~50 s the assembly cooling is started. Slight metallic melting at the elevation of 400 mm (100 mm below the hottest zone) is predicted with RELAP/IRS code (Figure 42), but intact geometry is maintained. The code ATHLET-CD demonstrates a short-term cladding temperatures escalation by 100 K at the elevation of 400 mm, but temperatures are not too high to melt. At the same time the code predicts higher (in comparison with the temperatures of claddings in the internal ring) shroud temperatures (due to larger available oxygen in the channel), hence the melting point are

reached on the shroud before flooding onset (see Figures 34 and 43). In the experiment, at the flooding stage the assembly continued heating up not only in the lower part, as it can be expected from the pre-test calculations, but also in the upper part (see Figures 37 – 39). Evidently, the post-test calculations with exact experimental conditions are needed for interpretation of the experiment at the flooding stage.

The calculated with various codes hydrogen generation at the flooding stages directly connected to the temperatures predicted. In the calculations where melting point of metal zirconium is reached (ATHLET-CD, RELAP/IRS), a small hydrogen mass up to 5 g is predicted at the flooding stage (Figure 41). The code SOCRAT gives extra hydrogen mass of ~35 g due to yield of melt on the surface of zirconium components and its oxidation. In the experiment at the flooding stage ~86 g of hydrogen was released due to strong melting of the assembly and oxidation of the melt formed.

3.2. Results of PARAMETER-SF4 experiment

The PARAMETER-SF4 experiment was performed at the test facility PARAMETER in FSUE SRI SIA "LUCH" on 21 July, 2009, with analytical support of the teams executing the pre-test calculations (see Section 3.1), the complete information on the results is presented in [8].

In the PARAMETER-SF4 experiment, the stage of severe LOCA with a core drying out, its heating-up to $\sim 1750°C$ in the air flow and water flooding from bottom was simulated.

The PARAMETER-SF4 experiment was conducted to study the behaviour of 19-rods model FA of VVER-1000 under simulated conditions of severe accident with air ingress, including:

- Study of temperature behaviour of the assembly under conditions of air ingress and subsequent bottom flooding;
- Post-test study of oxidation degree of the structural components of the model FA of VVER-1000 and of structural-phase changes in claddings of model FA;
- Study of the time history of oxygen consumption and hydrogen generation.

The process systems of PARAMETER test facility were prepared for the experiment according to the functional diagram (see Figure 26).

The experiment consisted of six stages:

- *preparation stage* (0 – 4506 s) – stabilization of the assigned flow rates of argon ($G_{Ar\ in} \approx 2$ g/s) and steam ($G_{st\ in} \approx 3.5$ g/s) at FA temperature (T_{FA}) $\approx 500°C$, check of state of the assembly and process systems;

- *assembly heating-up to temperature of $\approx 1200°C$* (4506 – 8000 s);

- *pre-oxidation* (8000 – 13886 s) – FA holdup at temperature of $\approx 1200^{\circ}$C in the hottest zone for $\sim$ 6000 s. The maximum temperature deviations in the hottest zone (1250 mm) – $\sim \pm 50^{\circ}$C;

- *the assembly cool down to temperature* $T_{FA} \approx 900^{\circ}$C (from 13886 to 16355 s);

- *air ingress into FA* (16035 – 17511 s) with subsequent (from 16355 s to 17434 s) assembly heating-up to FA maximum temperature of $\sim$ 1740°C in the hottest zone;

- *flooding* (17434 – 17908 s) – flooding of the bundle from bottom with water at the flow rate of Gbf $\approx$ 80 g/s.

Figures 68 and 69 present the results of measurement of the main experimental parameters: flow rate and temperature of argon ($G_{arg\ in}$, $T_{in.Ar}$) and steam ($G_{st\ in}$, $T_{in.st.}$) at the test section inlet; gas mixture flow rate G(R4) at outlet to special ventilation (Figure 68); electric parameters (Figure 69): power (P1), current (I1), voltage (U1).

Figure70 provides the thermocouples readings arranged over the length of fuel rod claddings throughout the experiment.

Figure 71 presents the results of measurement of volumetric concentration of oxygen by the OLCT20 oxygen measurement device and in sampling tanks, and the air flow rate at the test section inlet G(R6). Indications of OLCT20 are given in the on-line mode. In comparison of the indications of the continuous (OLCT20) and discrete (sampling) measurement system with calculated data the transport time should be considered.

Figure 72 gives the results of measurement of volumetric concentration of hydrogen by the hydrogen measurement system (SOV-3) and in sampling tanks, and also the flooding water flow rate G(R2).

Analysis of the results of hydrogen measurement by SOV-3 system showed that in the experiment at the pre-oxidation stage the hydrogen was generated in the amount of $\sim$ 21 g (Figure 73), and at the flooding stage of – $\sim$ 86 g. Maximum rate of hydrogen generation at the flooding stage was $\sim$ 0.6 g/s (see Figure 73).

3.3. Results of material studies of the SF4 model assembly

After completion of the PARAMETER-SF4 experiment the model assembly was encapsulated and sectioned, and the preliminary material studies of the tested model FA were performed, the results are presented in [8].

Encapsulation of the model FA was made inside the test section (before its withdrawal from the test section) to keep the bundle integrity. FA encapsulation procedure included resin supply in lower part of the bundle, that is bottom-top filling. Following this

procedure, the bundle was filled up to the elevations of ~ 250 …300 mm, and after that resin level rise stopped evidently due to flow path blockage at lower elevation. To complete the bundle encapsulation, resin was injected in the upper part.

After the compound hardened, the assembly was removed from the test section and cut over into fragments and slabs.

The preliminary analysis was made for the four cross-sections taken from the assembly upper and lower parts. The analysis of the cross-sections indicated the following:

At the elevation Z = 130 mm (top view) the assembly has no any visible damages practically (in the given section all fuel rod claddings and periphery rods kept their integrity, Figures 74, 75). There are cracks in some pellets of uranium dioxide. There are no fuel fragments in some pellets. However, crumbling of the pellets occurred probably in the course of the assembly sectioning or preparing of slabs.

The oxide scale on fuel rod claddings is thin and well connected with metal; the measured thickness of zirconium oxide varies within $4 - 9$ μm.

At the elevation Z = 260 mm the following was revealed:

- presence of large amount of melt in the space between rods that dissolved the fuel rod claddings (Figures 76, 77). EDX analysis of the melt indicates that it is metallic and have (U,Zr,O) composition (Figure 38). Formation of cracks in the solidified melt is a sign of its brittleness due to high content of the dissolved oxygen;

- oxidation of zirconium structural components and melt;

- presence of melt in fuel-clad gaps in some fuel rods;

- interaction of some claddings of fuel rod with UO_2 pellets.

Study of fuel rod cross-sections shows the sequence of phases typical for $Zr - UO_2$ interaction and external oxidation.

At the elevation Z = 300 mm (bottom view) practically all structural components of the model FA (including heaters) are degraded. One can see remains of two fuel rods only, Figure 78. The melt is porous. EDX analysis indicates that the melt contained not only uranium, zirconium, oxygen, but significant amount of tantalum as well (Figure 79).

At the elevation Z = 1200 mm (bottom view) the state of the assembly is characterized by complete absence of zirconium structural components (FA shroud, fuel rod claddings, spacer grids, thermocouples sheath) that is indicative of considerable exceeding the zirconium melting point at this region (Figure 80) though molten pool are absent. Remained fuel stacks (12 out of 18) are kept only due to tantalum heaters being in the given case the skeleton for the assembly. In some regions of the given section the

remains of oxide scales of fuel rod claddings and shroud are revealed (Figures 80, 81). Diameter of fuel pellets is less than original one noticeably due to dissolution of uranium dioxide by the melted zirconium that evidently relocated down on the fuel column surfaces (Figure 81). The traces of melt were found in the fuel-heater gap, the diameter of some heaters is less than original one as well.

Conclusions

1. Two 19-rods fuel bundles to be identical to VVER-1000 with respect to materials and geometry were tested under severe accident conditions including top flooding of the bundle of overheated to ~1600°C (PARAMETER-SF3 test) and bottom flooding of the bundle overheated to ~1750°C in air flow (PARAMETER-SF4 test).

2. Performed metallic layers thicknesses measurement allow estimation of SF2 и SF3 bundle oxidation degrees as well as hydrogen mass on the basis of zirconium amount that reacted with oxygen. Hydrogen masses estimated through measured layers thicknesses agree with directly measured total hydrogen release.

3. Results of the post-test numerical analysis and analytical studies of PARAMETER-SF2 and PARAMETER-SF3 experiments performed under ISTC Project No.3690 indicated that, in spite of complicated character of these experiments, the sets of experimental data are self-consistent and can be used for verification of computer codes, their thermohydraulic and physical-chemical models under severe accidents conditions including the flooding stage.

4. Performed studies indicated that in SF2 and SF3 test pronounced cladding spallation was observed, but no hydrogen release during quenching. In the same time, in SF1 test the significant hydrogen release was observed during quenching of partially molten bundle. Thus, the PARAMETER tests series demonstrated strong effect of melt formation on hydrogen release, and it should be taken into account in severe accident management strategy.

5. Conducted PARAMETER-SF4 test indicated quite good codes capacity to predict the bundle temperature evolution under conditions with low air flow rate. In the same time, comparing calculated and measured data set in details one can see the air oxidation model deficiencies that needs to be improved. The measured data improve our knowledge and can be used for verification of the codes that treat overheated core degradation under air ingress conditions.

References

1. Analysis of material studies of WWER-1000 model assembly tested at the PARAMETER-SF2 experiment under the conditions of severe accident with top and bottom flooding. Report on scientific work under ISTC Project No.3690, FSUE SRI SIA "LUCH", pp 45, 2008.

2. Protocol on the results of PARAMETER-SF2 experiment, pp 51, 2007.

3. Protocol on the results of PARAMETER-SF3 experiment, pp 45, 2008.

4. Minutes of a Task Group Meeting on Pre-Test Calculational Support for the PARAMETER-SF4 Experiment, WP14-1, Forschungszentrum Karlsruhe, 1st September 2008.

5. Emilie BEUZET, Jean-Sylvestre LAMY, PARAMETER-SF4 pre-test calculation with MAAP4.07, ISTC status meeting, Podolsk, 29 -30 July 2009.

6. Ch. Bals, K. Trambauer, Final PARAMETER SF4 pre-test calculation with ATHLET-CD, ISTC status meeting, Podolsk, 29 -30 July 2009.

7. Jon Birchley, PARAMETER SF4 final pre-test calculation, ISTC status meeting, Podolsk, 29 -30 July 2009.

8. Protocol on the results of PARAMETER-SF4 experiment, pp 55, 2009.

FIGURES
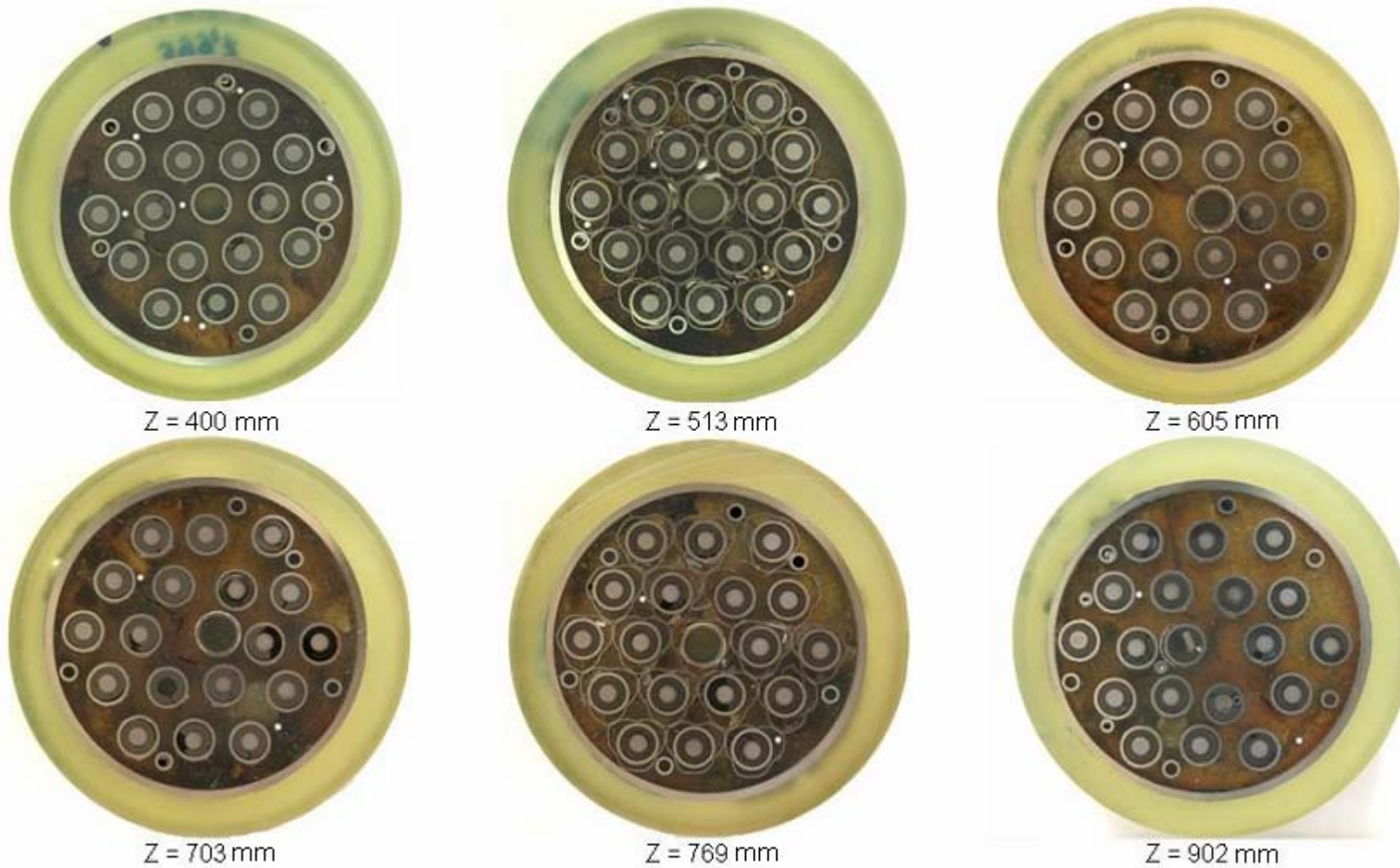
Figure 1. Photos of the assembly cross-sections slabs within the elevations of Z ~ 400…900 mm.
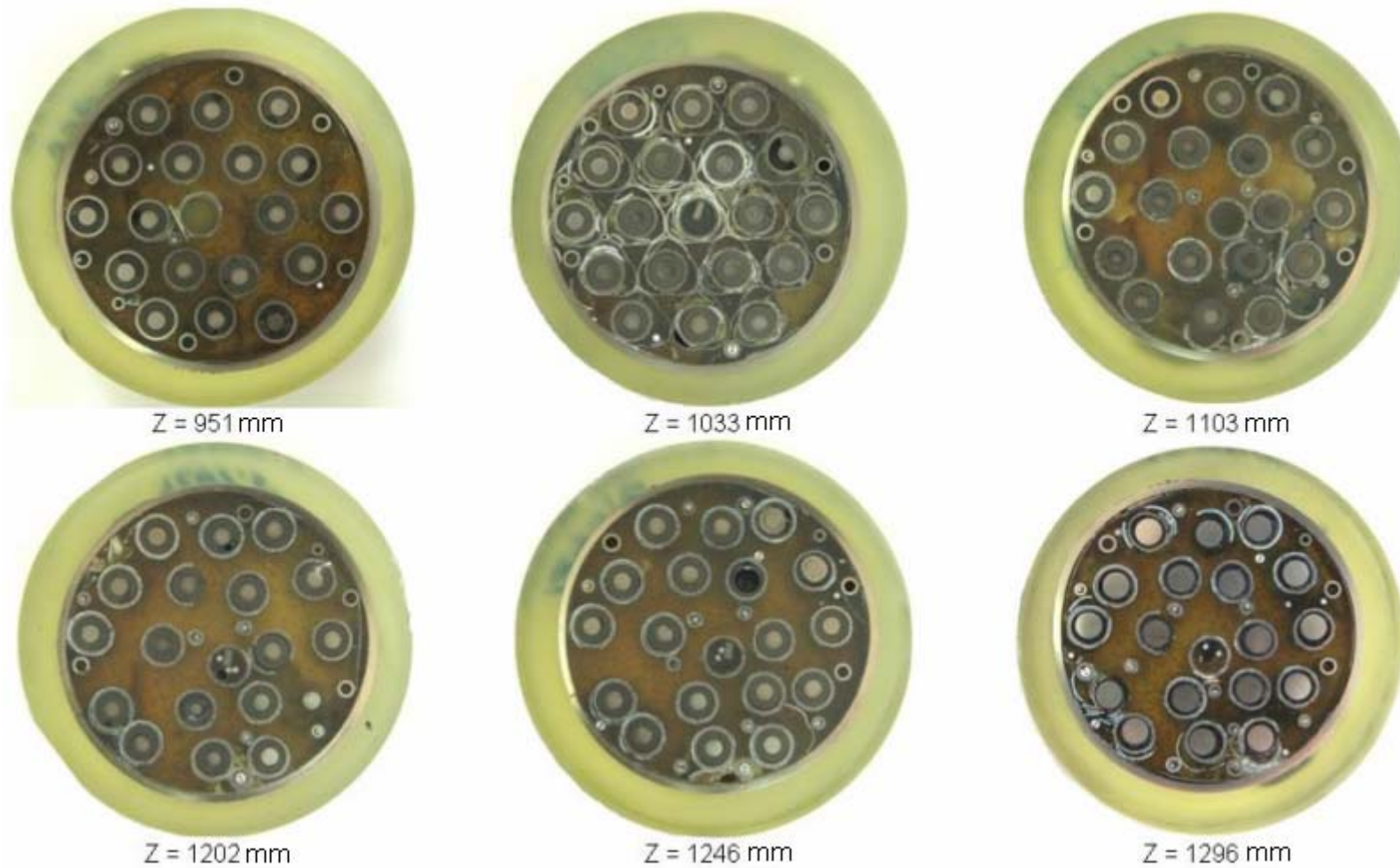
Figure 2. Photos of the assembly cross-sections slabs within the elevations of Z ~ 950…1300 mm.
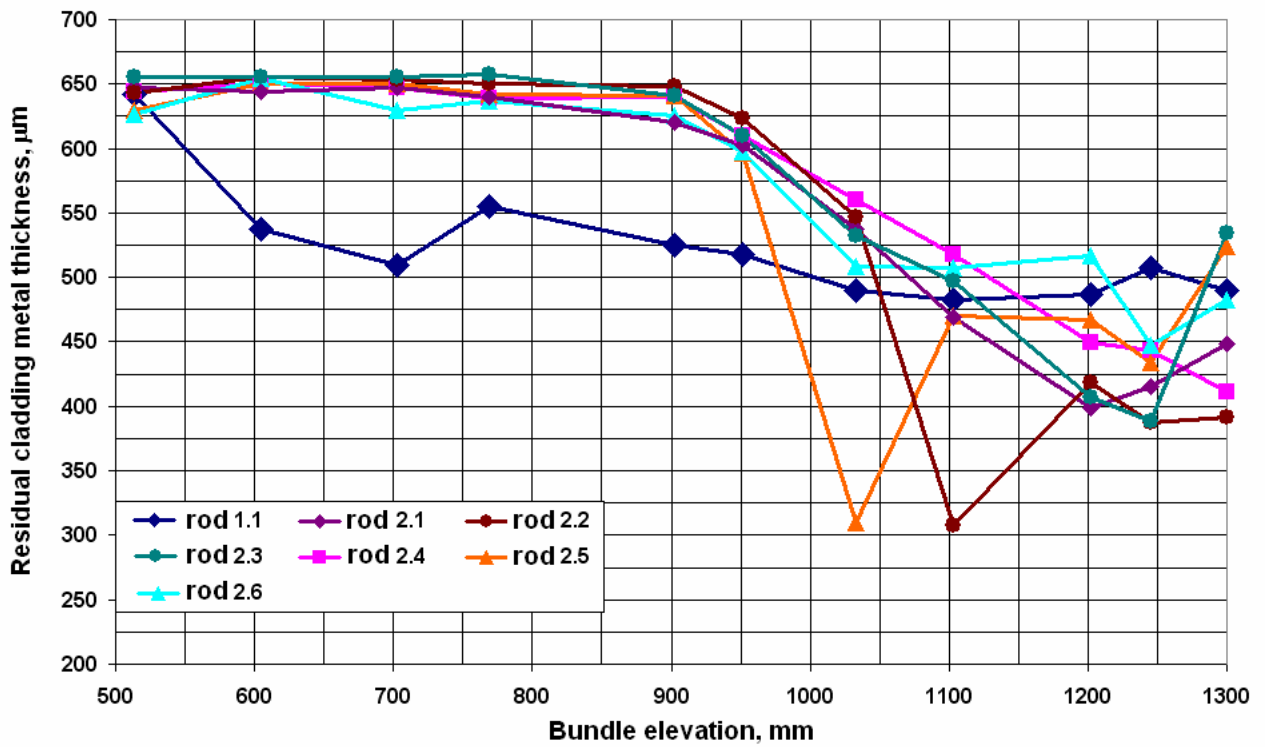
Figure 3. Distribution of thickness of the remained metal part of claddings of fuel rods in the second row over heated zone.
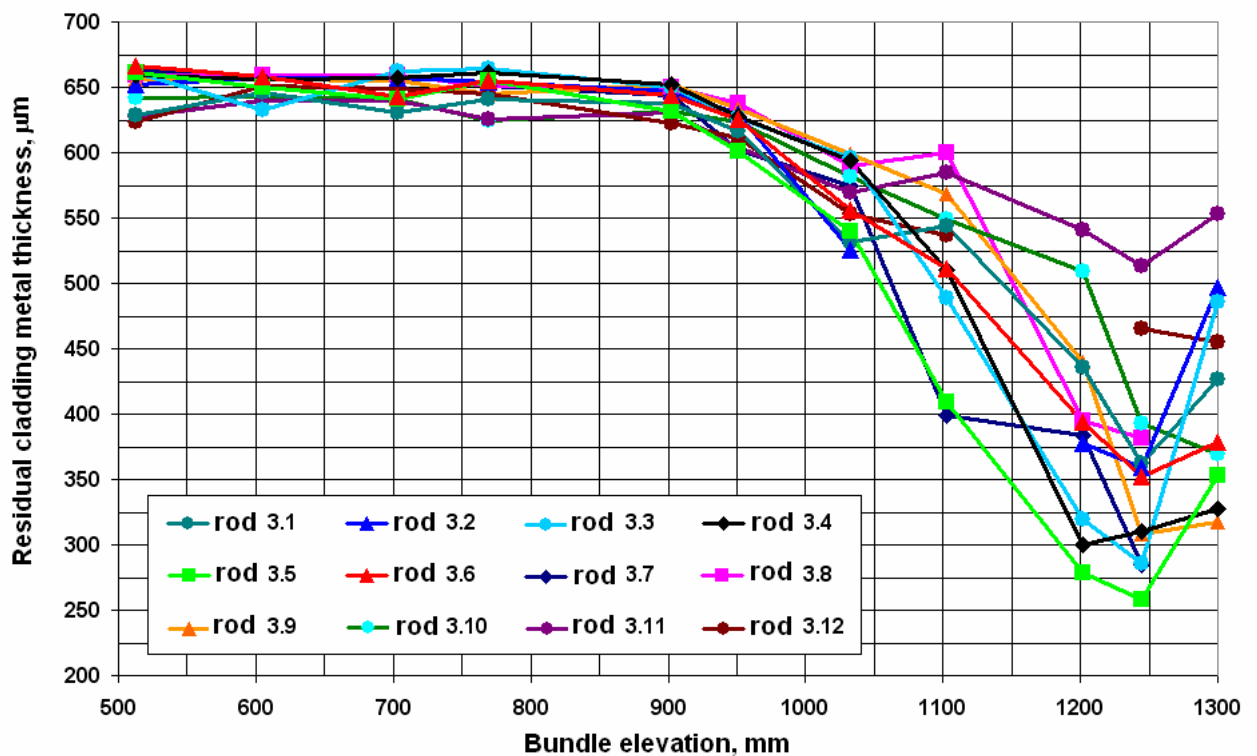
Figure 4. Distribution of thickness of the remained metal part of claddings of fuel rods in the third row over heated zone.
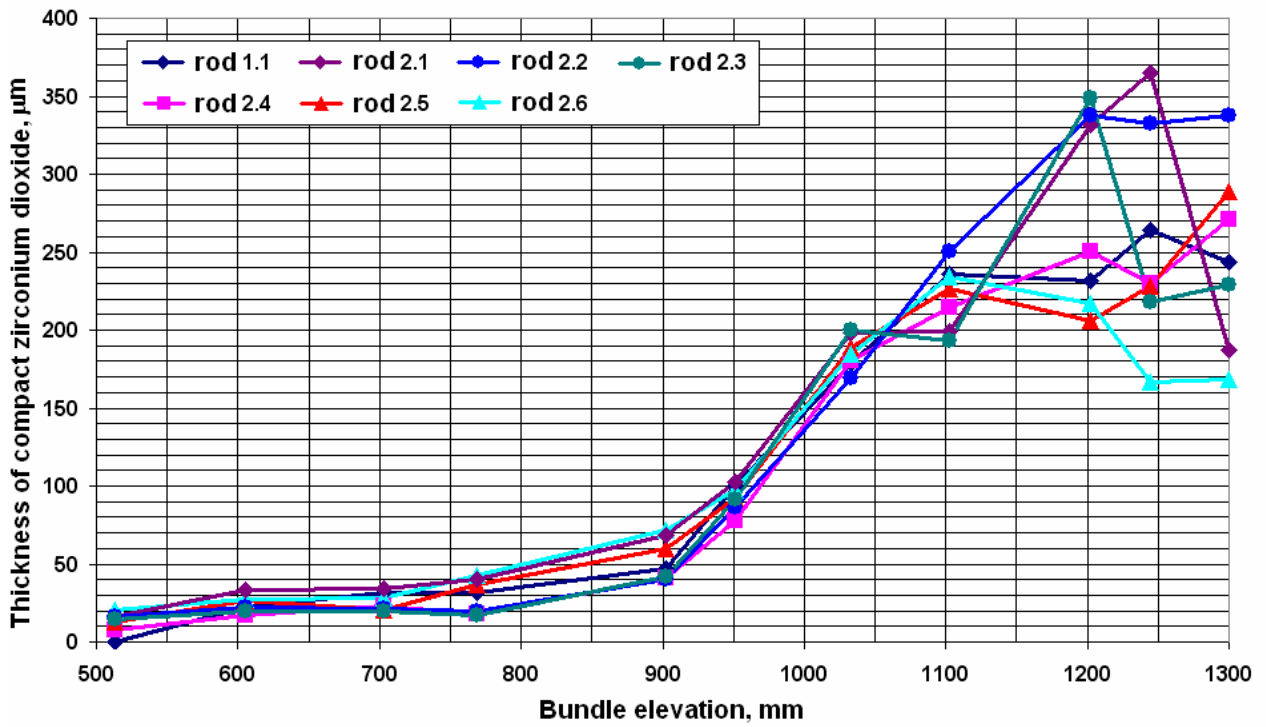
Figure 5. Distribution of thickness of the compact ZrO_2 layer on external surface of fuel rods in the second row over heated zone.
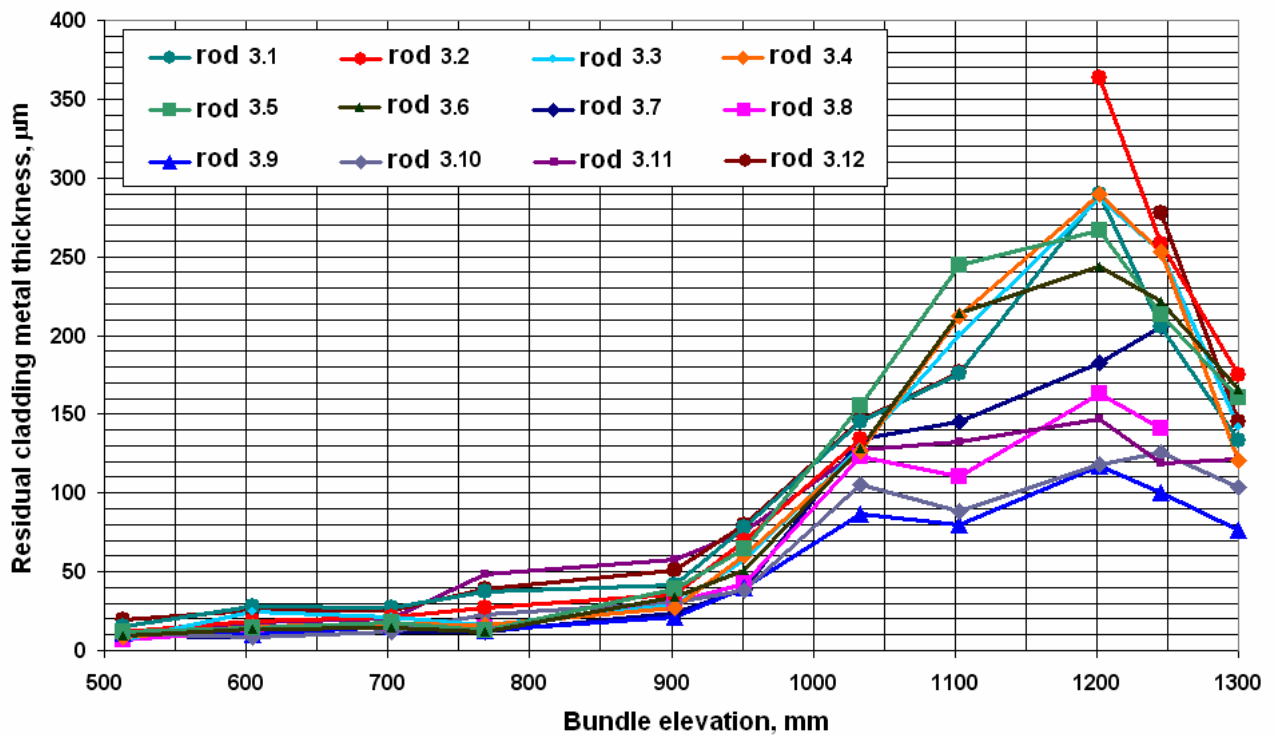
Figure 6. Distribution of thickness of the compact ZrO_2 layer on external surface of fuel rods in the third row over heated zone.
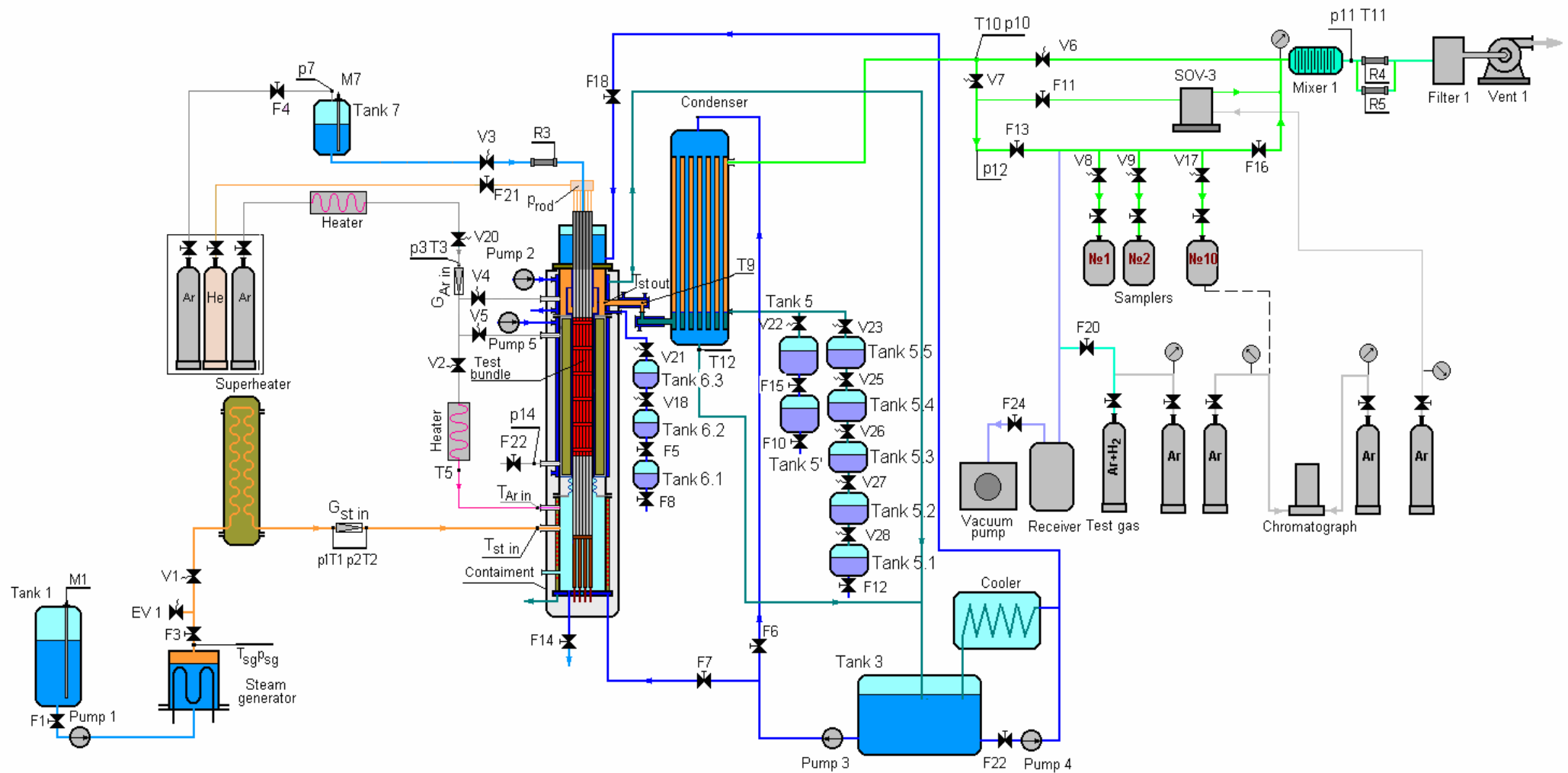
Figure 7. Flow diagram of the PARAMETER test facility in PARAMETER-SF3 experiment.
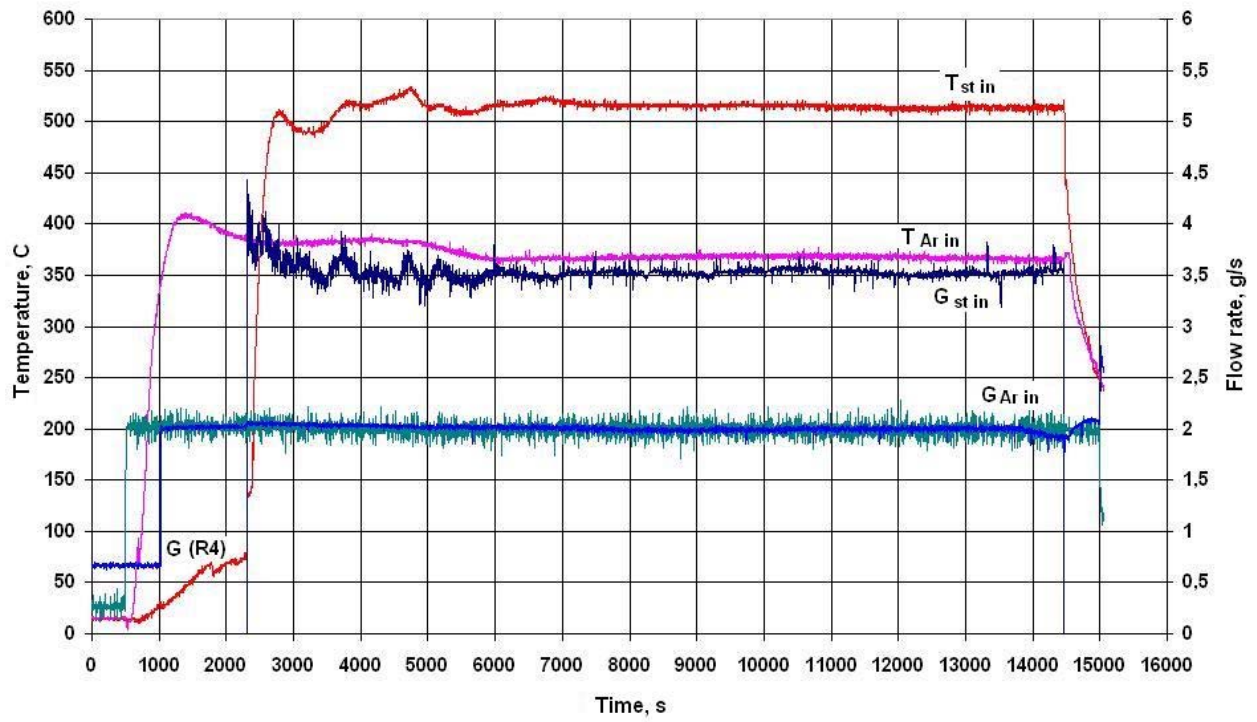
Figure 8. Steam (G $_{st\ in}$, T $_{st\ in}$) and argon (G $_{Ar\ in}$, T $_{Ar\ in.}$) parameters at the inlet to the test section and gas mixture flow rate G(R4) at the outlet to the special ventilation.
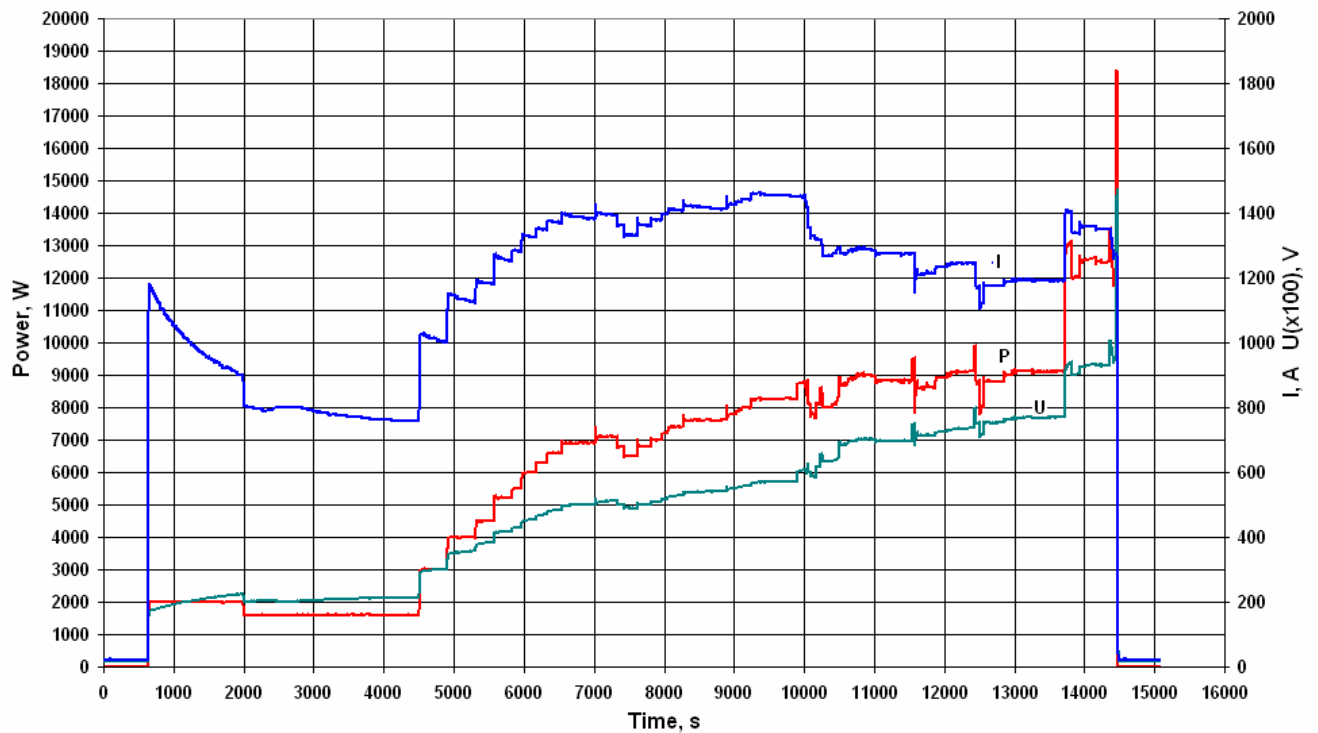
Figure 9. Power supply.

38
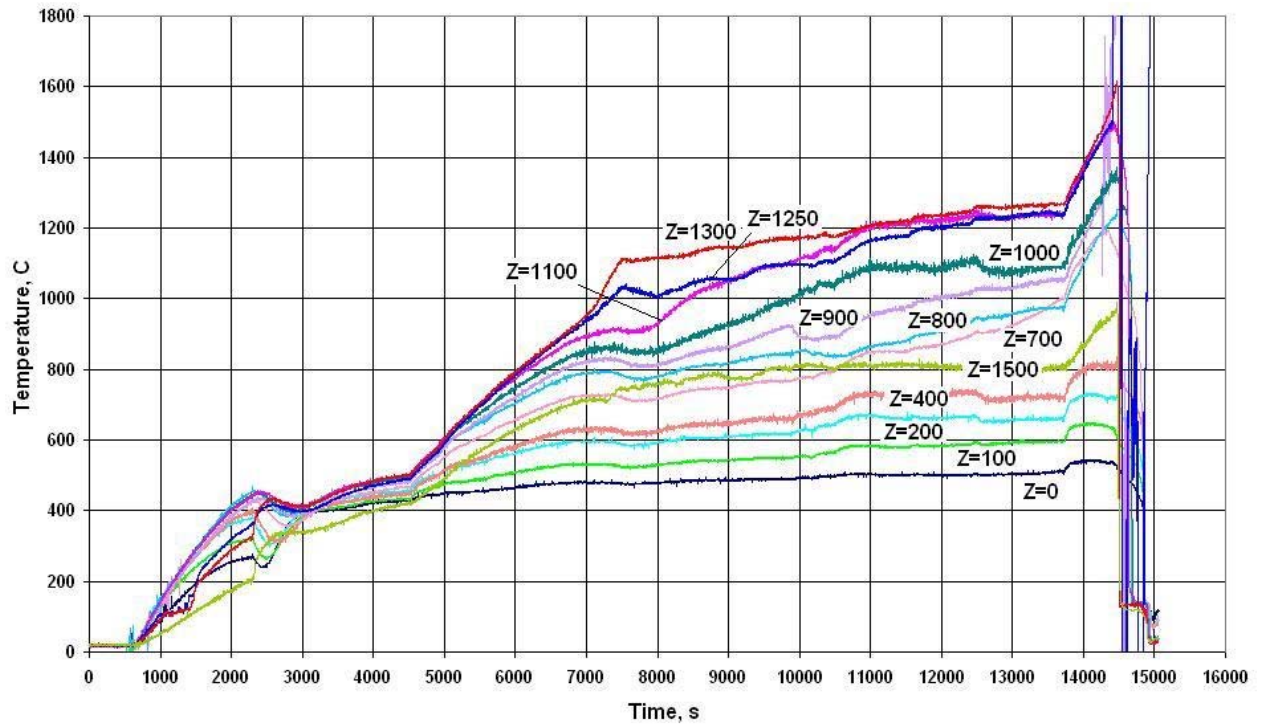
Figure 10. Readings of thermocouples on fuel rod claddings at different elevations.
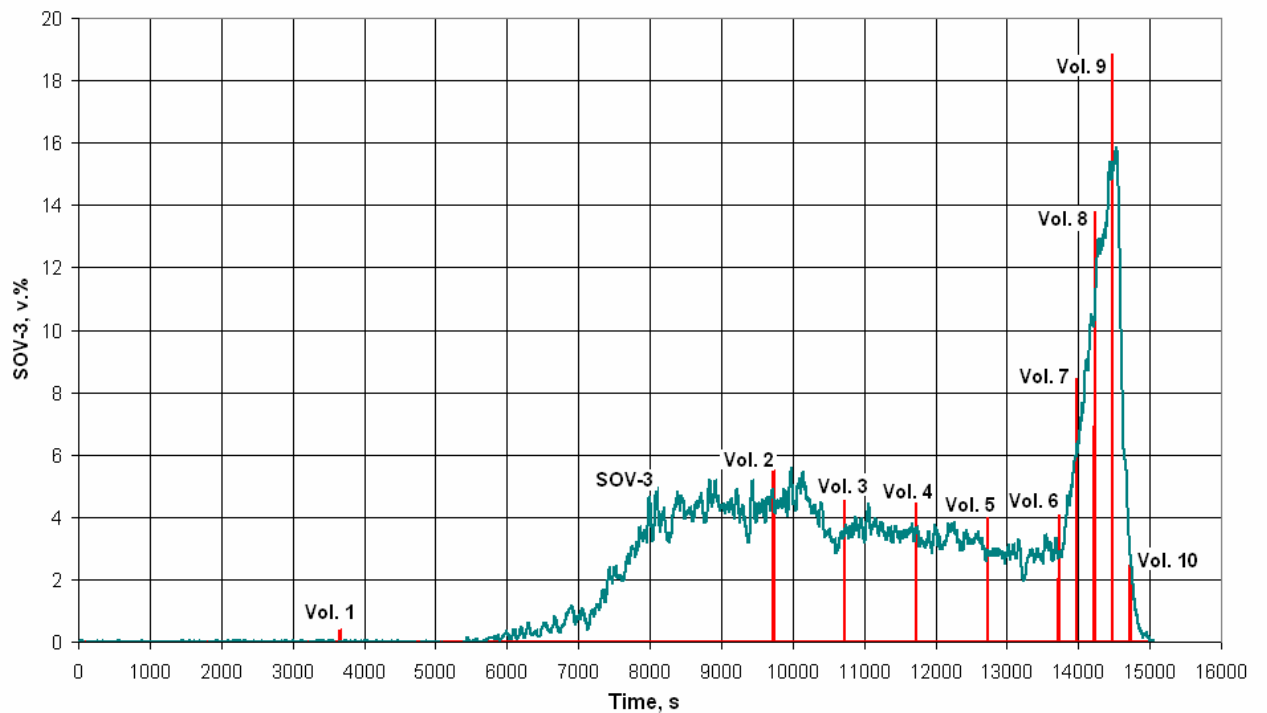
Figure 11. Volumetric hydrogen concentration measured by continuous (SOV-3) and discrete (Vol.) hydrogen monitoring systems.
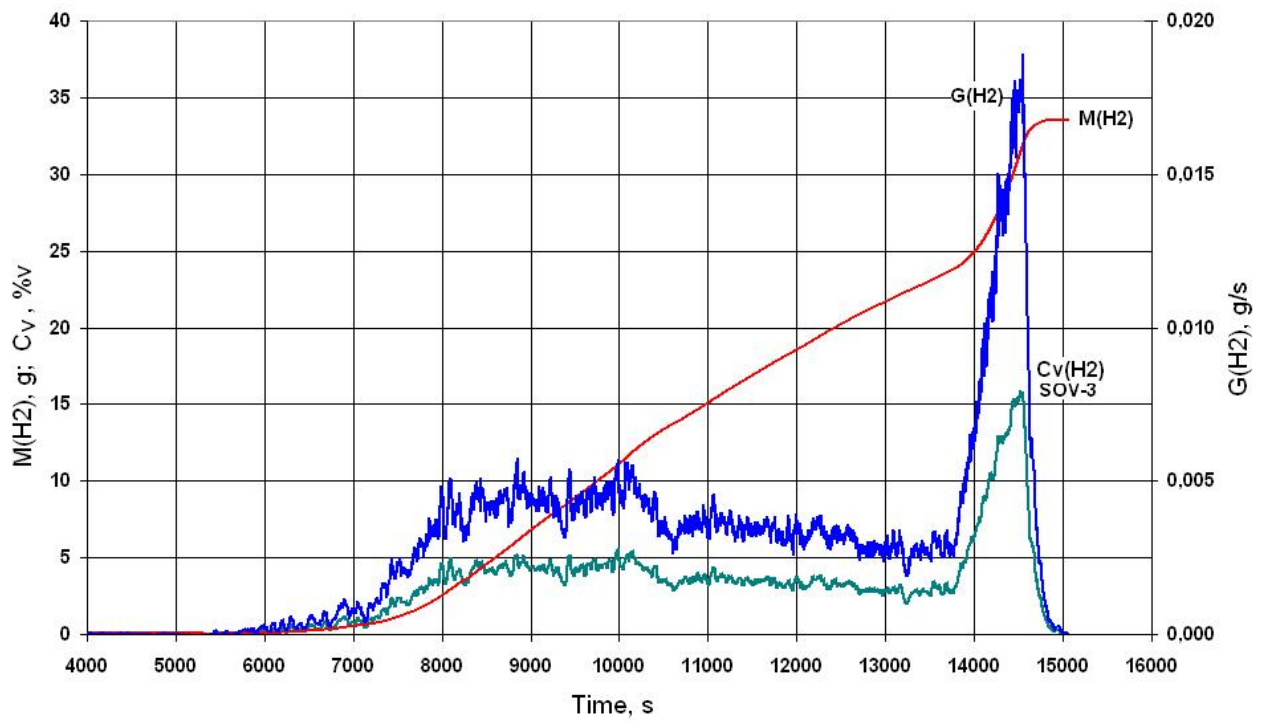
Figure 12. Released hydrogen mass and generation rate.

500 mm

600 mm

700 mm

800 mm

900 mm

1000 mm

Figure 13. Photos of the assembly cross-sections within the range of Z ~ 500…1000 mm elevations.

1100 mm

1200 mm

1250 mm

1300 mm

1400 mm

1500 mm

Figure 14. Photos of the assembly cross-sections slabs within the range of Z ~ 1100…1500 mm elevations.
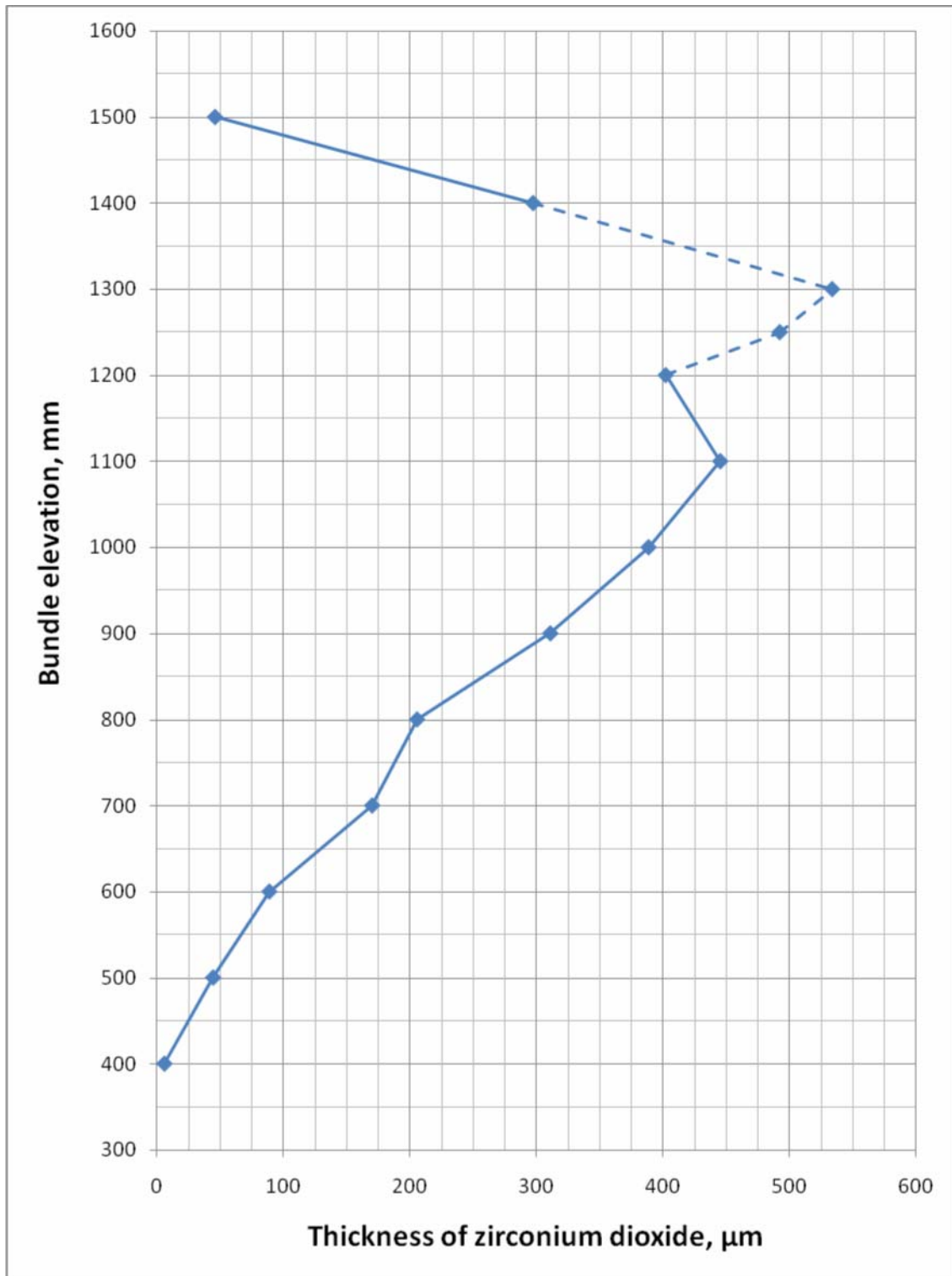
Figure 15. Distribution of the averaged thickness of calculated oxide scale on cladding surfaces over SF3 assembly length.
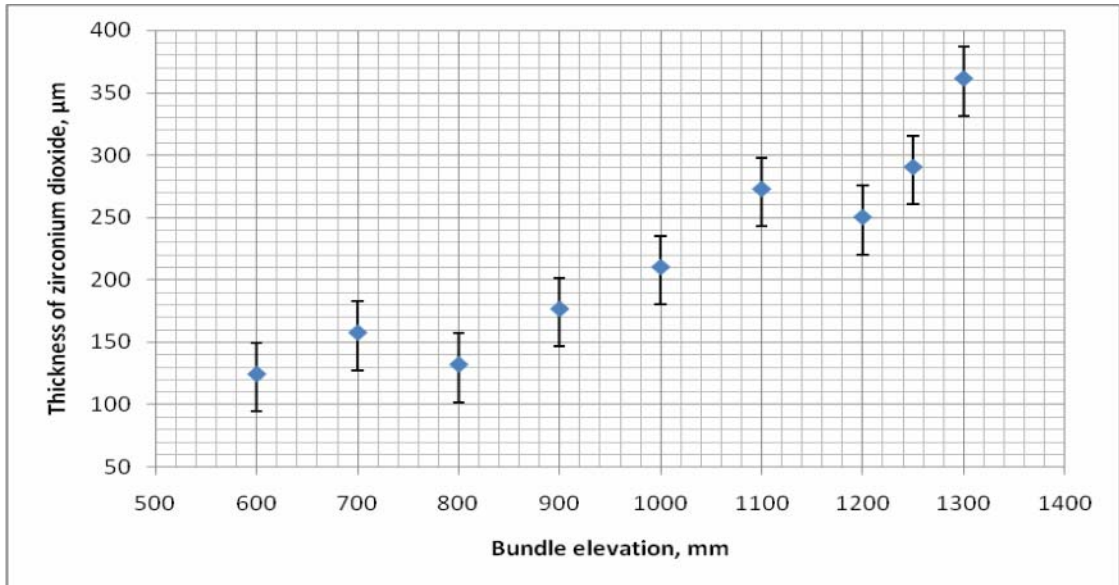
Figure 16. Distribution of the calculated ZrO$_2$ thickness on internal surfaces of the shroud (minimum and maximum values corresponds to minimum and maximum shroud wall thickness measured) over SF3 assembly length.

Further on, in Figures 17 – 81 the abbreviations are given according to the list:

Computer code	Designation in the legend in graphs
SOCRAT	SOCRAT
ICARE/CATHARE	ICARE
RELAP/SCDAPSIM MOD3.2	RELAP
PARAM-TG	PARAM-TG
ATHLET-CD	ATHLET-CD
MAAP4	MAAP4
SCDAP/RELAP/FZK-PSI	RELAP/IRS
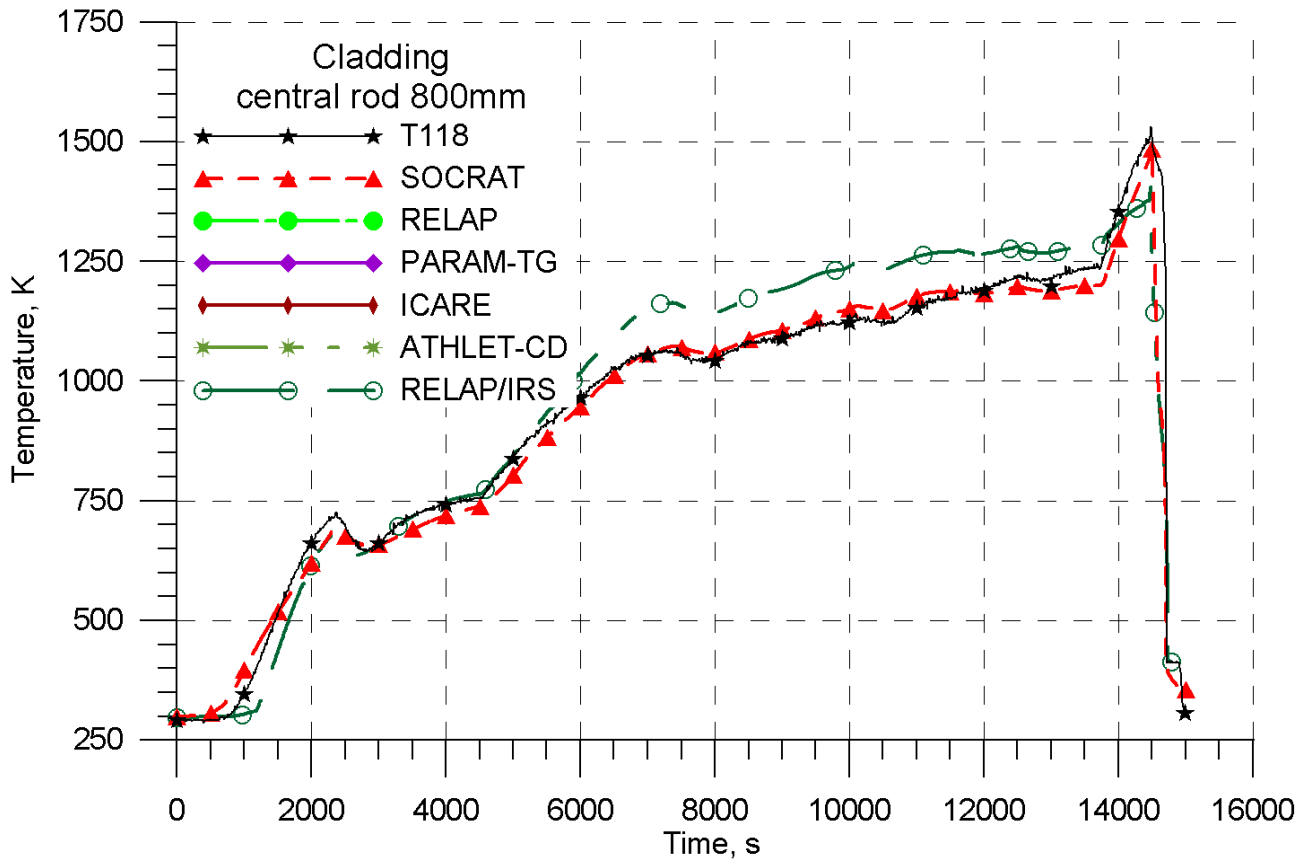
Figure 17. Cladding temperature of the central fuel rod at elevation 800 mm.
PARAMETER-SF3 experiment.
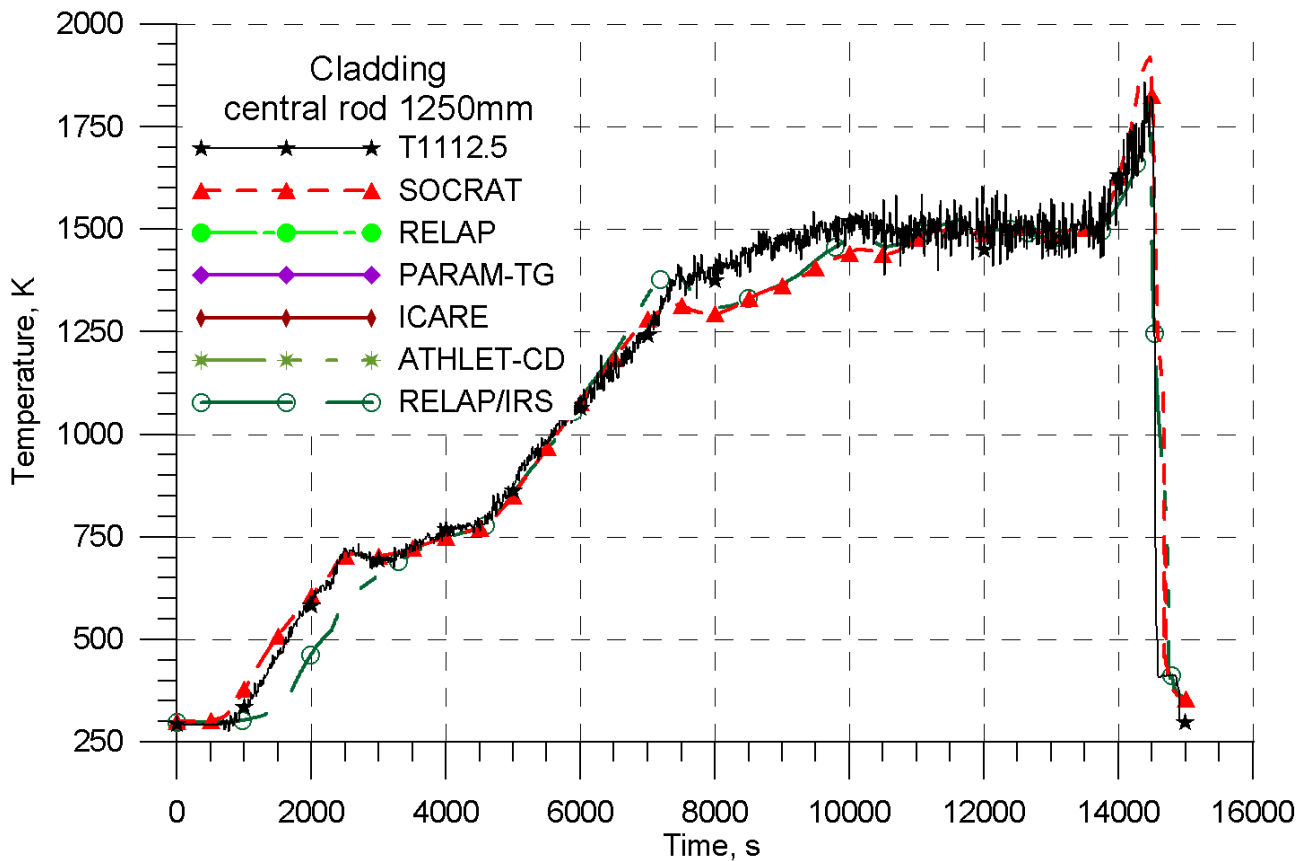
Figure 18. Cladding temperature of the central fuel rod at elevation 1250 mm.
PARAMETER-SF3 experiment.
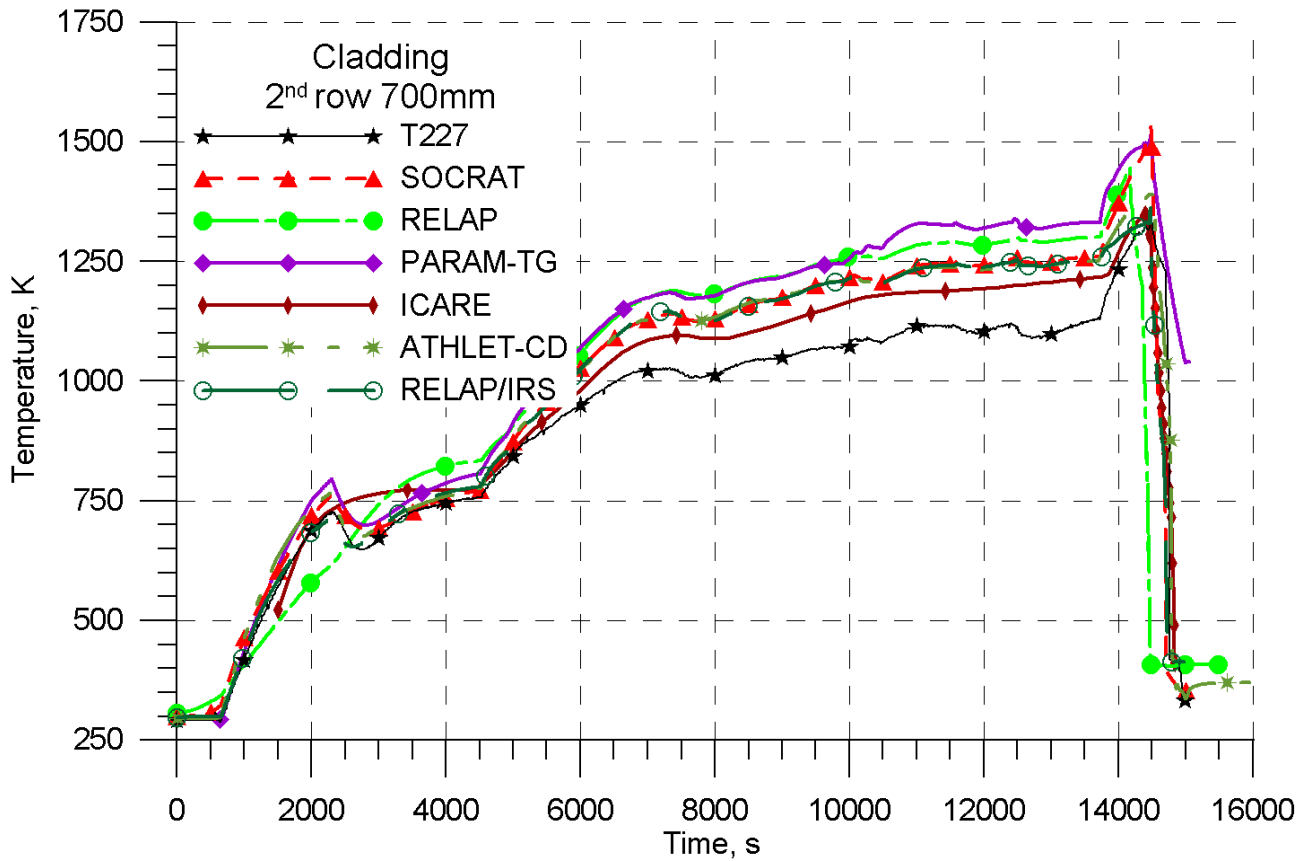
Figure 19. Cladding temperature of fuel rod in the second row at elevation 700 mm.
PARAMETER-SF3 experiment.
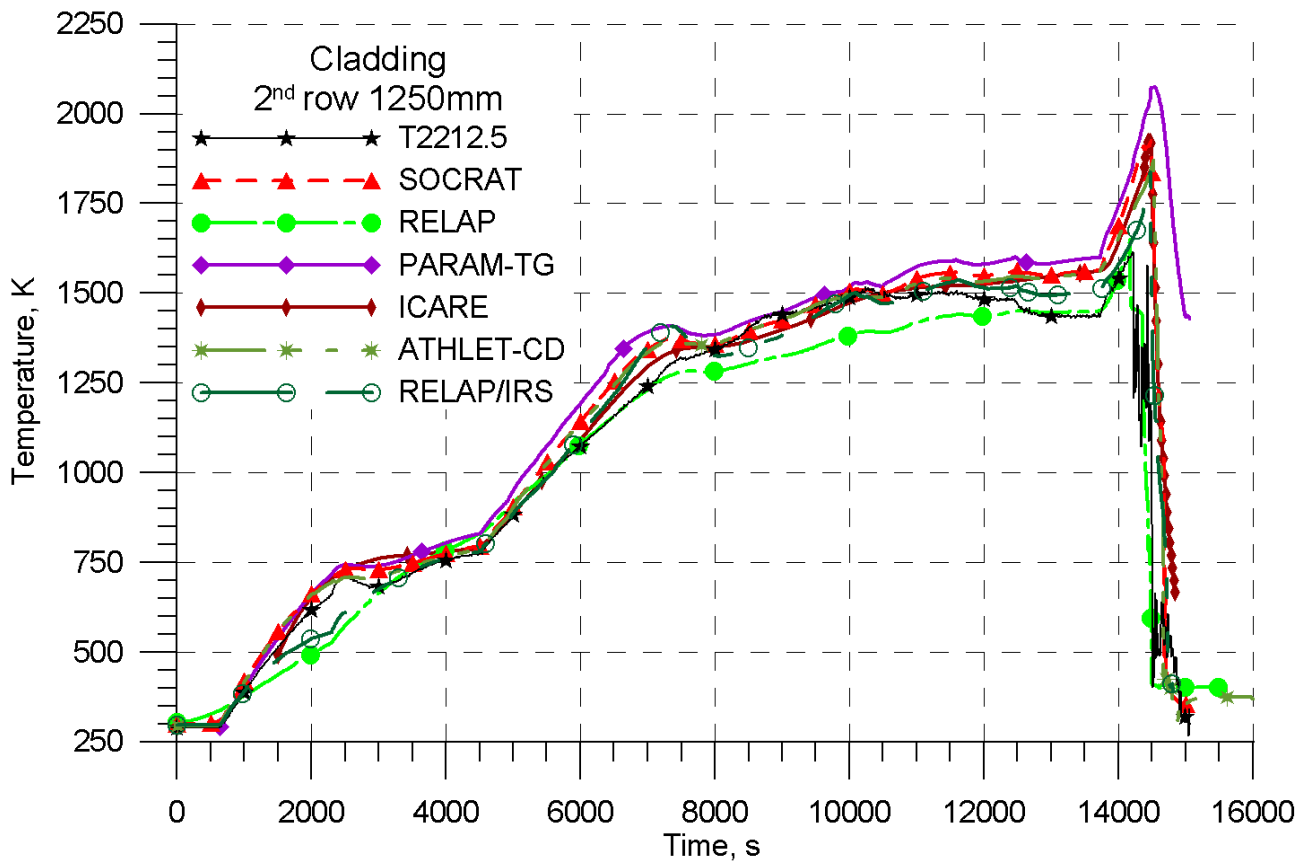
Figure 20. Cladding temperature of fuel rod in the second row at elevation 1250 mm.
PARAMETER-SF3 experiment.
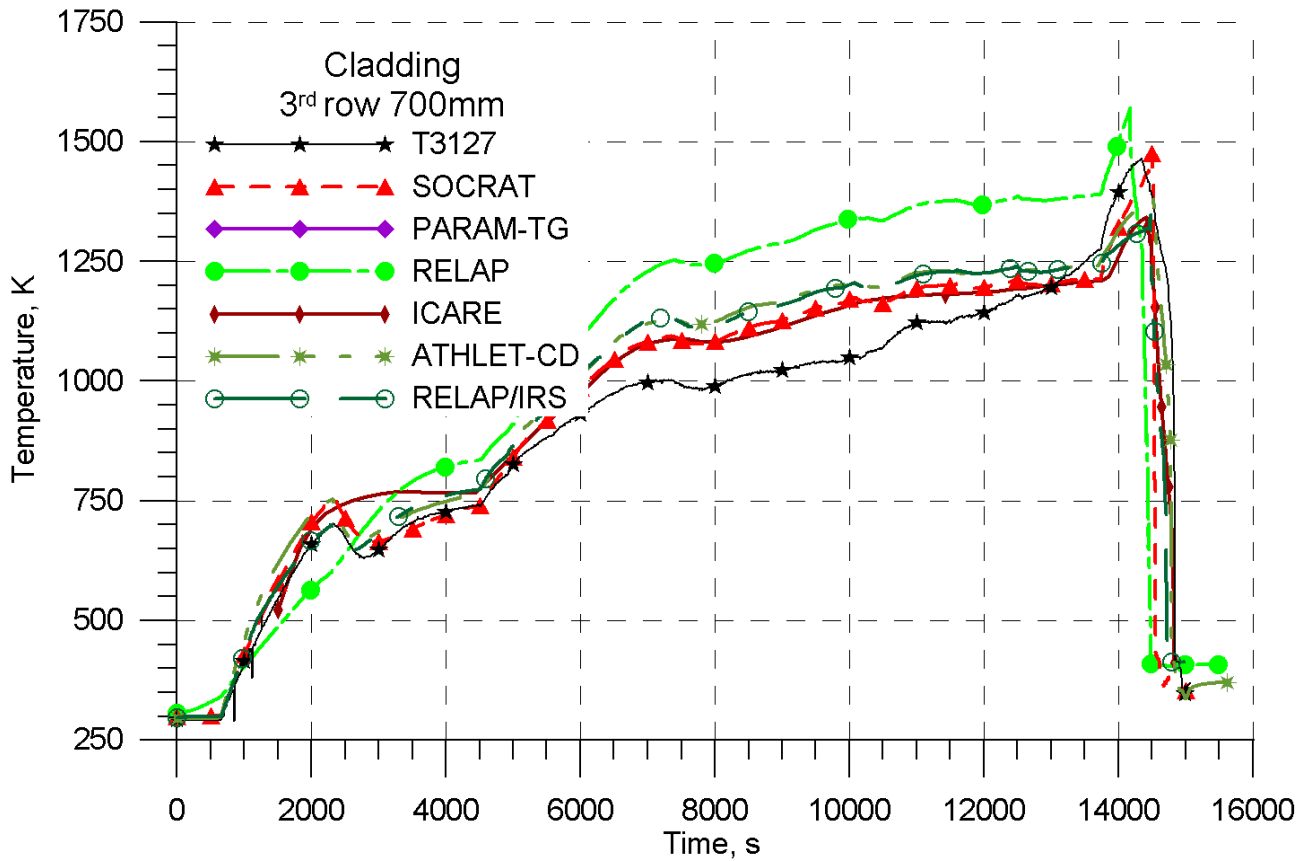
Figure 21. Cladding temperature of fuel rod in the third row at elevation 700 mm.
PARAMETER-SF3 experiment.
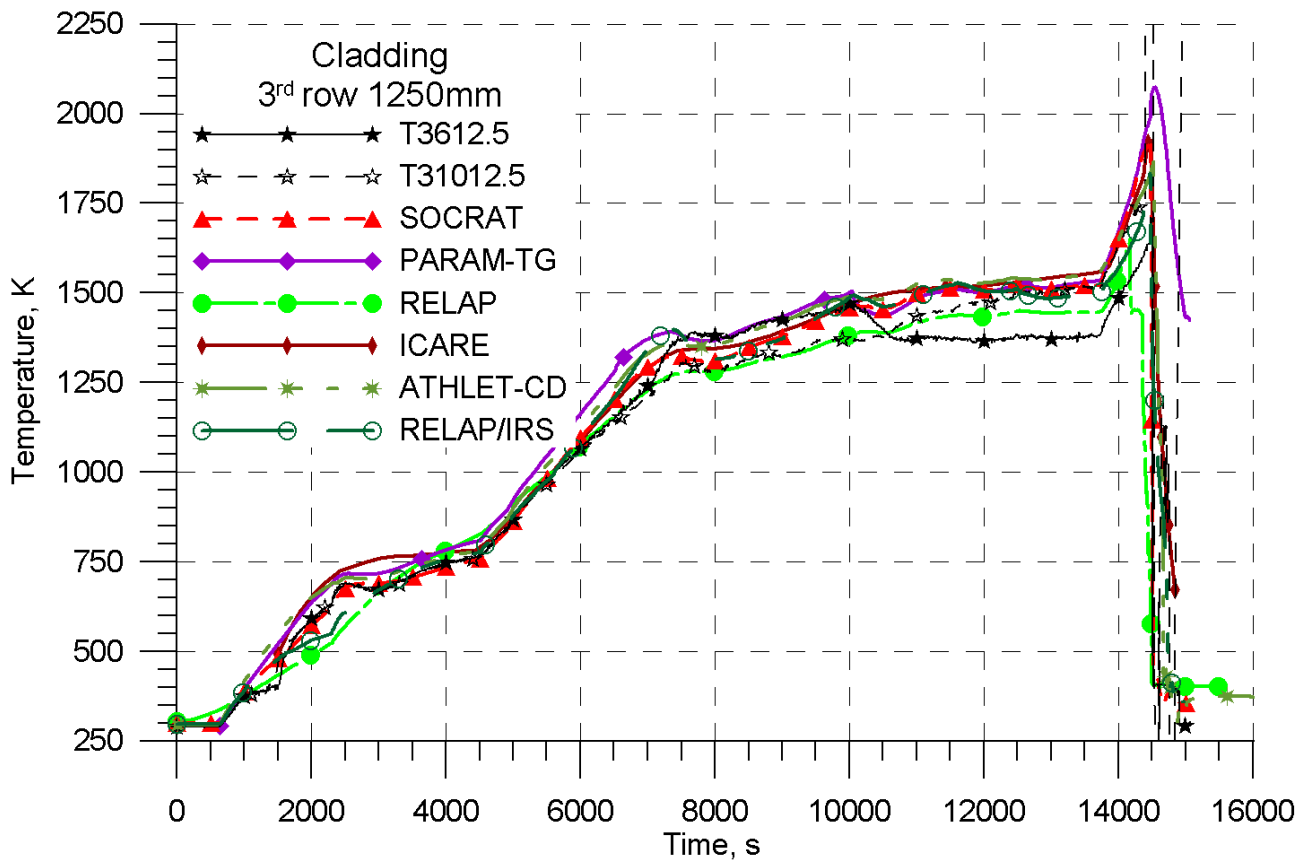
Figure 22. Cladding temperature of fuel rod in the third row at elevation 1250 mm.
PARAMETER-SF3 experiment.
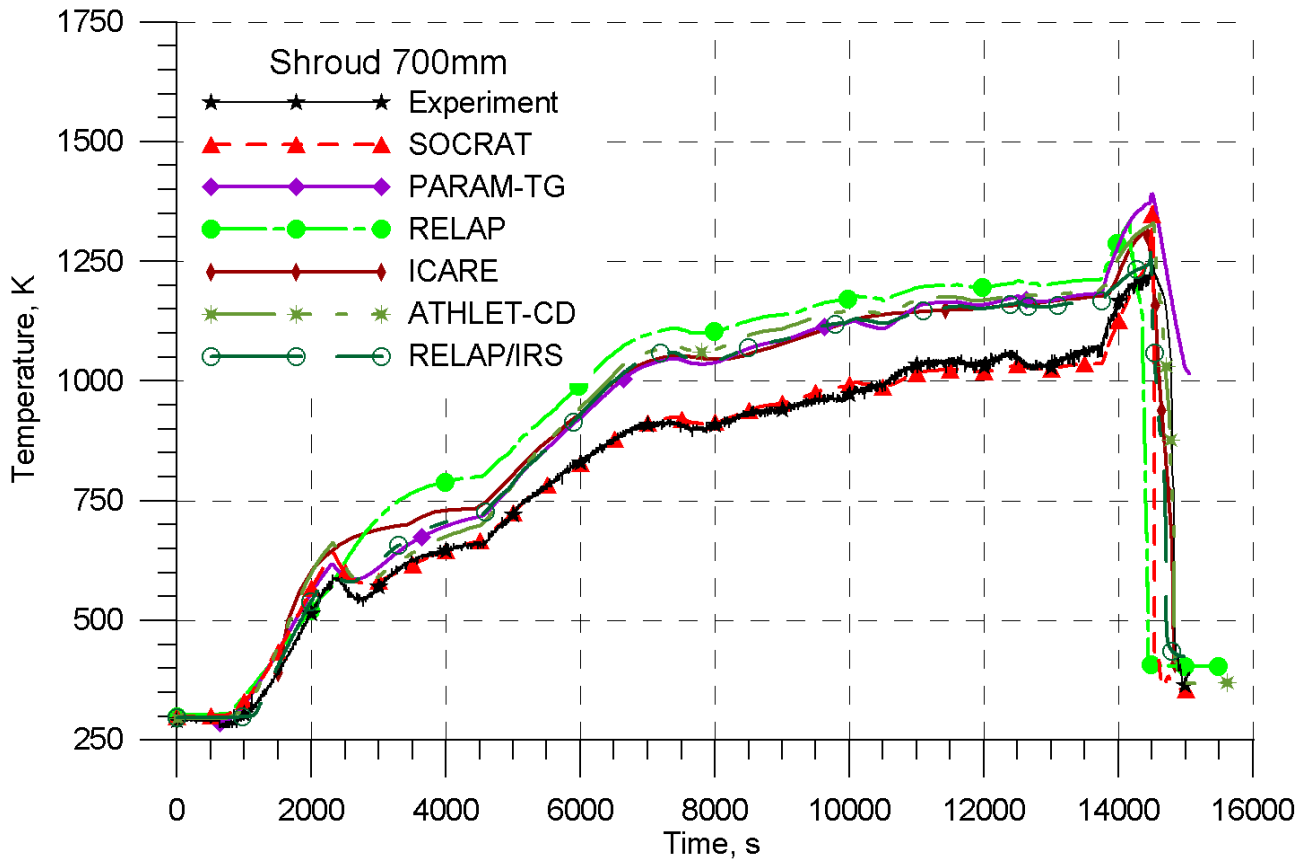
Figure 23. Shroud temperature at elevation 700 mm. PARAMETER-SF3 experiment.
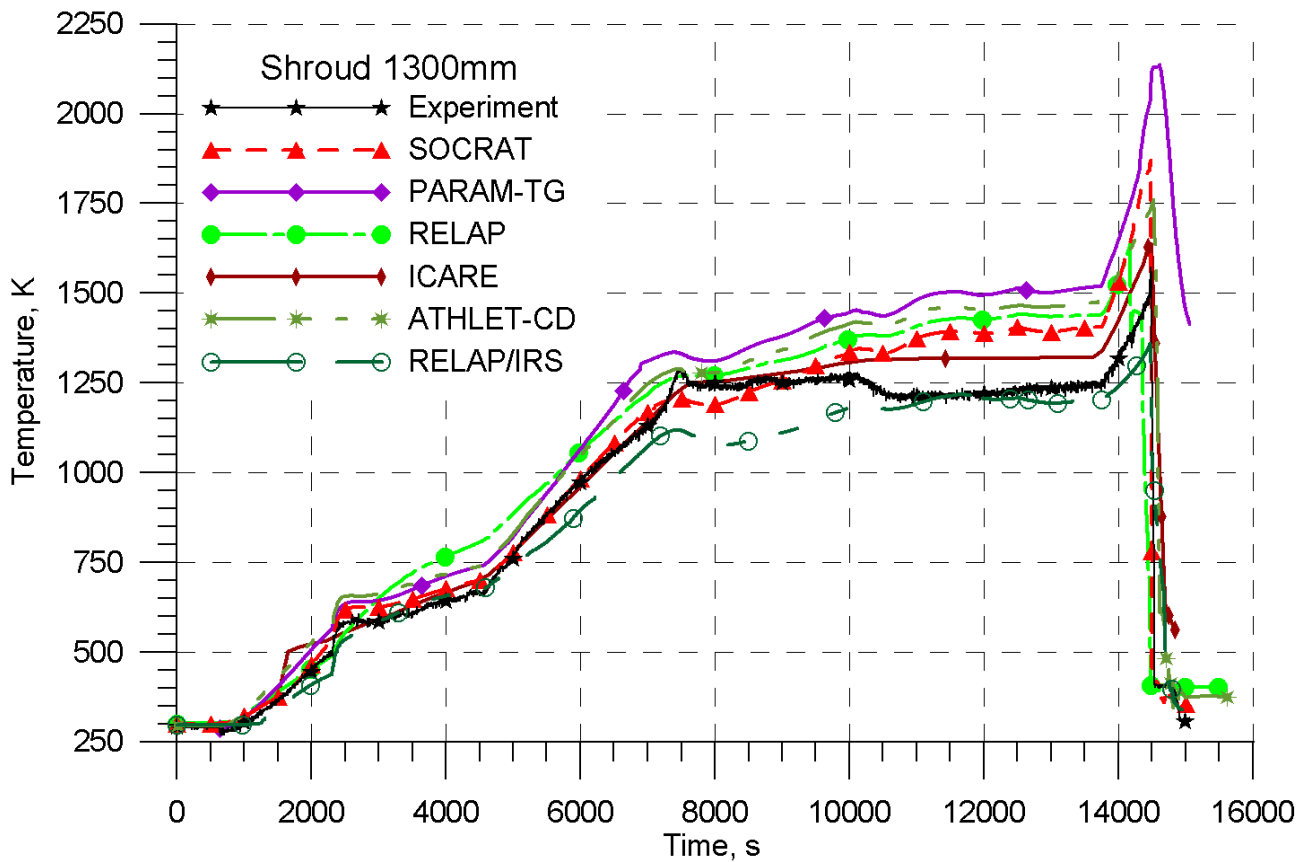
Figure 24. Shroud temperature at elevation 1300 mm. PARAMETER-SF3 experiment.
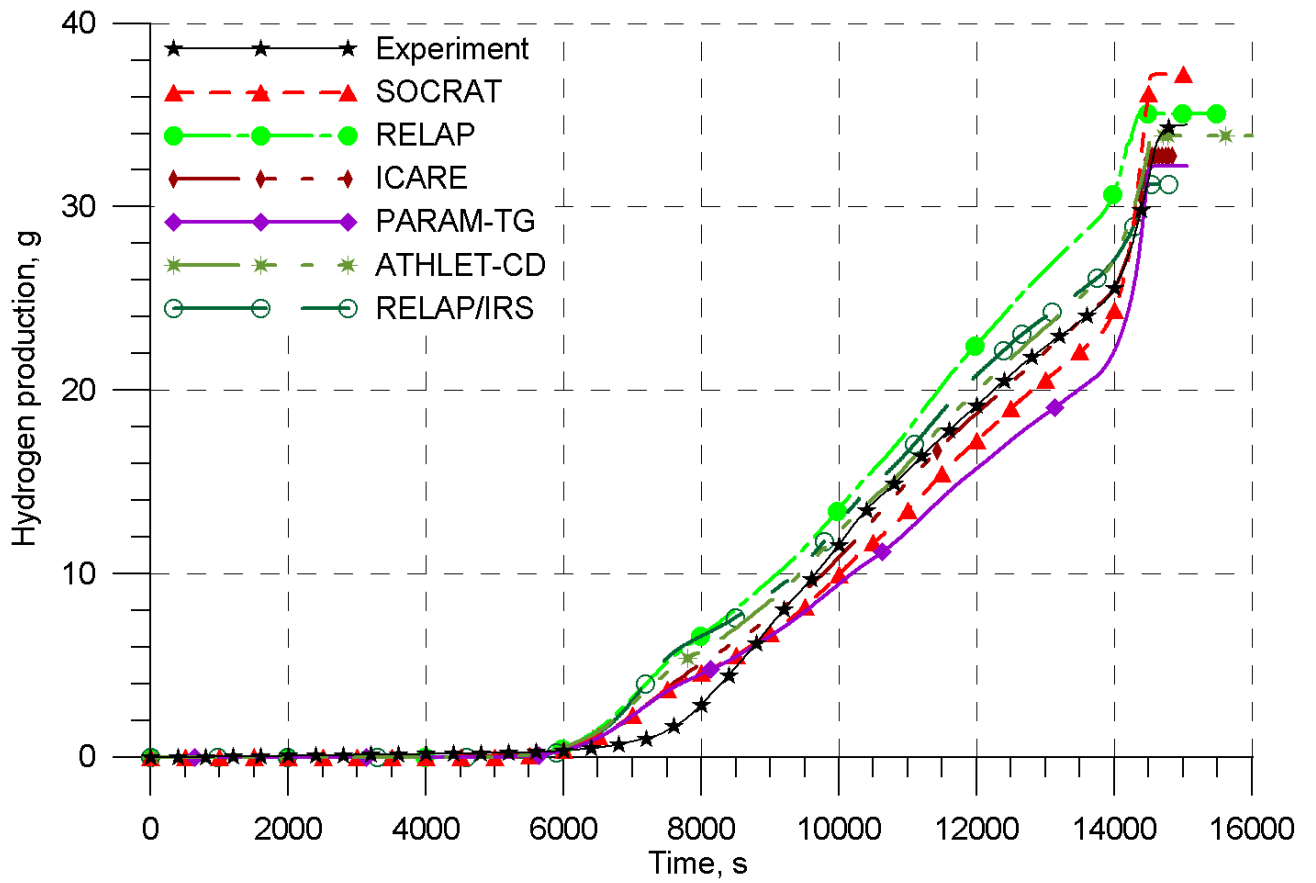
Figure 25. Integral release of hydrogen. PARAMETER-SF3 experiment.
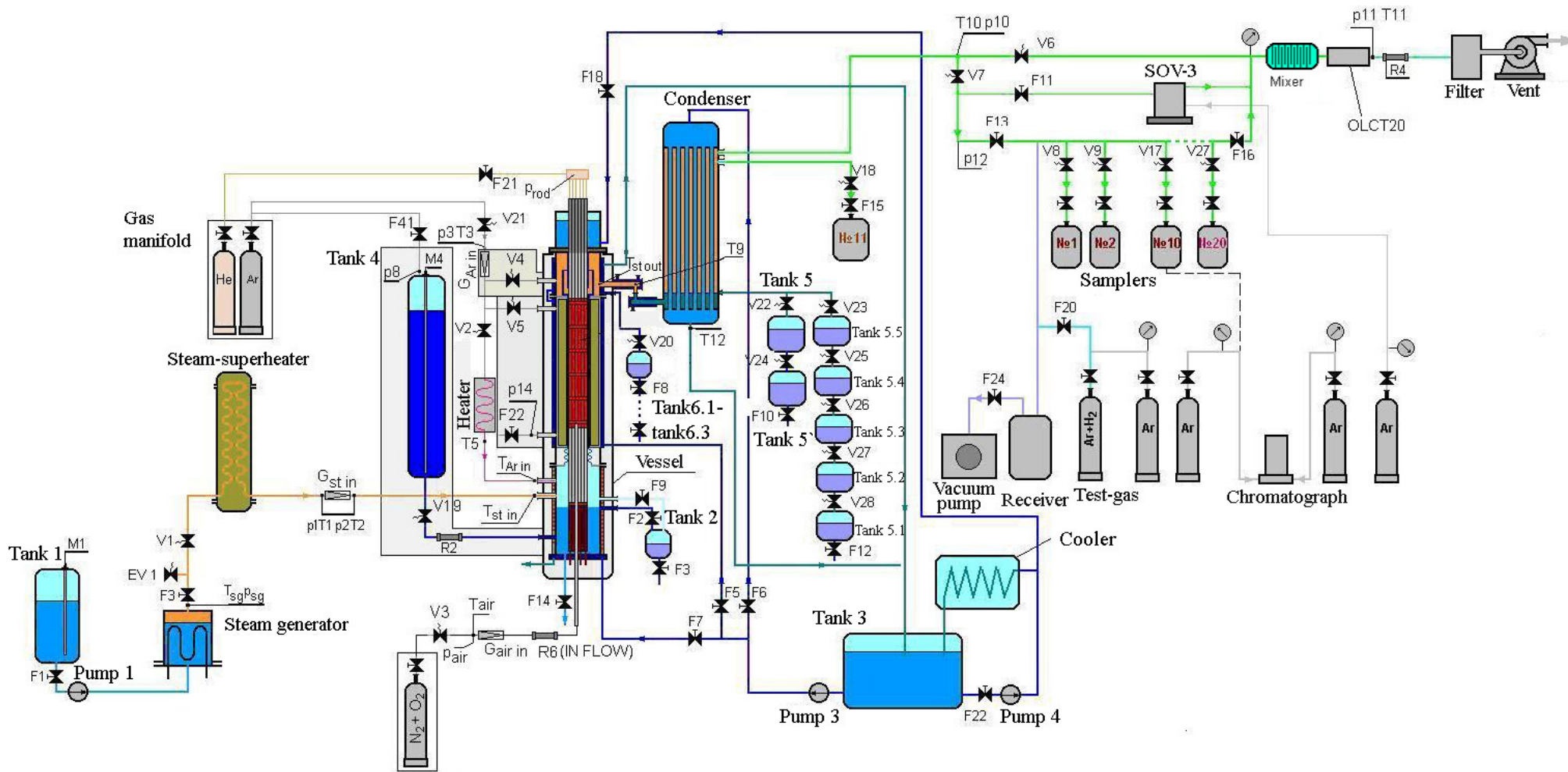
Figure 26. Functional diagram of the PARAMETER test facility in PARAMETER-SF4 experiment.
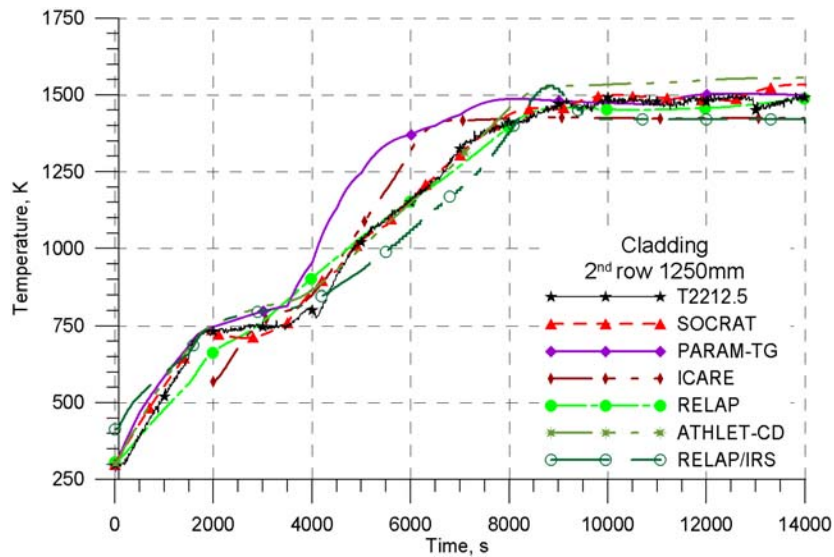
Figure 27. Cladding temperature of the 2nd row fuel rods at the pre-heating and pre-oxidation stages. PARAMETER-SF4 experiment. Air flow rate 0.5 g/s.
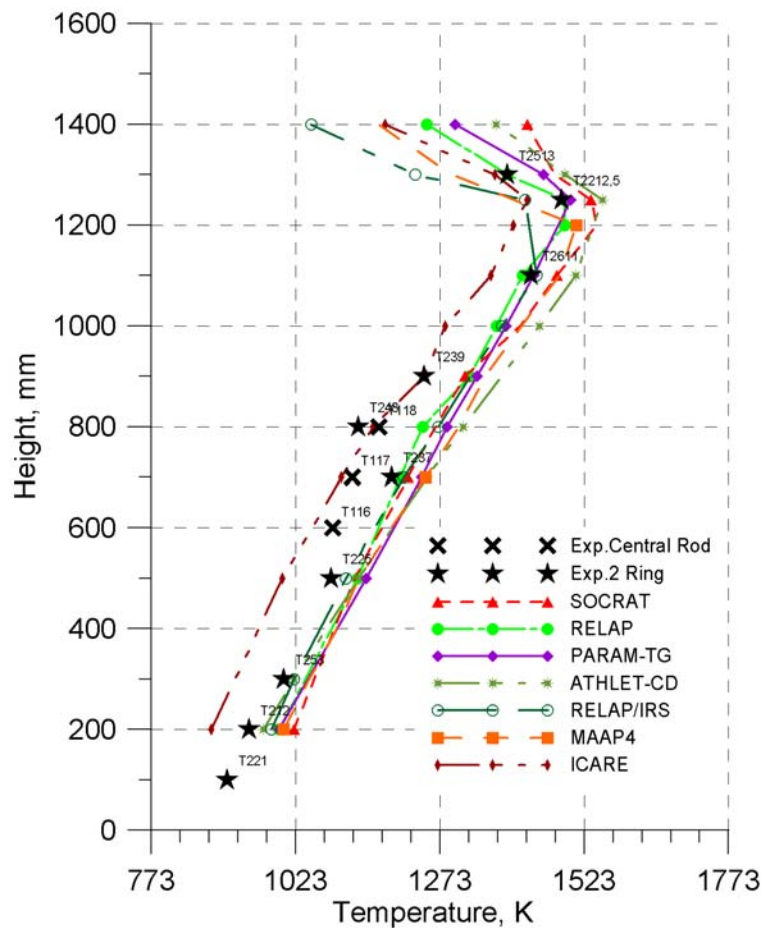
Figure 28. Axial temperature profile by the end of the pre-oxidation stage (t=13950 s). PARAMETER-SF4 experiment. Air flow rate 0.5 g/s.
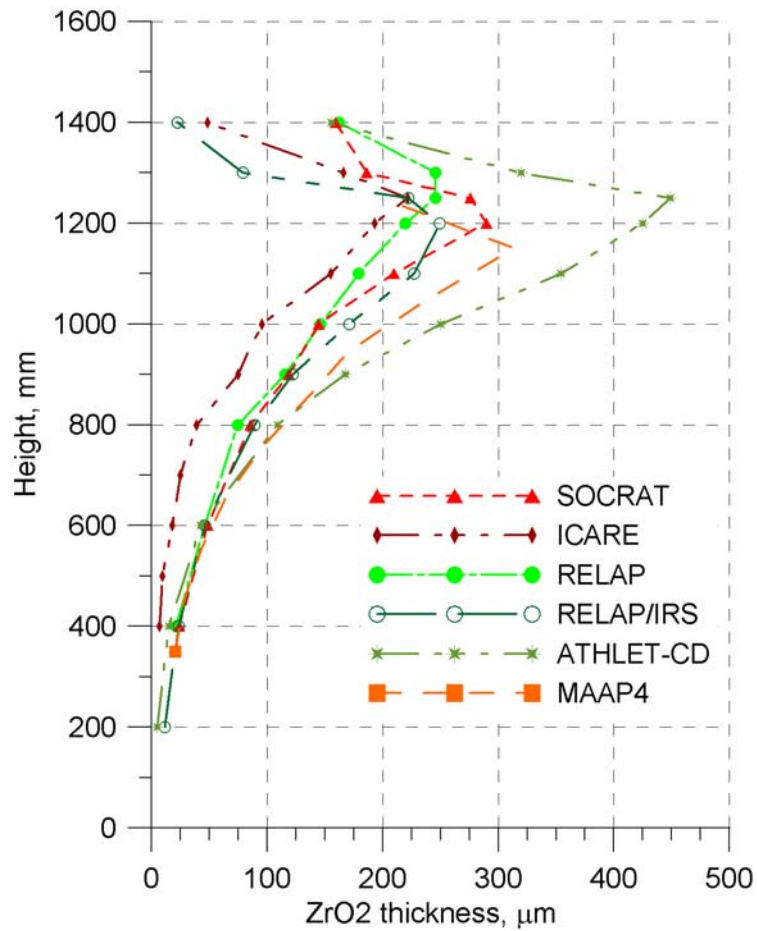
Figure 29. Distribution of oxide scale thickness on cladding surfaces by the end of pre-oxidation stage (t=13950 s). PARAMETER-SF4 experiment. Air flow rate 0.5 g/s.
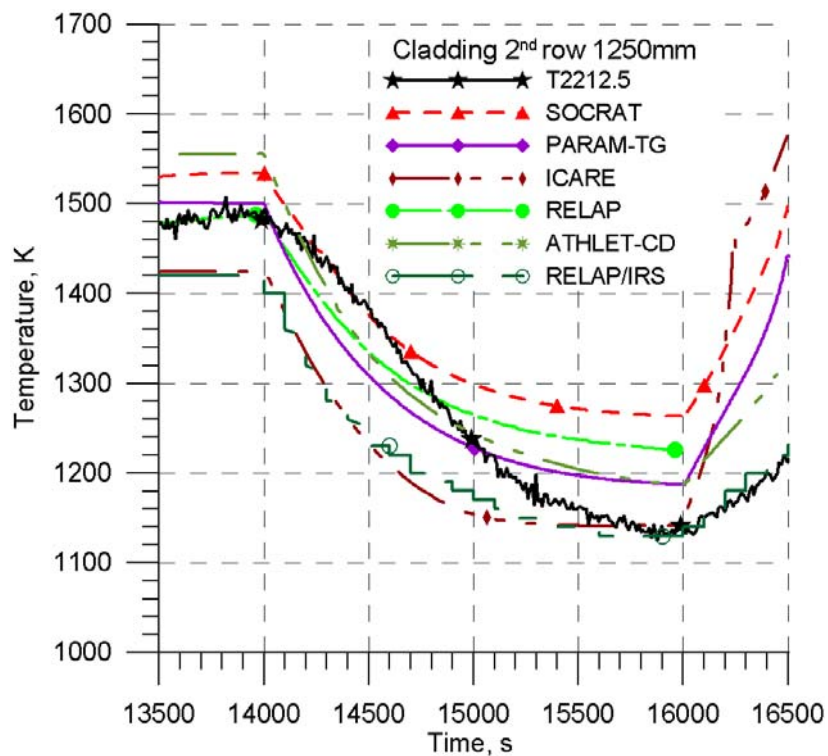
Figure 30. Cladding temperature of the 2nd row fuel rods at the cool down stage. PARAMETER-SF4 experiment. Air flow rate 0.5 g/s.
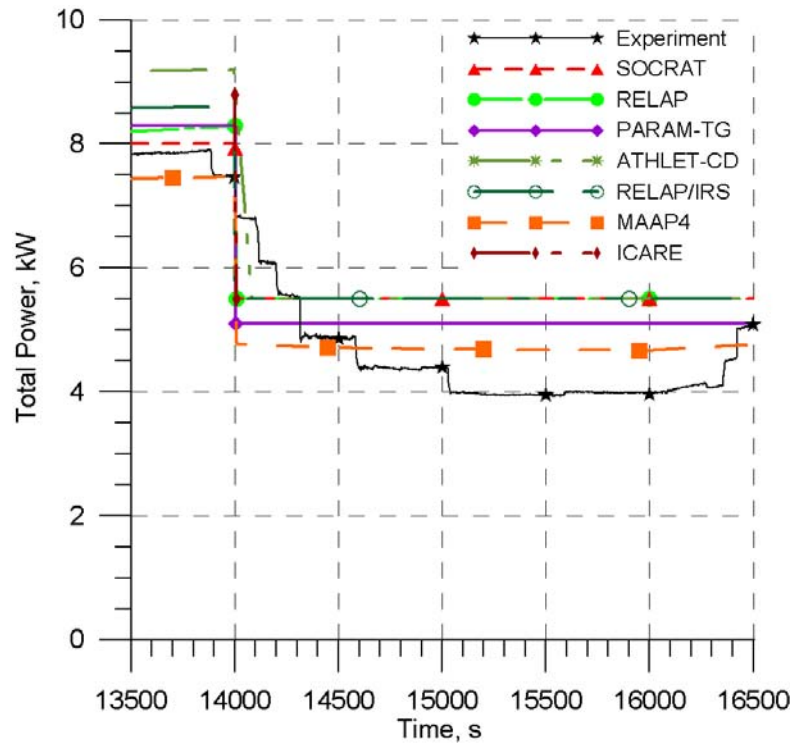
Figure 31. Electric power at the cool down stage.
PARAMETER-SF4 experiment. Air flow rate 0.5 g/s.
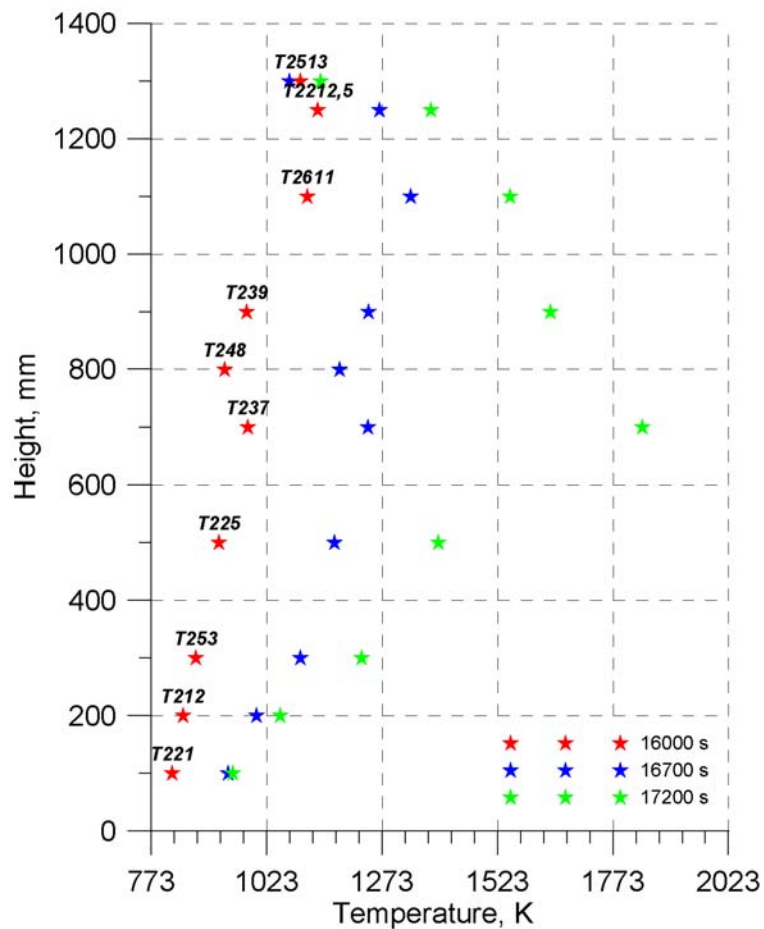
Figure 32. Profile of the measured cladding temperature over the assembly length
at the air ingress stage at different time moments. PARAMETER-SF4 experiment.
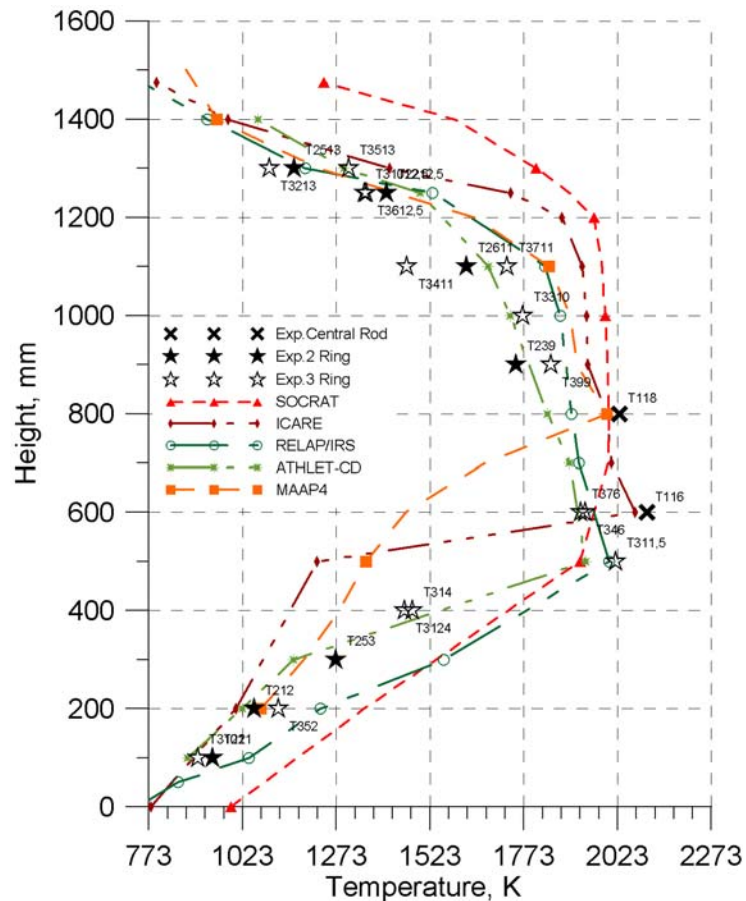
Figure 33. Distribution of fuel rod cladding temperature over the assembly length before flooding onset. PARAMETER-SF4 experiment. Air flow rate 0.5 g/s.
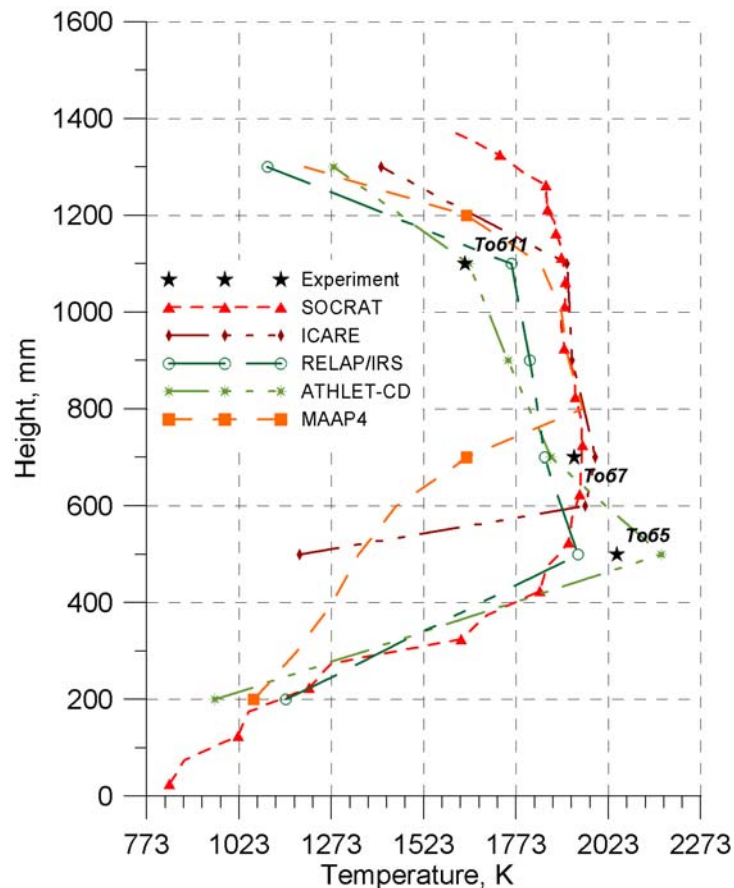
Figure 34. Distribution of shroud temperature over the assembly length before flooding onset. PARAMETER-SF4 experiment. Air flow rate 0.5 g/s.
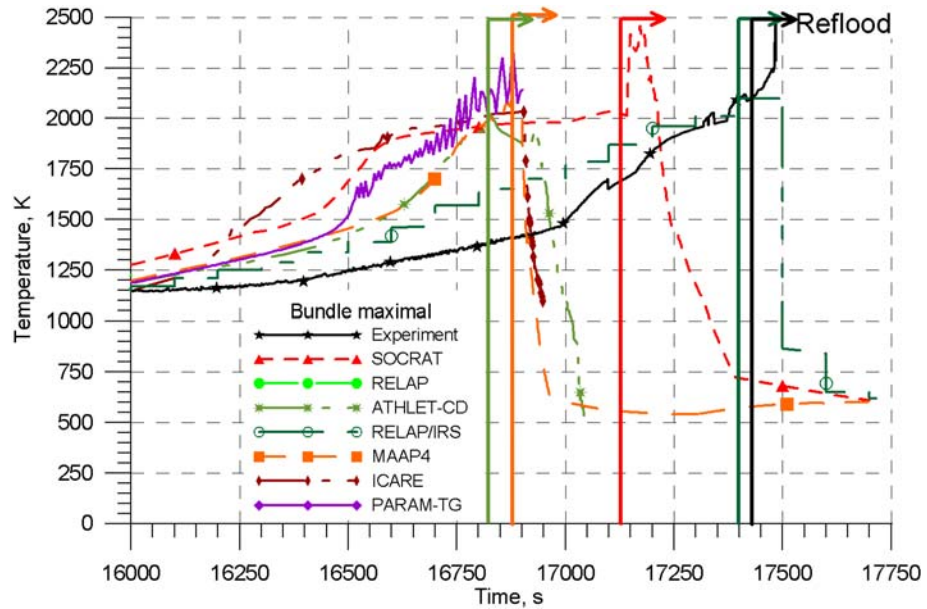
Figure 35. Maximum temperature in the assembly (fuel rod claddings)
at the air ingress stage. PARAMETER-SF4 experiment. Air flow rate 0.5 g/s.
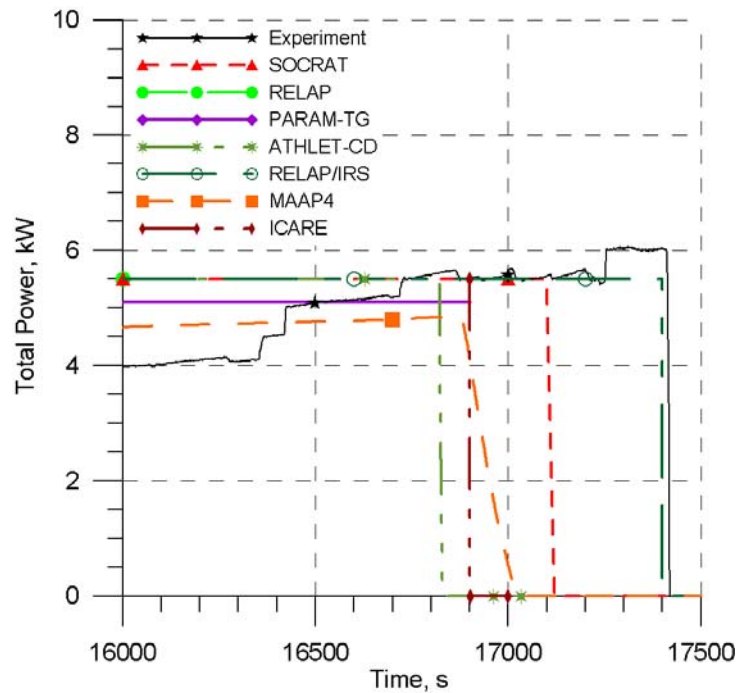
Figure 36. Electric power at the air ingress stage.
PARAMETER-SF4 experiment. Air flow rate 0.5 g/s.
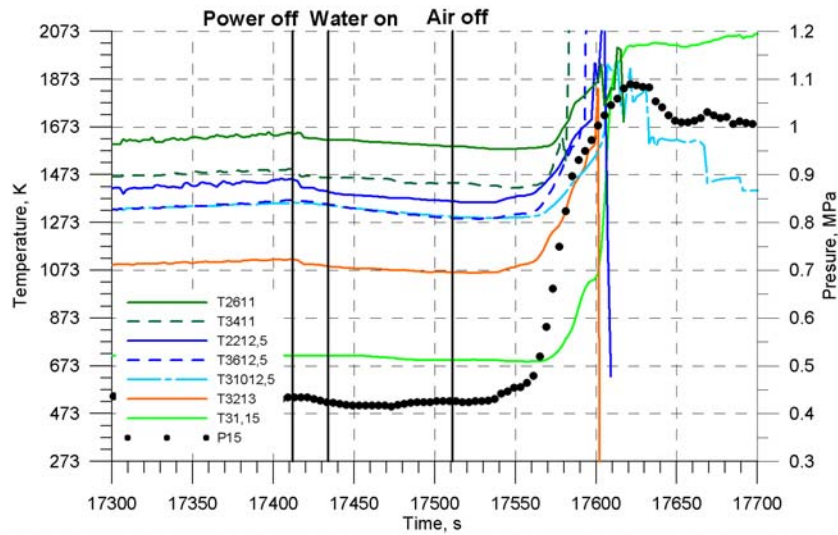
Figure 37. Thermocouples readings in the assembly upper part (1100-1500 mm) at the flooding stage. PARAMETER-SF4 experiment.
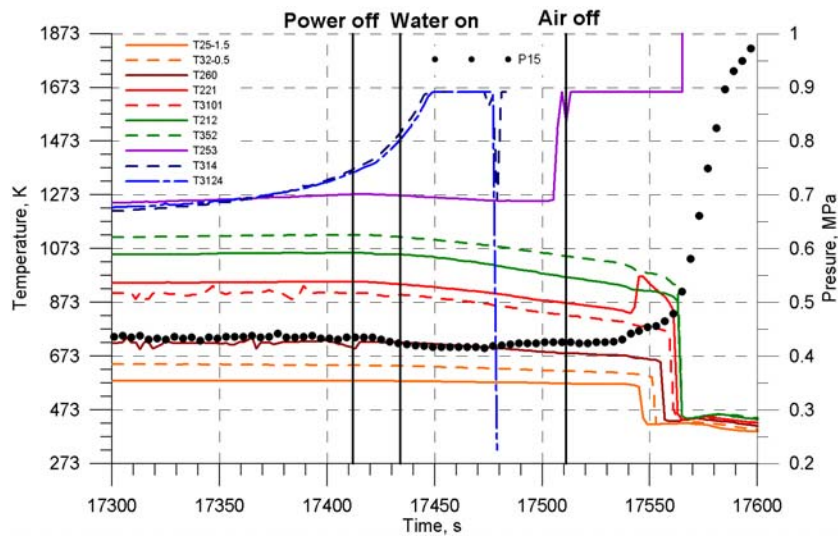
Figure 38. Thermocouples readings in the assembly lower part (-150÷400 mm) at the flooding stage. PARAMETER-SF4 experiment.
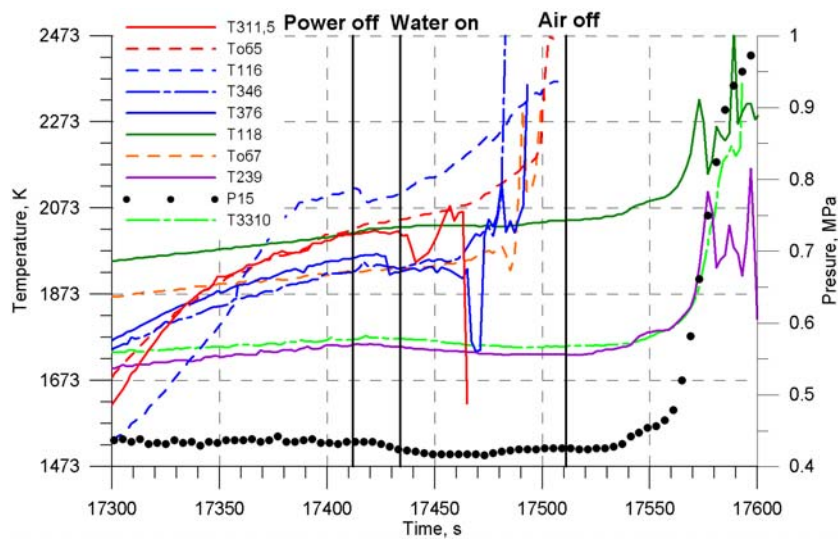
Figure 39. Thermocouples readings in the assembly middle part (500÷1000 mm) at the flooding stage. PARAMETER-SF4 experiment.
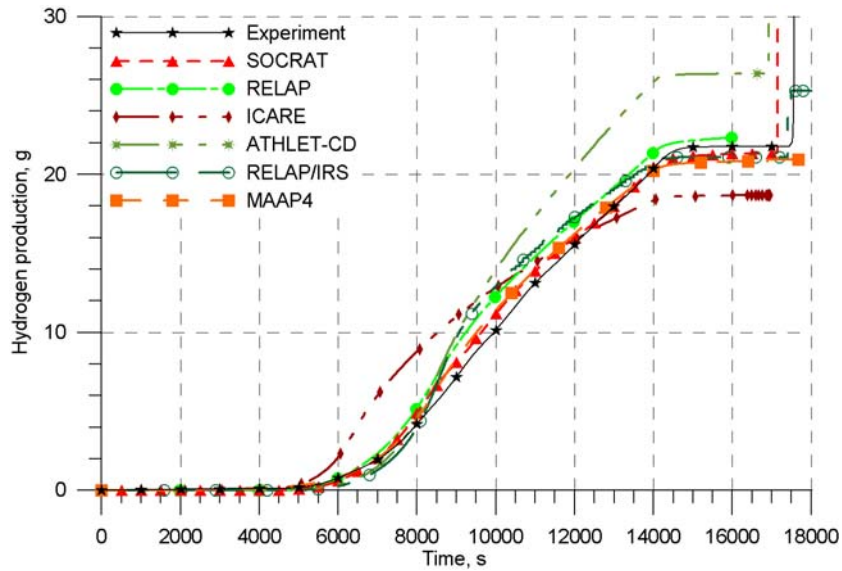
Figure 40. Hydrogen generation at the pre-heating and pre-oxidation stages.
PARAMETER-SF4 experiment. Air flow rate 0.5 g/s.
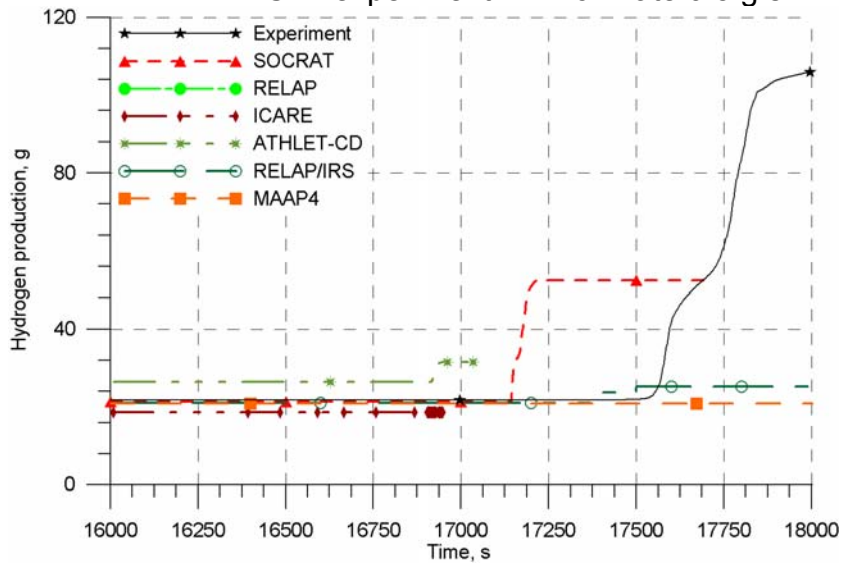
Figure 41. Hydrogen generation at the flooding stage.
PARAMETER-SF4 experiment. Air flow rate 0.5 g/s.
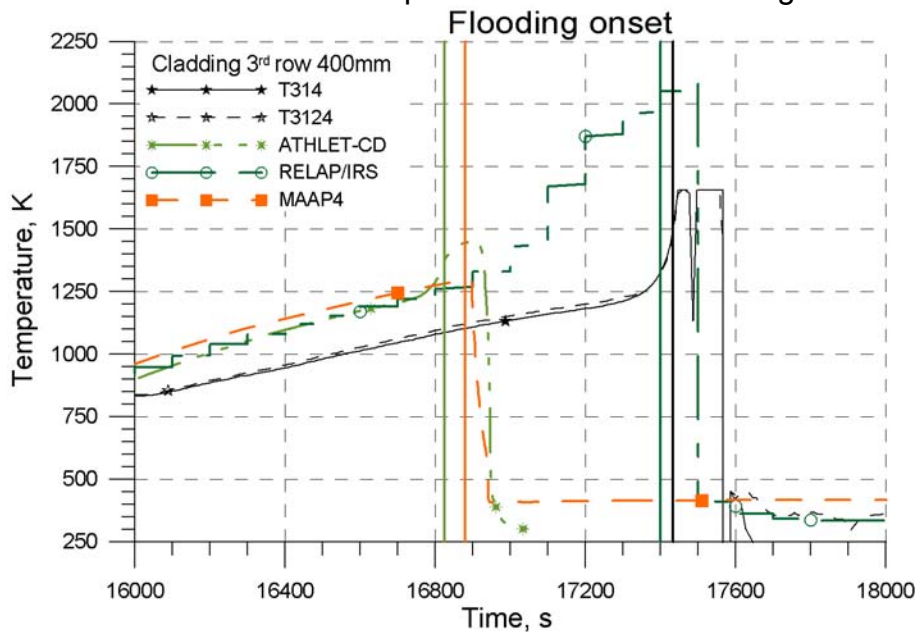
Figure 42. Temperature of fuel rod claddings at elevation 400 mm.
PARAMETER-SF4 experiment. Air flow rate 0.5 g/s.
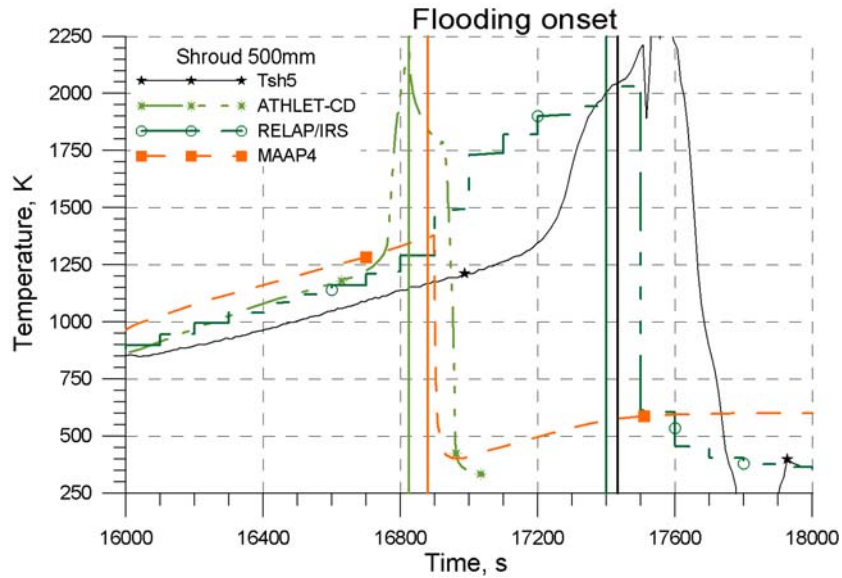
Figure 43. The shroud temperature evolution at elevation 500 mm.
PARAMETER-SF4 experiment. Air flow rate 0.5 g/s.
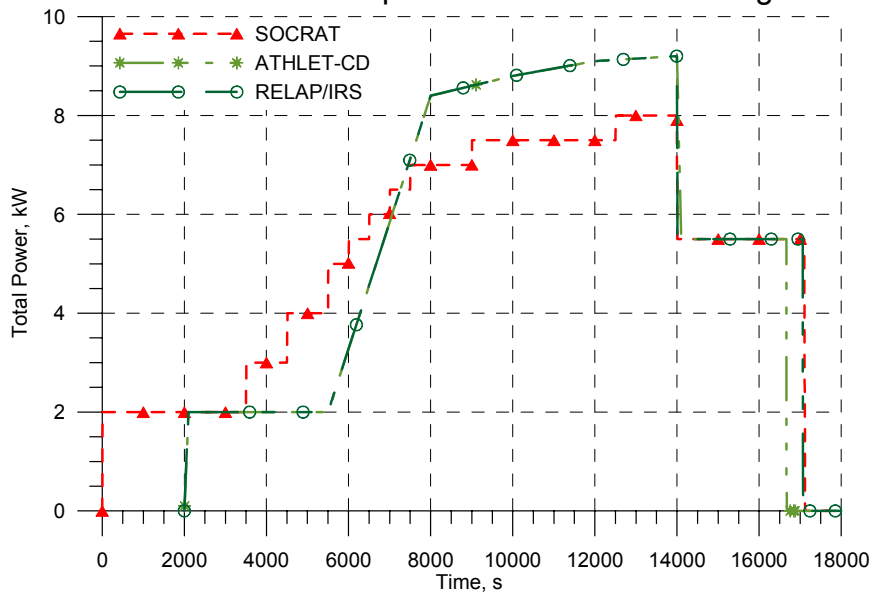
Figure 44. Electric power versus time. PARAMETER-SF4 experiment.
Air flow rate 0.8 g/s.
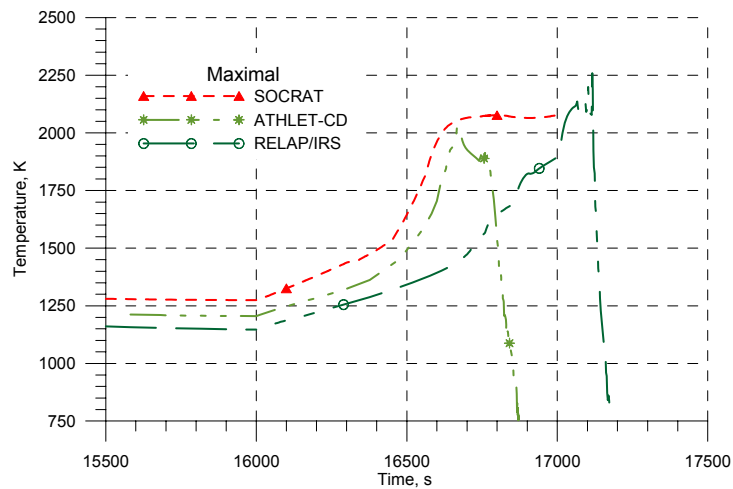
Figure 45. Maximum temperature behaviour at the air ingress.
PARAMETER-SF4 experiment. Air flow rate 0.8 g/s.
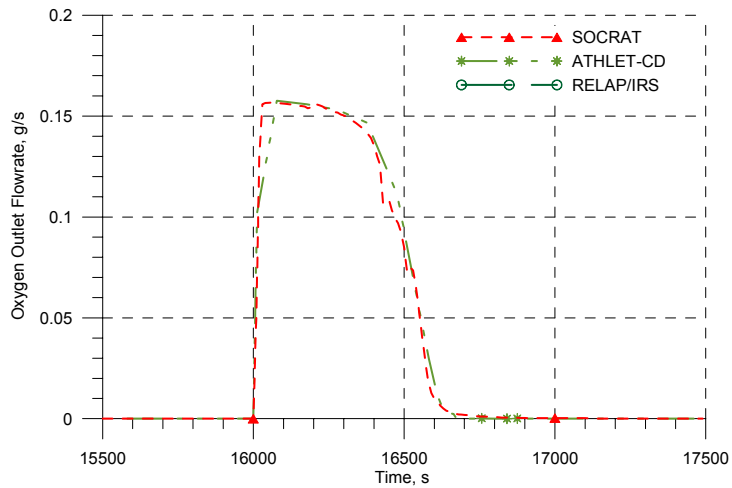
Figure 46. Oxygen flow rate at the assembly outlet.
PARAMETER-SF4 experiment. Air flow rate 0.8 g/s.
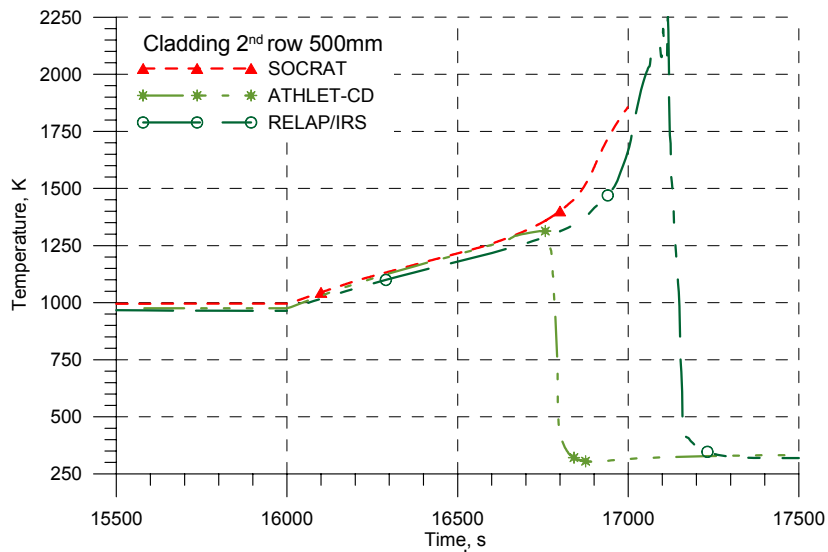
Figure 47. Cladding temperature of the 2nd row fuel rods at elevation 500 mm.
PARAMETER-SF4 experiment. Air flow rate 0.8 g/s.
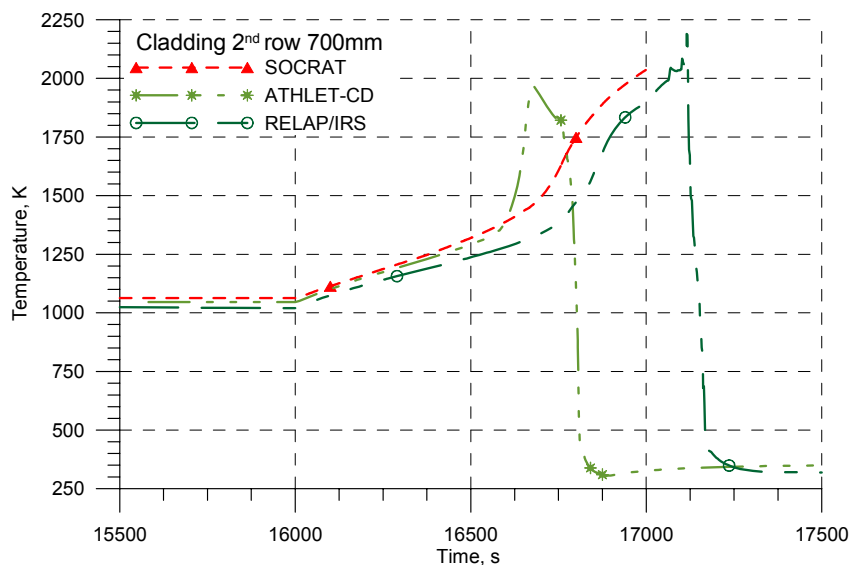
Figure 48. Cladding temperature of the 2nd row fuel rods at elevation 700 mm.
PARAMETER-SF4 experiment. Air flow rate 0.8 g/s.
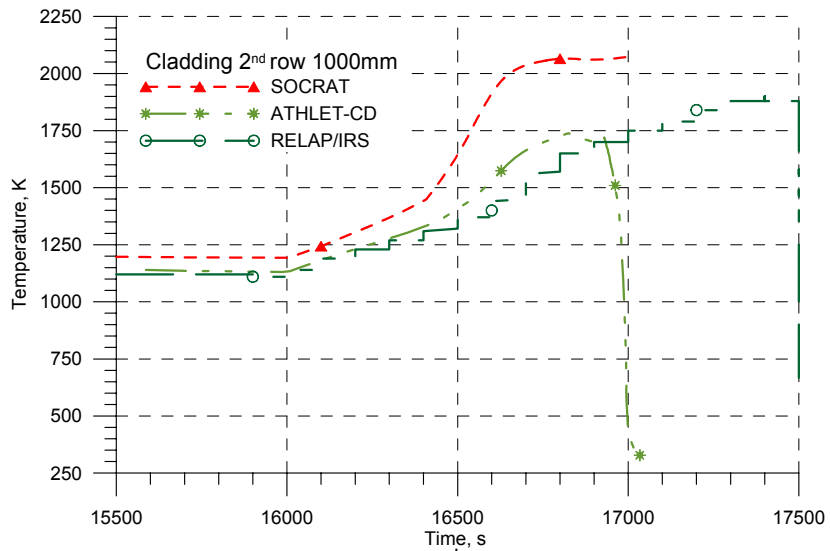
Figure 49. Cladding temperature of the 2nd row fuel rods at elevation 1000 mm. PARAMETER-SF4 experiment. Air flow rate 0.8 g/s.
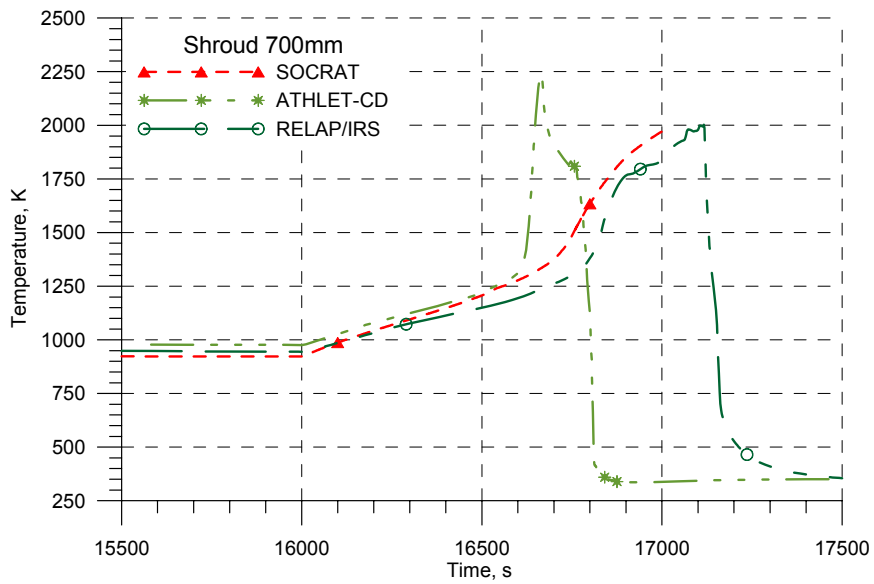
Figure 50. Shroud temperature at elevation 700 mm. PARAMETER-SF4 experiment. Air flow rate 0.8 g/s.
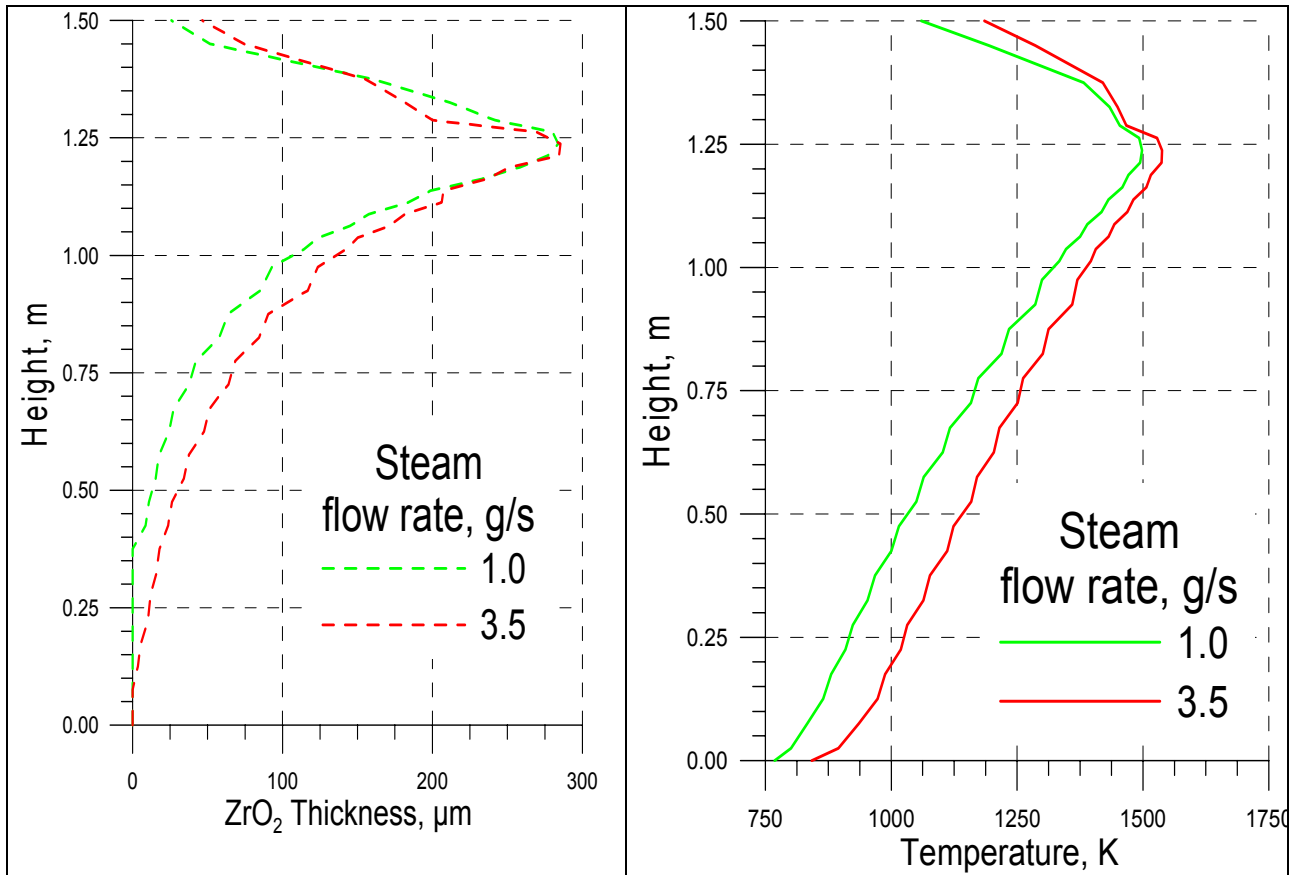
Figure 51. Temperature profile and distribution of the oxide scale thickness on cladding surfaces at the end of the pre-oxidation stage. Studies of SOCRAT code sensitivity to steam flow rate. PARAMETER-SF4 experiment.
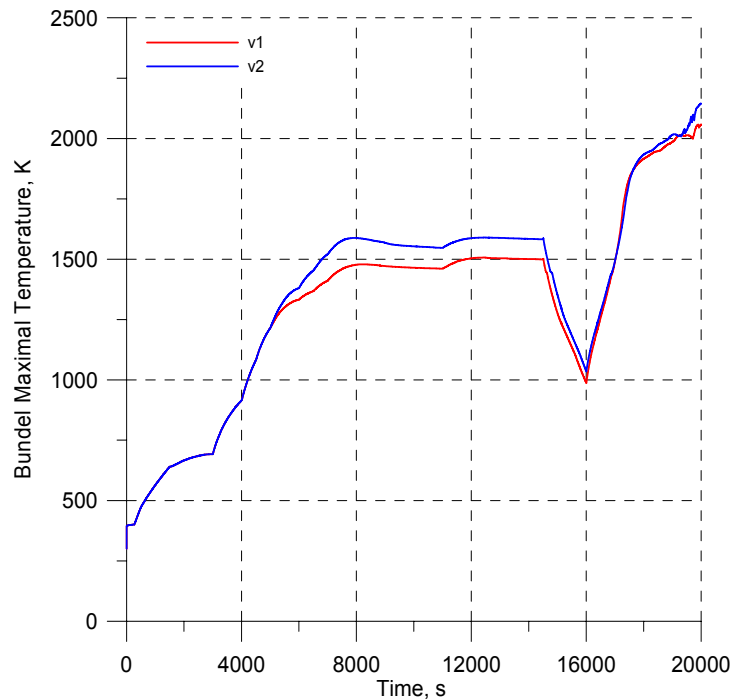
Figure 52. Maximum temperature as a function of time. PARAMETER-SF4 experiment. Studies of SOCRAT code sensitivity to oxide scale thickness. Steam flow rate 3.5 g/s, argon flow rate 4 g/s, air flow rate 0.33 g/s.
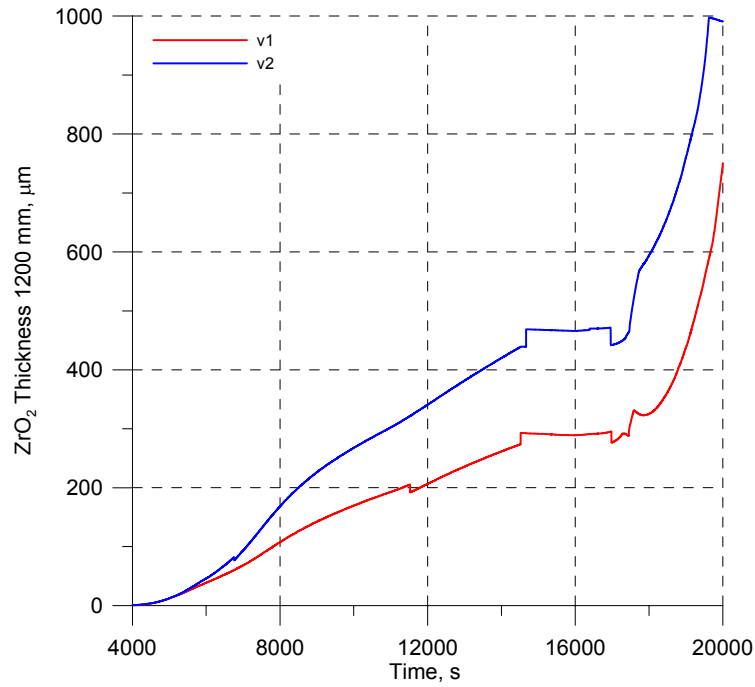
Figure 53. Oxide scale thickness on fuel rod cladding surfaces as a function of time. PARAMETER-SF4 experiment. Studies of SOCRAT code sensitivity to oxide scale thickness. Steam flow rate 3.5 g/s, argon flow rate 4 g/s, air flow rate 0.33 g/s.
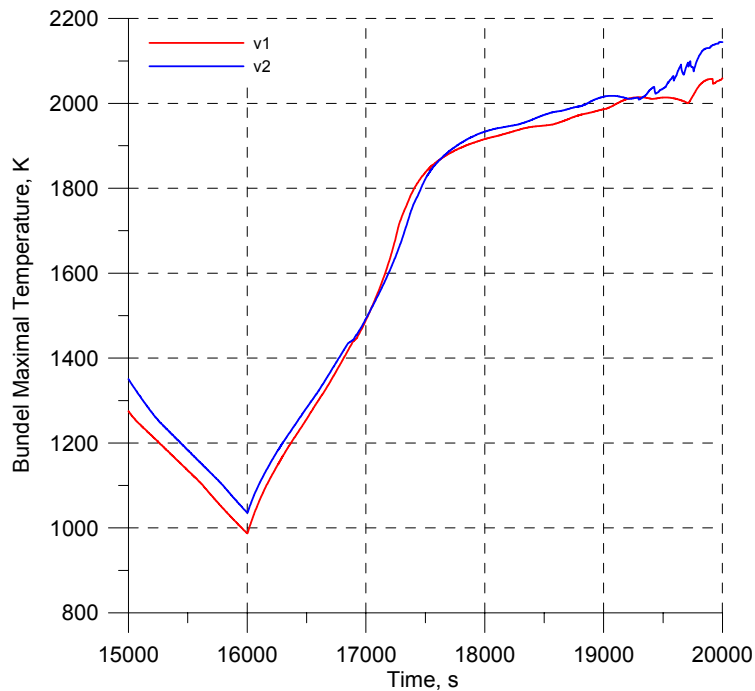
Figure 54. Maximum temperature of fuel rod claddings at the air ingress stage. PARAMETER-SF4 experiment. Studies of SOCRAT code sensitivity to oxide scale thickness. Steam flow rate 3.5 g/s, argon flow rate 4 g/s, air flow rate 0.33 g/s.
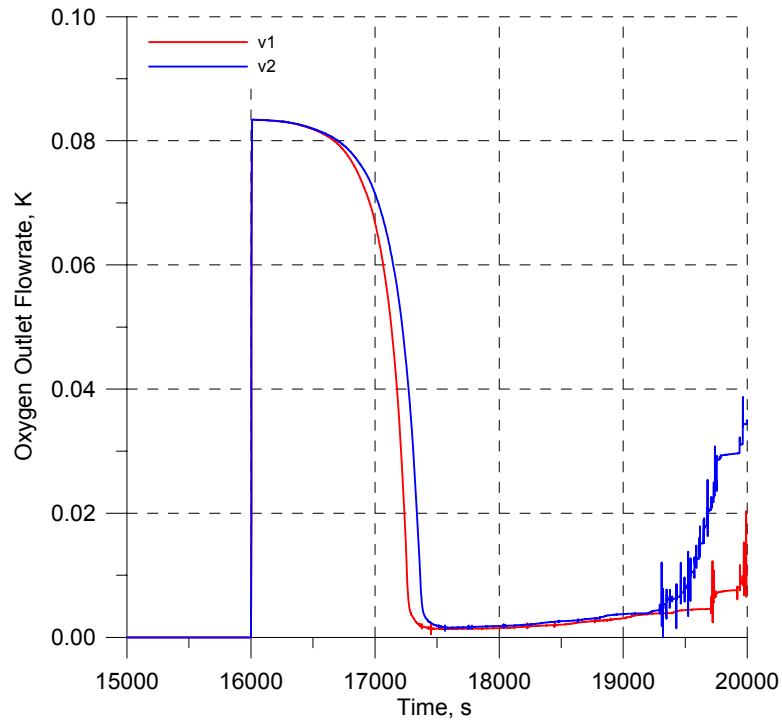
Figure 55. Oxygen flow rate at the assembly outlet. PARAMETER-SF4 experiment. Studies of SOCRAT code sensitivity to oxide scale thickness. Steam flow rate 3.5 g/s, argon flow rate 4 g/s, air flow rate 0.33 g/s.
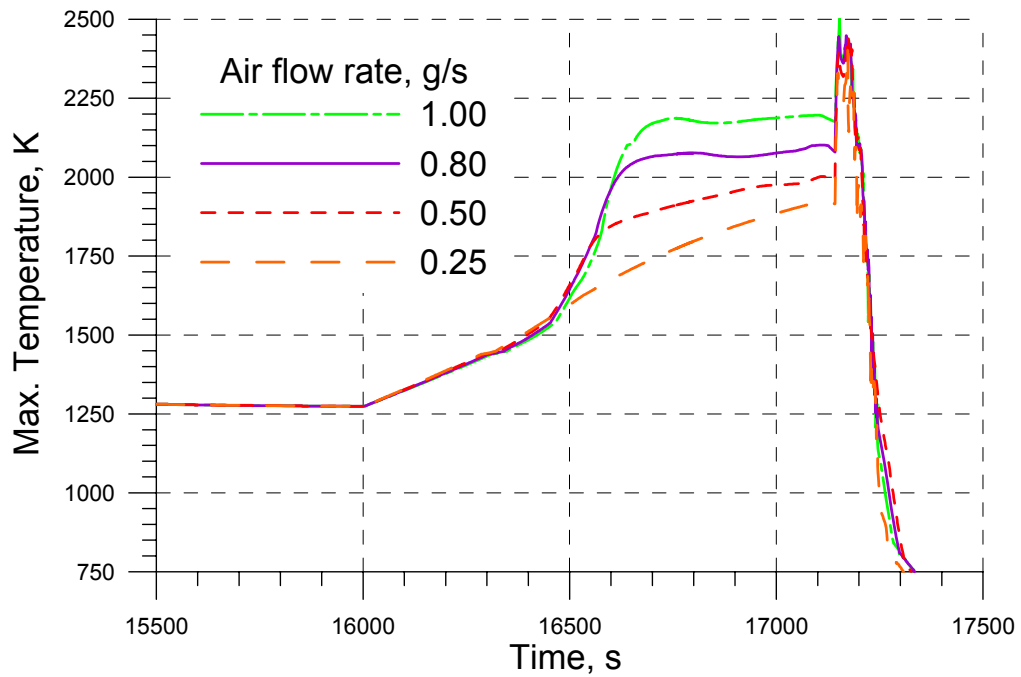
Figure 56. Maximum temperature of fuel rod claddings at the air ingress stage. PARAMETER-SF4 experiment. Studies of SOCRAT code sensitivity to air flow rate. Steam flow rate 3.5 g/s, argon flow rate 2 g/s.
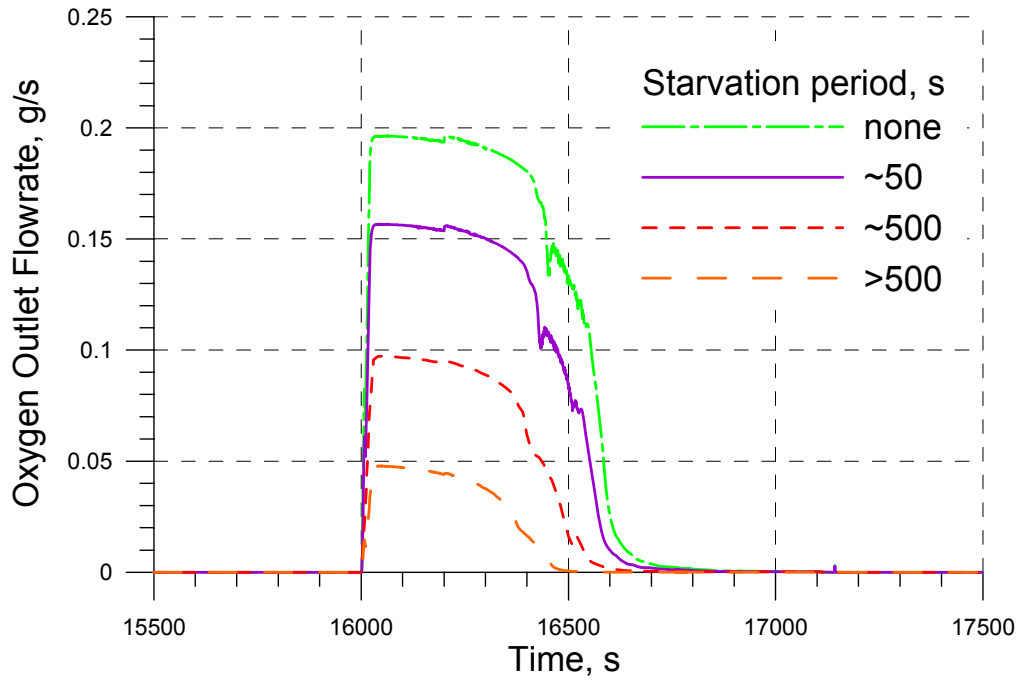
Figure 57. Oxygen flow rate at the assembly outlet. PARAMETER-SF4 experiment. Studies of SOCRAT code sensitivity to air flow rate. Steam flow rate 3.5 g/s, argon flow rate 2 g/s.
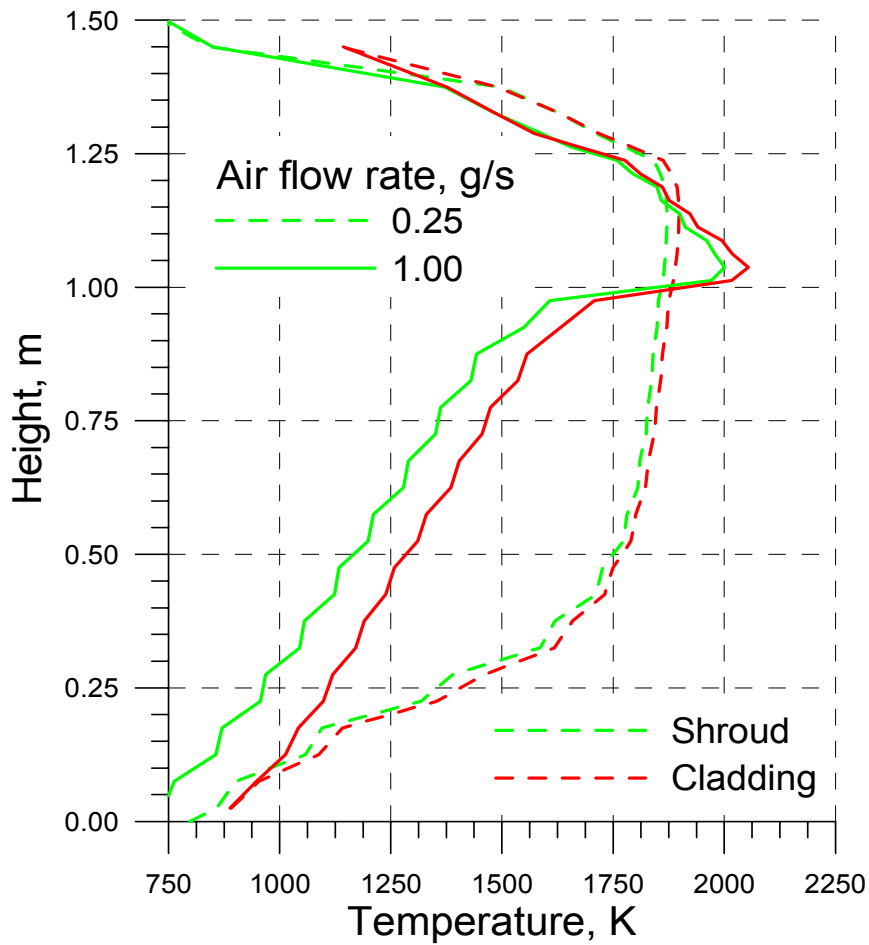
Figure 58. Temperature profile at the end of the air ingress stage. PARAMETER-SF4 experiment. Studies of SOCRAT code sensitivity to air flow rate. Steam flow rate 3.5 g/s, argon flow rate 2 g/s.
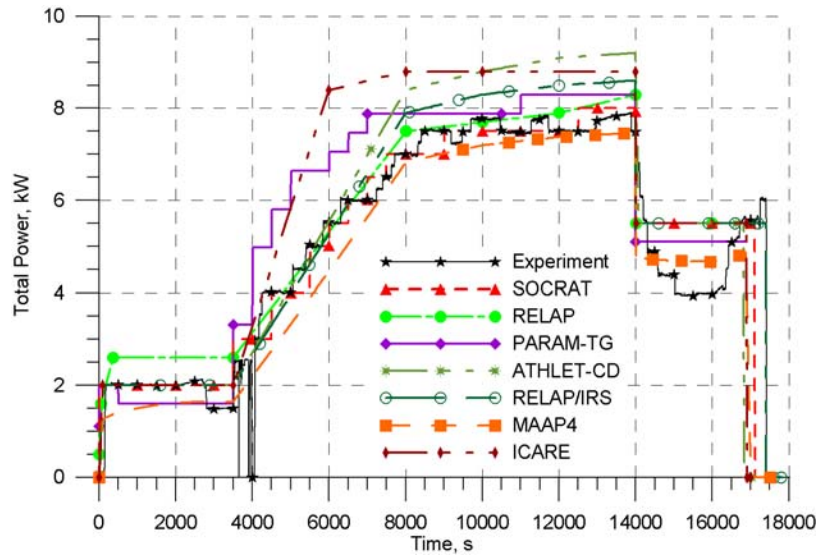
Figure 59. Electric power supply. PARAMETER-SF4 experiment. Air flow rate 0.5 g/s.
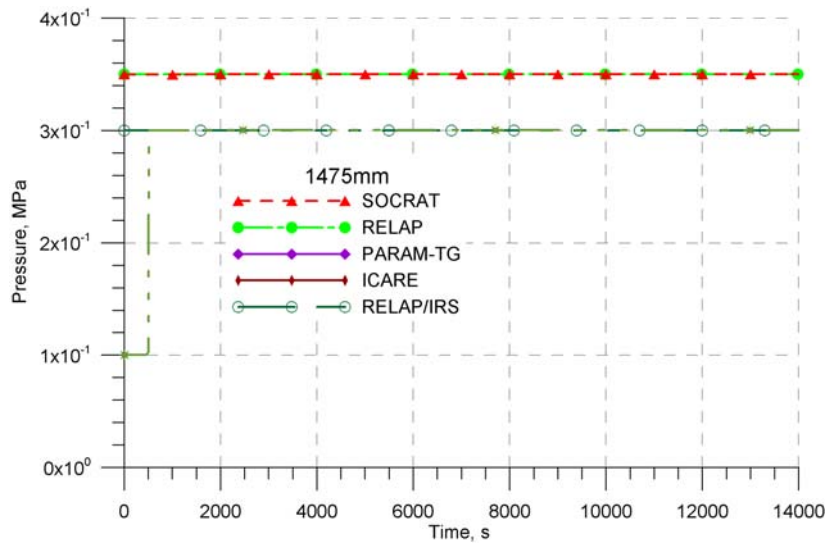
Figure 60. System pressure. PARAMETER-SF4 experiment. Air flow rate 0.5 g/s.
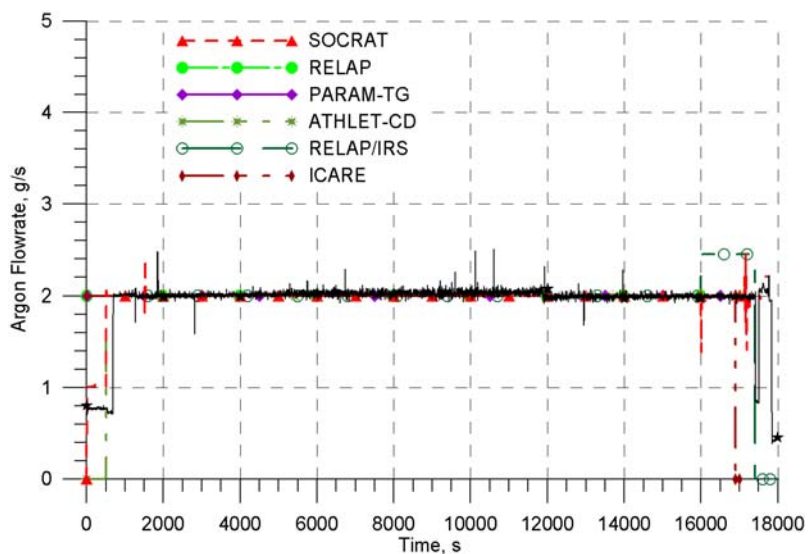
Figure 61. Argon flow rate at inlet. PARAMETER-SF4 experiment.
Air flow rate 0.5 g/s.
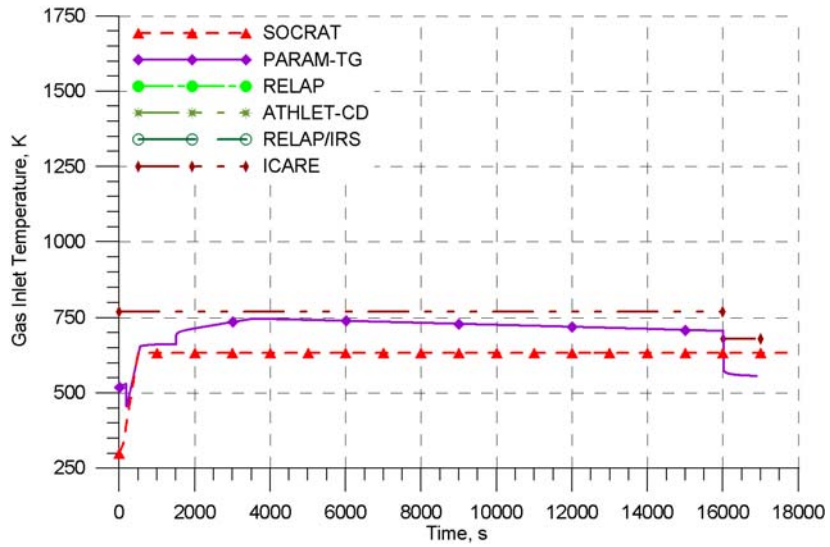
Figure 62. Argon temperature at inlet. PARAMETER-SF4 experiment.
Air flow rate 0.5 g/s.
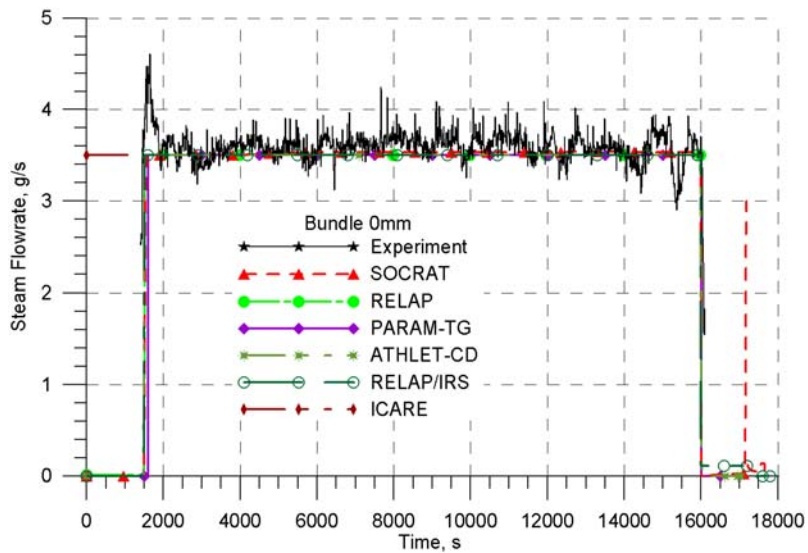
Figure 63. Steam flow rate at inlet. PARAMETER-SF4 experiment.
Air flow rate 0.5 g/s.
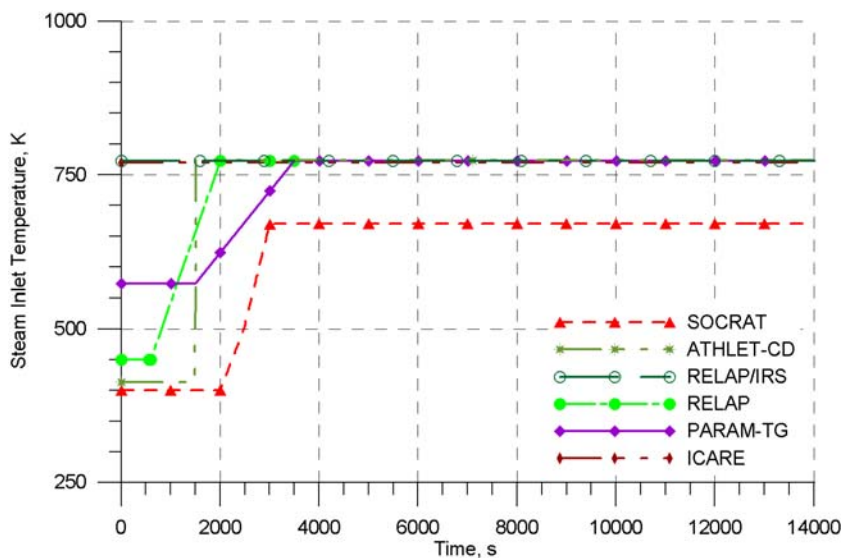
Figure 64. Steam temperature at inlet. PARAMETER-SF4 experiment.
Air flow rate 0.5 g/s.
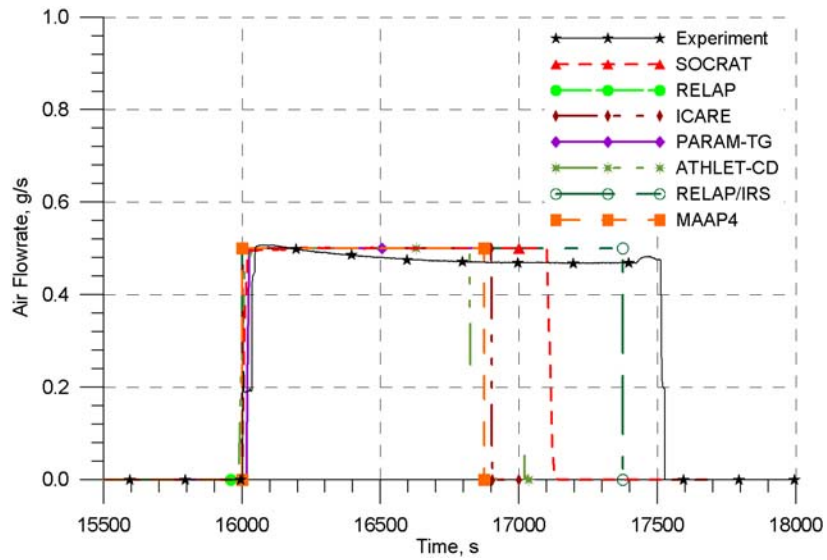
Figure 65. Air flow rate at inlet. PARAMETER-SF4 experiment.
Air flow rate 0.5 g/s.
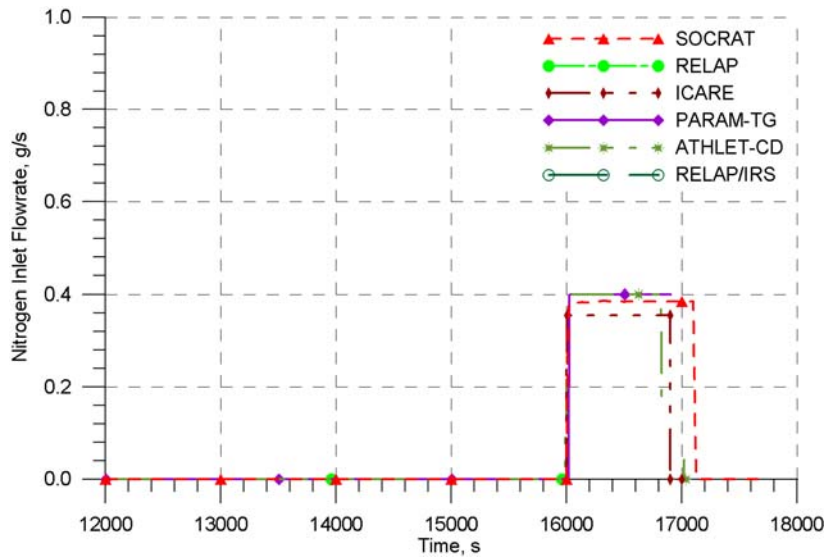
Figure 66. Nitrogen flow rate at inlet. PARAMETER-SF4 experiment.
Air flow rate 0.5 g/s.
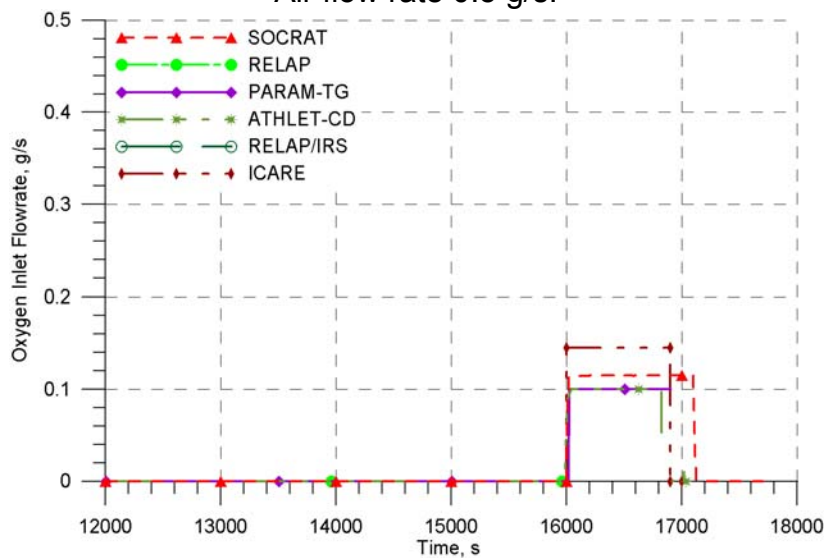
Figure 67. Oxygen flow rate at inlet. PARAMETER-SF4 experiment.
Air flow rate 0.5 g/s.
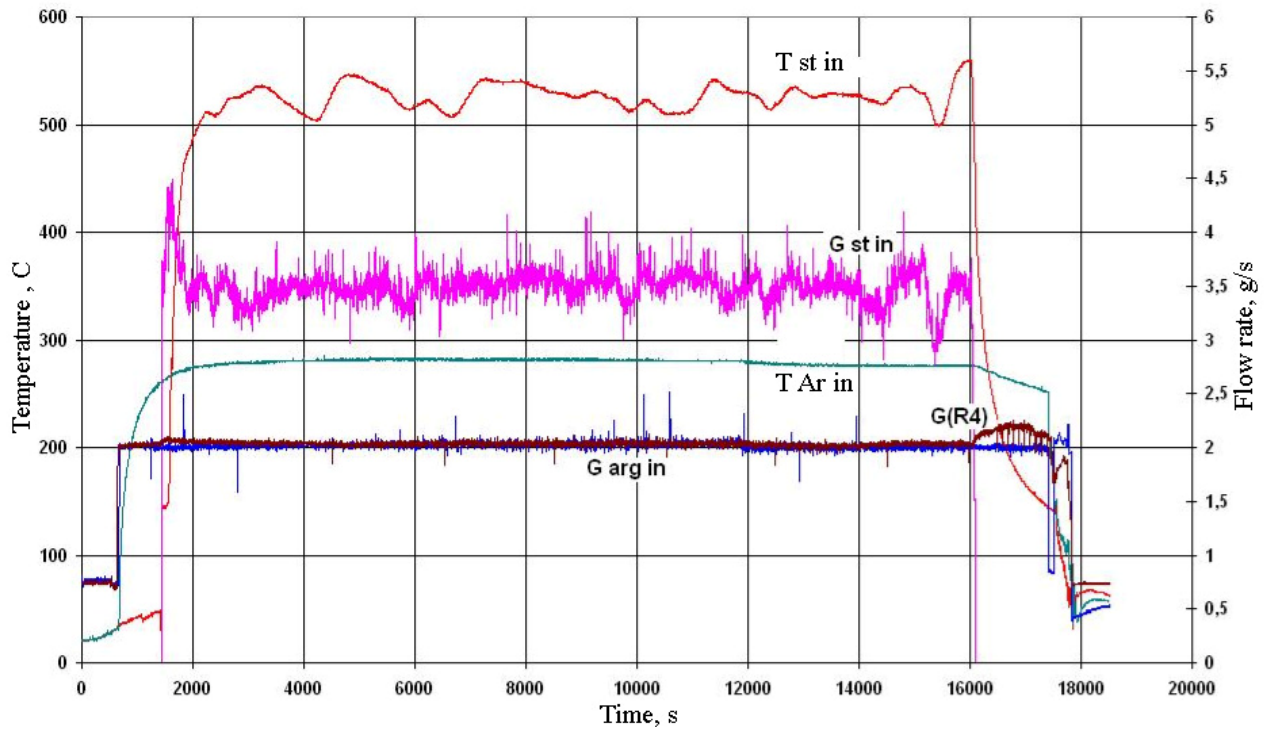
Figure 68. Steam (G $_{st\ in}$, T $_{st\ in}$) and argon (G $_{Ar\ in}$, T $_{Ar\ in.}$) parameters at the inlet to the test section and gas mixture flow rate G(R4) at the outlet to the special ventilation.
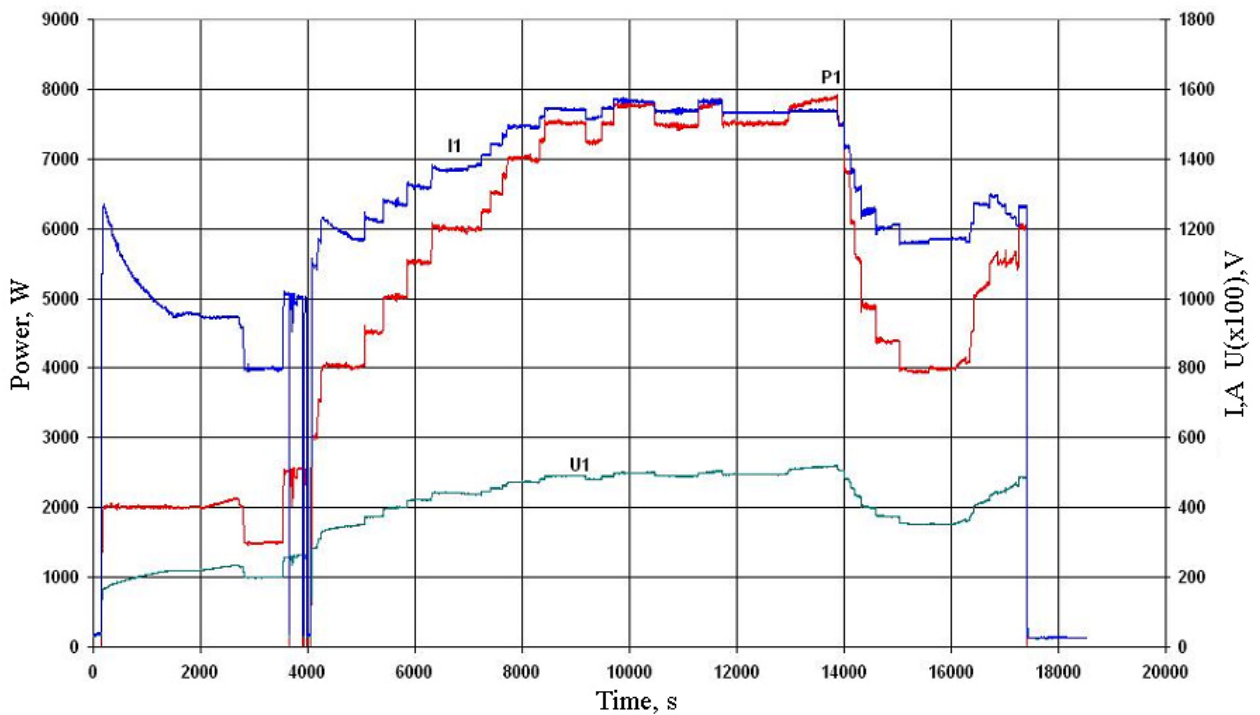
Figure 69. Power supply.
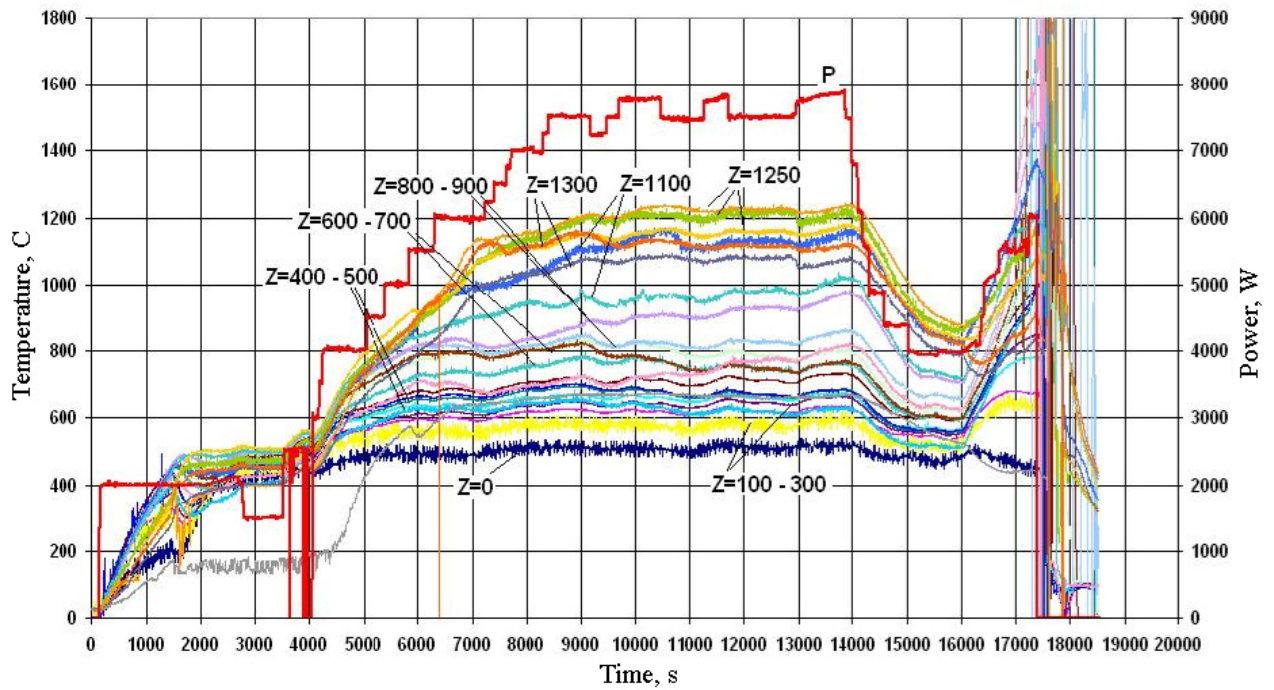
Figure 70. Thermocouples readings located over the height of fuel rods,
and electric power supply (P).
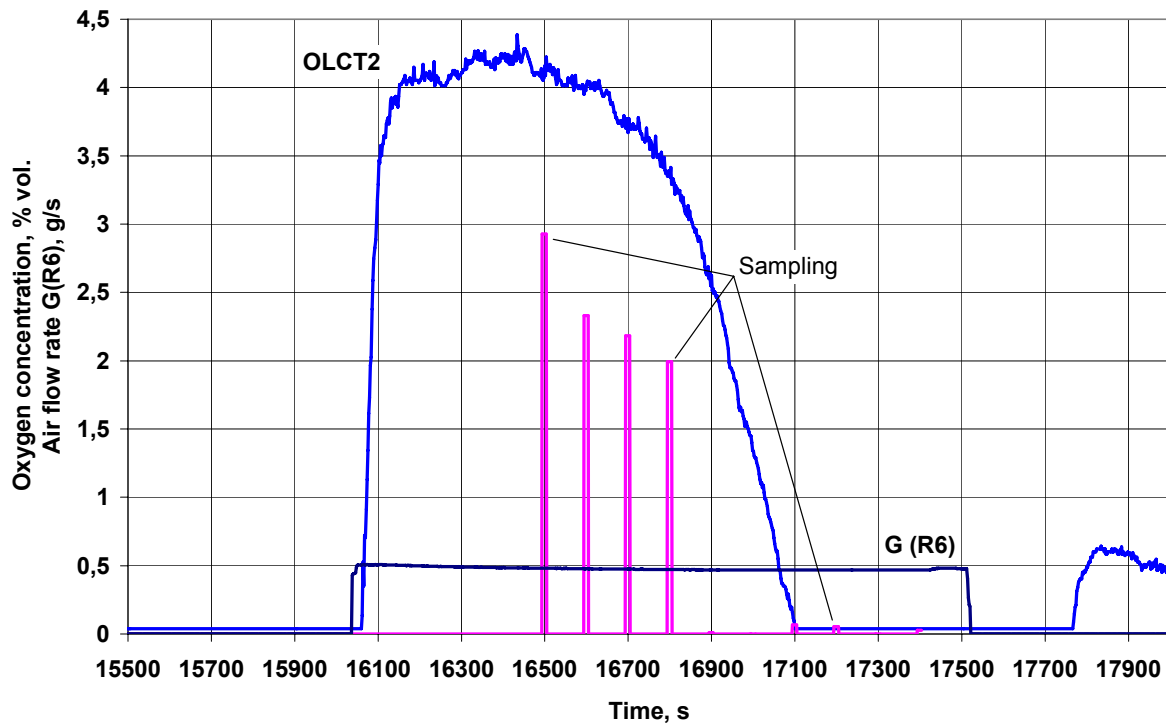
Figure 71. Volumetric oxygen concentration measured with the systems of continuous
(OLCT20) and discrete (Sampling) oxygen monitoring and air flow rate
at the test section inlet G(R6).
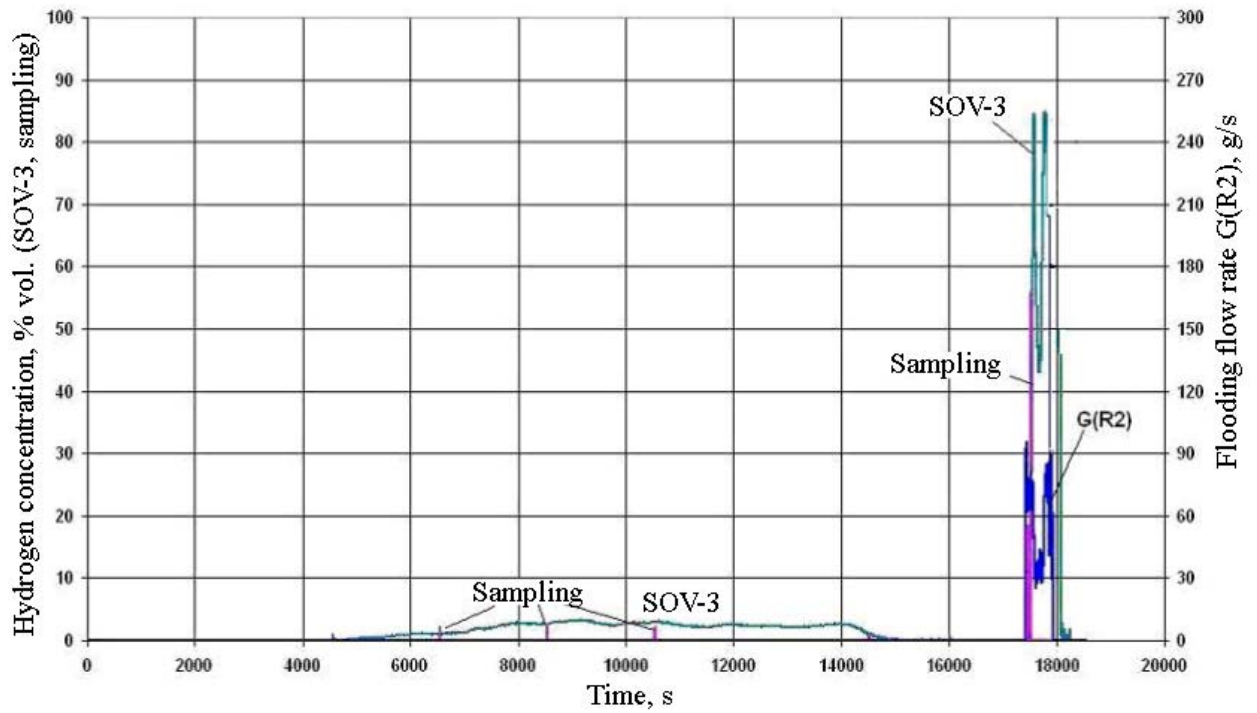
Figure 72. Volumetric hydrogen concentration measured with the systems of continuous (SOV-3) and discrete (Sampling) hydrogen monitoring, flooding water flow rate G(R2).
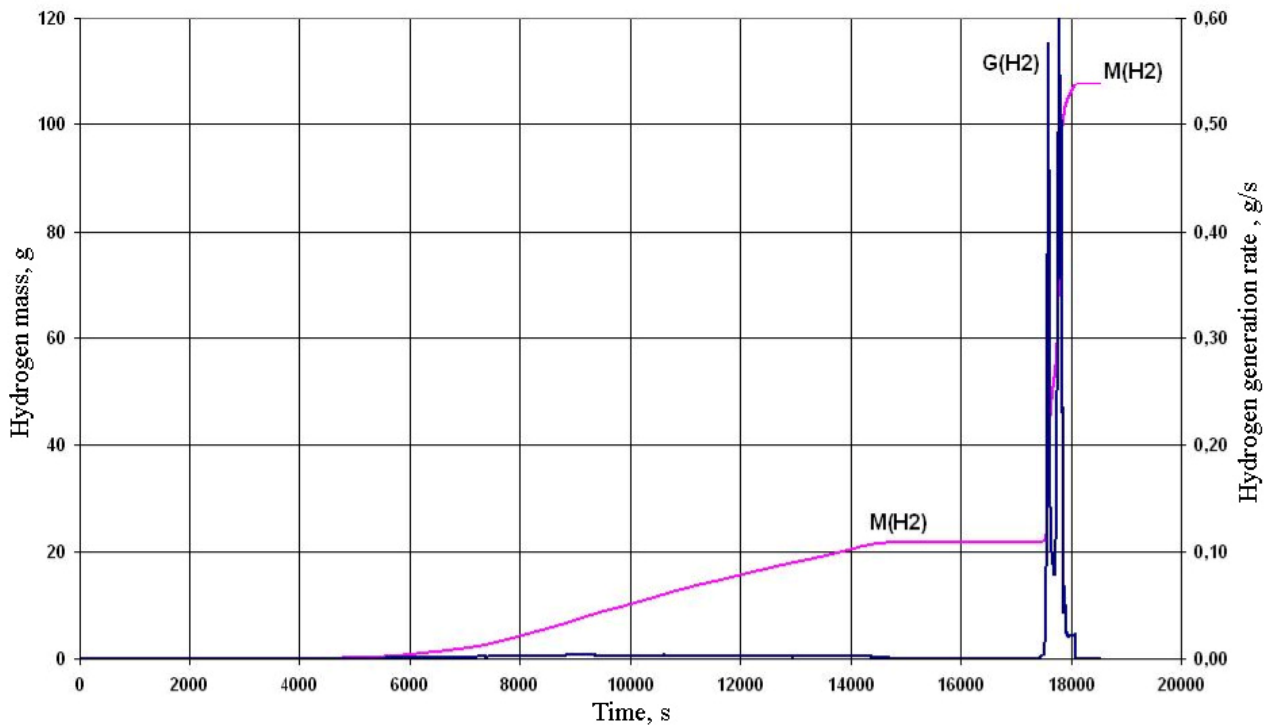
Figure 73. Released hydrogen mass and generation rate.

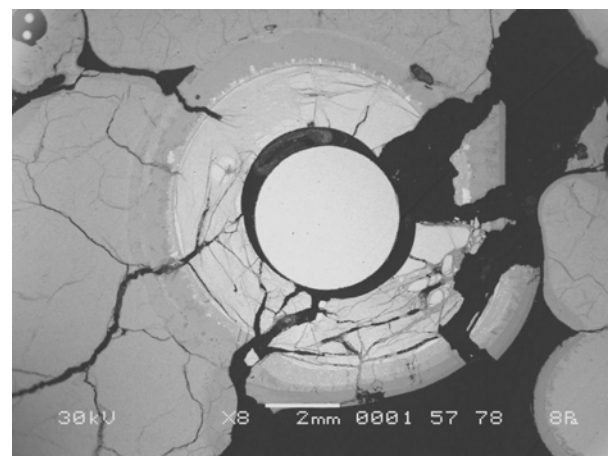Figure 74. Assembly cross-section at the elevation of Z = 130 mm (top view).

| a | b |
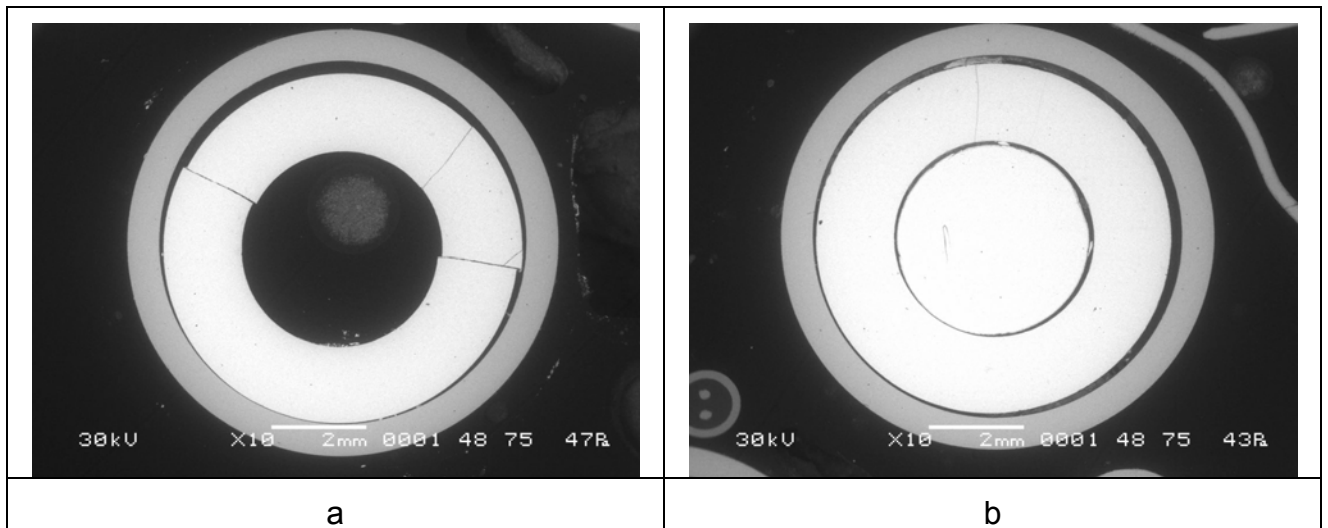
Figure 75. Photos of fuel rod simulators at the elevation of Z = 130 mm:
a – fuel rod 1.1; b – fuel rod 2.4.
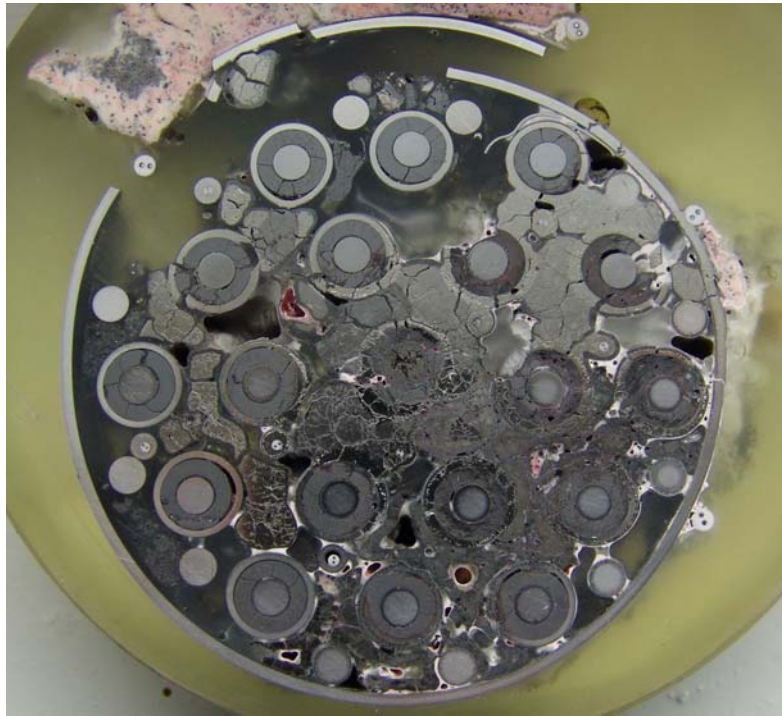
Figure 76. Assembly cross-section at the elevation of Z = 260 mm (top view).
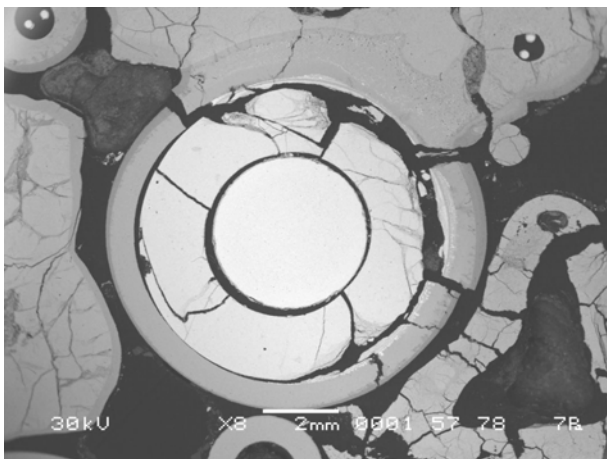
a
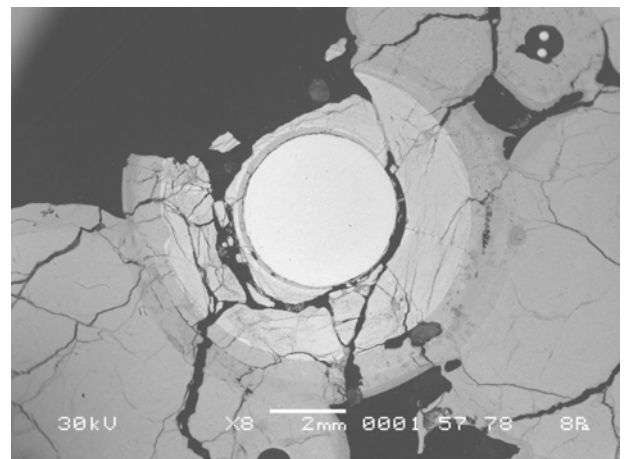
b
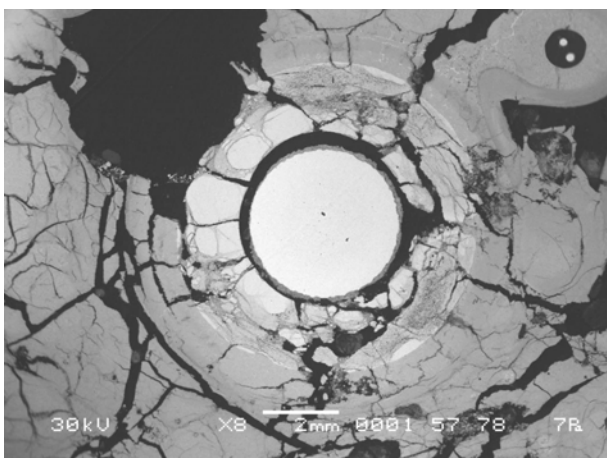
c

d

Figure 77. Cross-section of fuel rod simulators at the elevation of Z = 260 mm:
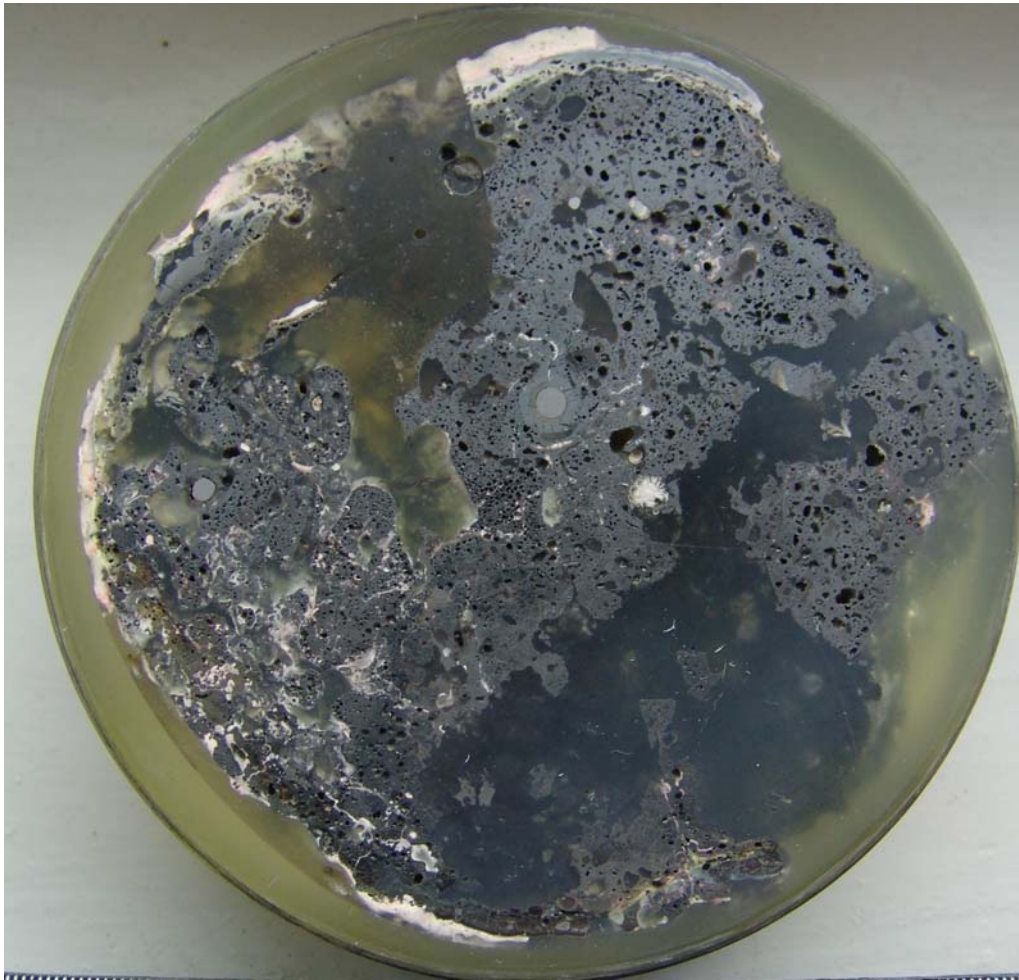a – fuel rod 2.1; b – fuel rod 2.4; c – fuel rod 2.5; d – fuel rod 3.8.

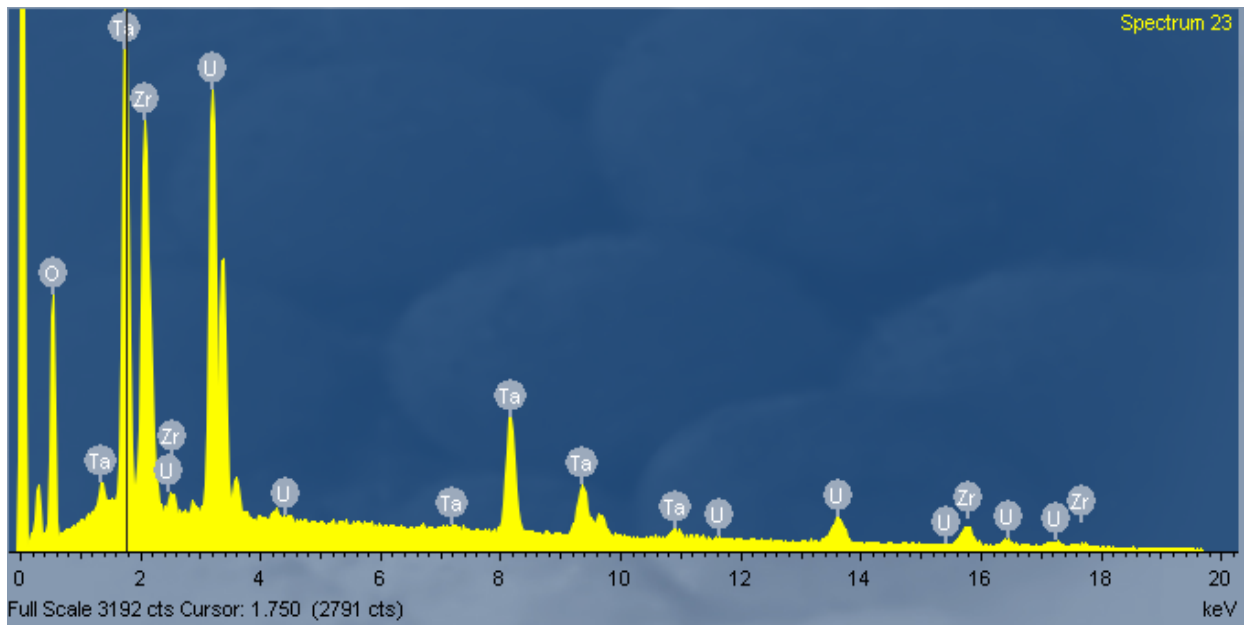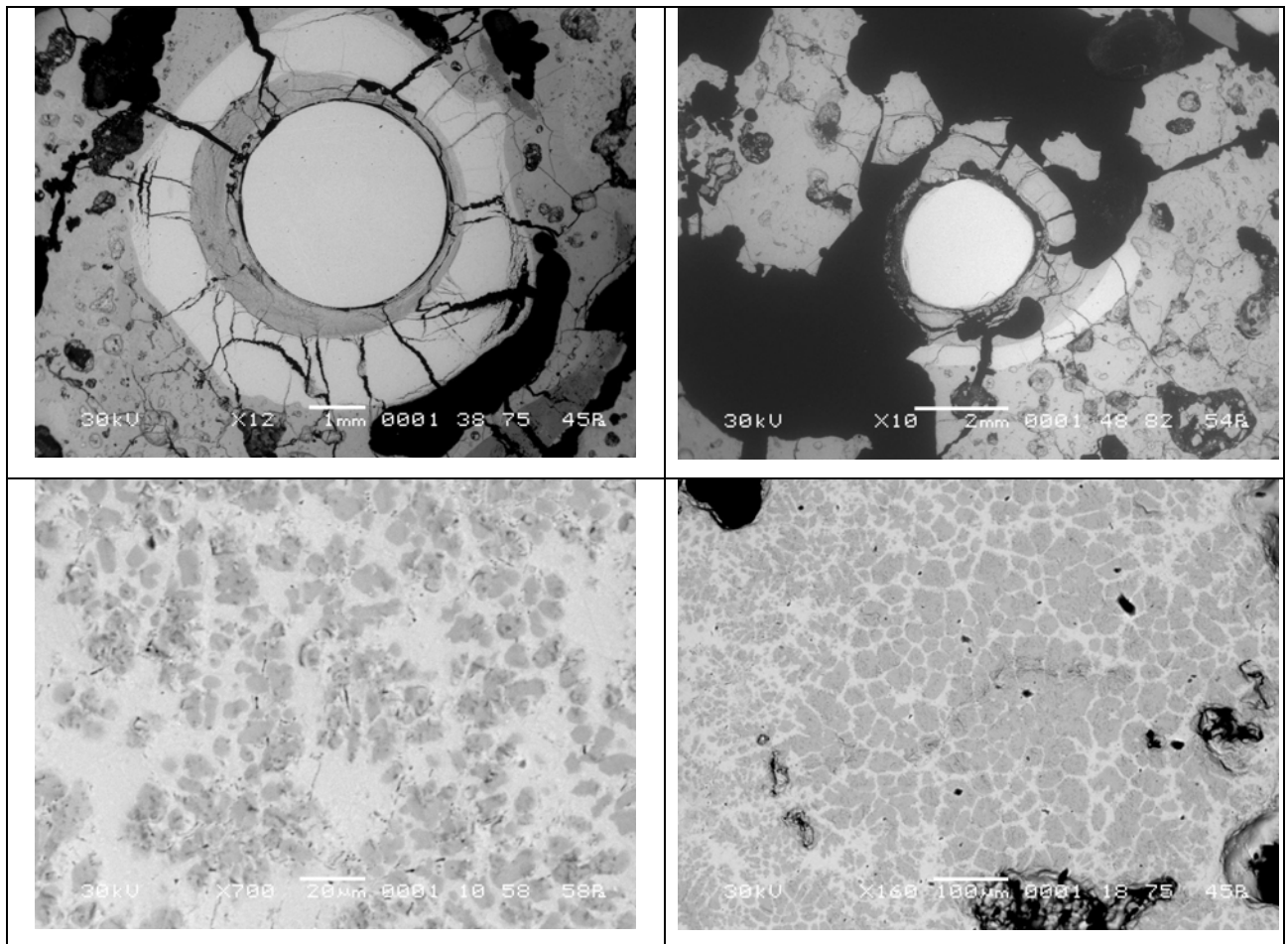Figure 78. Assembly cross-section at the elevation of Z = 300 mm (bottom view).

Figure 79. Cross-section of fuel rod simulators and structure of the melt
at the elevation of Z = 300 mm.

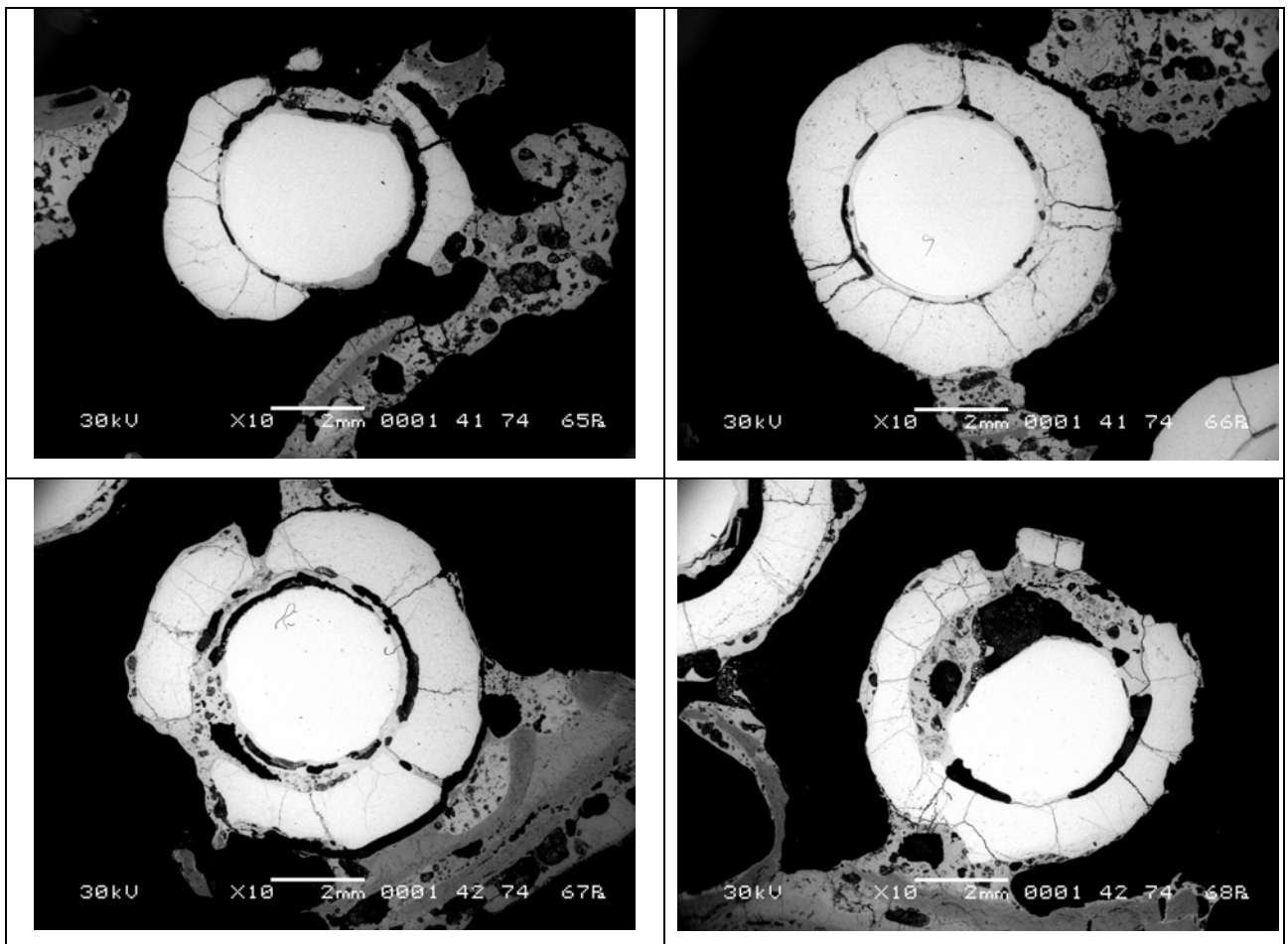Figure 80. Assembly cross-section at the elevation of Z = 1200 mm (bottom view).

Figure 81. Cross-section of fuel rod simulators at the elevation of Z = 1200 mm.